Charles University, Faculty of Science

Department of Botany

Study programme: Botany

Mgr. Kateřina Woodard

Quantitative shape analysis of diatom frustules: asymmetry, allometry and morphospace structure

Kvantitativní tvarová analýza rozsivkových frustul: asymetrie, allometrie a struktura tvaroprostorů

Ph.D. Thesis

Supervisor: Prof. RNDr. Jiří Neustupa, Ph.D.

Prague, 2023

Věnováno RNDr. Jiřímu Macelovi

Author's declaration

I hereby declare that I have written this thesis independently using listed references. I did not submit this thesis nor its part for any other academic degree or diploma.

Prohlášení autorky

Čestně prohlašuji, že jsem nepředložila práci ani její části k získání jiného nebo stejného akademického titulu a že jsem práci zpracovala samostatně za použití citované literatury.

In Prague, January 2023 Kateřina Woodard

Poděkování

Děkuji svému učiteli dr. Jiřímu Macelovi za to, že mě přivedl se studiu bio-logie. Prof. Aloisii Poulíčkové děkuji za poskytnutí rozsivkových kmenů. Dr. Janě Kulichové děkuji za uvedení do algologické laboratoře. Celé své rodině děkuji za podporu, a zvlášť svojí mamince, která se starala o vnoučata, když jsem pracovala na disertaci. Ze srdce děkuji školiteli Jiřímu Neustupovi za trpělivost a inspiraci.

Acknowledgements

I thank my teacher Dr. Jiří Macela for bringing me to study bio-logy. I thank Prof. Aloisie Poulíčková for providing the with diatom strains to me. I thank Dr. Jana Kulichová for introducing me to the algology laboratory. I thank my whole family for their support, especially my mother who took care of the grandchildren while I worked on my dissertation. My heartfelt thanks to my supervisor Jiří Neustupa for his patience and inspiration.

List of scientific articles included in the thesis

Article 1

Woodard, K.; Kulichová, J.; Poláčková, T. & Neustupa, J. (2016). Morphometric allometry of representatives of three naviculoid genera throughout their life cycle. Diatom Research 31: 231–242. DOI: 10.1080/0269249X.2016.1227375, IF (2016): 1.714

Article 2

Woodard, K. & Neustupa, J. (2016). Morphometric asymmetry of frustule outlines in the pennate diatom *Luticola poulickovae* (Bacillariophyceae). Symmetry 8: 150. DOI: 10.3390/sym8120150, IF (2016): 1.457

Article 3

Woodard, K. & Neustupa, J. (2022). Geometric morphometrics of bilateral asymmetry in *Eunotia bilunaris* (Eunotiales, Bacillariophyceae) as a tool for the quantitative assessment of teratogenic deviations in frustule shapes. Symmetry 14: 42. DOI: 10.3390/sym14010042, IF (2021): 2.940

Article 4

Woodard, K. & Neustupa, J. (submitted). Morphometric variation and allometric trajectories in the genus *Eunotia* (Bacillariophyceae, Eunotiophycideae). Submitted to "Biological Shape Analysis - Proceedings of the International Symposium".

Authors' Contributions

Article 1: KW, JK and JN designed the study; KW conducted the culturing experiments, microscopic work and analysed the data; TP participated on the data analysis; KW wrote the manuscript and JN reviewed and edited the manuscript.

Article 2: KW and JN designed the study; KW cultured the strains and conducted light microscopy of frustules and analysed the data; KW wrote the manuscript and JN reviewed and edited the manuscript.

Article 3: KW and JN designed the study and analysed the data; JN sampled the diatoms; KW conducted light microscopy of frustules; KW wrote the manuscript and JN reviewed and edited the manuscript.

Article 4: JN designed the study; KW acquired and analysed the data; KW wrote and edited the manuscript.

On behalf of all the co-authors, I declare the keynote participation of Kateřina Woodard in completing the research and writing the papers, as described above.

In Prague, January 17, 2023 Jiří Neustupa

Abstract

This thesis is focused on geometric morphometrics of allometric and asymmetric variation in frustule shape of raphid pennate diatoms. While pronounced shape changes of diatom frustules related to their size reduction were many times reflected in diatom research, formal quantitative evaluation of these patterns has been rarely attempted. My thesis used semilandmark based geometric morphometrics of frustule outlines in analyses of morphological phenomena related to size reduction throughout mitotic phase of the life cycle, such as allometry, symmetry of frustules and their asymmetric deviations. The analyses showed that morphological allometry represents the dominant element of shape variation in several naviculoid species, such as *Luticola poulickovae*, *Navicula cryptocephala*, *Sellaphora pupula*. Shape changes during size reduction throughout the vegetative part of these taxa mostly involved a simultaneous increase in circularity of valve outlines and disparity among cells. On the other hand, asymmetry of valves proved to be unrelated to size changes within populations. However, the morphometric analyses of *Luticola poulickovae* revealed that there was a subtle but significant side-oriented asymmetry of valve outlines that is related to the position of the primary and secondary valve sides. In addition, pronounced individual asymmetric deviations often occur in natural diatom population as result of environmental stress. Morphometric analyses of asymmetry in *Eunotia bilunaris* showed that these shape deviations actually affected valve outlines with different frequency and the analysis identified specific regions of the frustule that may be particularly sensitive to stress. While the subsequent analysis of size reduction series in multiple species of the genus *Eunotia* showed that most species have relatively closely similar allometric shape trajectories. a few taxa exhibited more divergent ontogenetic allometric patterns, which might indicate their increased potential for morphological evolutionary diversification. With these analyses, I wanted to show that geometric morphometrics of diatom frustules may provide useful insights into patterns of shape dynamics related to ontogenetic processes or environmental effects.

Abstrakt

Tato práce je zaměřena na geometricko morfometrický výzkum alometrické a asymetrické variability ve tvaru frustul raphidních penátních rozsivek. Dřívější studie zabývající se výzkumem rozsivek mnohokrát zaznamenaly vztah tvarové variability a zmenšování frustul v průběhu vegetativního cyklu. Formální kvantitativní analýza těchto patrností se ovšem v literatuře vyskytuje jen poměrně vzácně. Ve své dizertaci jsem použila semilandmarkovou geometrickou morfometriku obrysů frustul pro analýzy morfologických fenoménů alometrie, symetrie a asymetrických odchylek spojených s redukcí jejich velikosti v průběhu mitotické fáze životního cyklu. Provedené analýzy ukázaly, že morfologická alometrie představuje dominantí část tvarové variability u několika studovaných navikuloidních rodů jako je *Luticola poulickovae*, *Navicula cryptocephala* a *Sellaphora pupula*. Tvarové změny v průběhu velikostní redukce u těchto taxonů zahrnovaly simultánní zvýšení cirkularity obrysů valv a disparity mezi buňkami. Dynamika asymetrie valv ovšem nebyla s velikostními změnami korelovaná. Morfometrické analýzy druhu *Luticola poulickovae* ovšem ukázaly, že jejich frustuly vykazovaly také subtilní ale signifikantní stranově orientovanou asymetrii valvárních obrysů, která souvisí s pozicí primární a sekundární strany valv. Výrazné individuální asymetrické odchylky se ovšem v rozsivkových populacích vyskytují zejména v důsledku environmentálního stresu. Morfometrické analýzy asymetrie u druhu *Eunotia bilunaris* ukázaly, že tyto tvarové deviace se v rámci její obrysů vyskytují pouze v několika úsecích, které tedy mohou být obzvláště sensitivní k působení vnějšího stresu. Následné analýzy velikostních sérií u jednotlivých druhů rodu *Eunotia* ukázaly, že většina druhů měla relativně podobné alometrické tvarové trajektorie, u několika druhů se ovšem prokázala velmi divergentní alometrická dynamika, která by mohla indikovat jejich zvýšený potenciál k evoluční a morfologické diferenciaci. Pomocí těchto analýz jsem chtěla ukázat, že geometrická morfometrika rozsivkových frustul může poskytnout užitečné vhledy pro pochopení jejich tvarové dynamiky spojené s ontogenetickými procesy a environmentálními vlivy.

Contents

1. Introduction.....**11**

2. Morphometric allometry of representatives of three naviculoid genera throughout their life cycle.....**29**

3. Morphometric asymmetry of frustule outlines in the pennate diatom *Luticola poulickovae* (Bacillariophyceae).....**52**

4. Geometric morphometrics of bilateral asymmetry in *Eunotia bilunaris* (Eunotiales, Bacillariophyceae)as a tool for the quantitative assessment of teratogenic deviations in frustule shapes.....**70**

5. Morphometric variation and allometric trajectories in the genus *Eunotia* (Bacillariophyceae, Eunotiophycideae).....**89**

6. Key results and Conclusions.....**109**

1. Introduction

The topic of this thesis is morphological variation of diatom frustules. My ambition was to study the shape dynamics of the frustules as a phenomenon, not to explain it through morphogenetic or other hidden mechanisms. In this work, the diatom frustule shapes are examined from the outside, as is typical for a biological research approach that has been lately addressed as biological shape analysis (Bookstein, 2013). The tradition of this approach can be traced back to the paradigmatic work "On Growth and Form" (Thompson, 1942), which was firmly rooted in the concepts of biological structuralism. Thus, this dissertation is also partly related to this school of thought in modern biology. Development of ideas and methods in biological structuralism started in the 1980s together with the progress in multivariate biostatistics and geometry. Undoubtedly, one of the most active fields in this line of biological thought is geometric morphometrics (Cooke & Terhune, 2015; Bookstein, 2019).

This thesis uses geometric morphometrics for exploring questions and testing hypotheses related to morphological allometry and asymmetry of pennate diatoms. It is composed of three published research articles, one submitted book chapter and a brief theoretical introduction that deals with the aspects of diatom biology and morphology that is relevant in the context of the thesis.

The core subject of my research was the phenomenon of quantitative morphological allometry and shape variability of raphid pennate diatoms related especially to their vegetative size reduction cycle. In addition, a related topic of asymmetry in frustule outlines throughout their vegetative size reduction phase was also investigated. The final part of this thesis is directly focused on the frustule outline asymmetry, especially in the context of their teratogenic deviations from species-specific morphology occurring in polluted habitats.

Diatom morphology, morphogenesis and allometry

Diatoms (Bacillariophyceae) are ubiquitous stramenopile microalgae with peculiar morphology and life cycle. They occur in oceanic, freshwater and soil habitats worldwide and they have substantial impact on the ocean carbon and silica cycles (Round et al., 1990; Smetacek, 1999; Kooistra et al., 2007). Based on the morphology, morphometrics, ecology and mating experiments, it has been estimated that the number of extant diatom species might exceed 100 000 (Mann, 1999; Mann & Vanormelingen, 2013).

Diatom silica cell wall (frustule) is a finely ornamented structure composed of two valves

that are joined by overlapping girdle bands, creating a box like morphology (Round et al., 1990). The valves are ornamented with pores, processes, spines, hyaline areas and other features that may or may not be specific for species and genera (Cox, 2012) (Fig. 1).

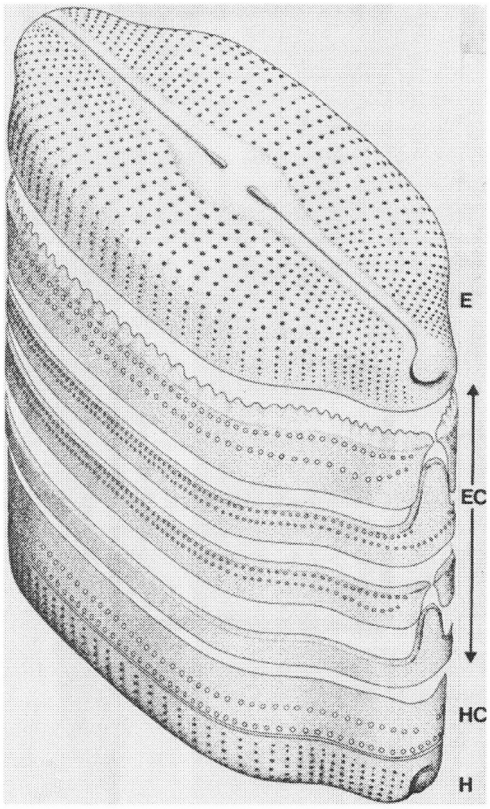

Figure 1. Exploded view of the frustule of a naviculoid diatom, showing the epivalve (E), epicingulum containing 4 bands (EC), the incomplete hypocingulum (HC) and the hypovalve (H). After Round et al. (1990).

The shape and symmetry of the frustules together with the mode of sexual reproduction and the plastid arrangement is reflected in the traditional diatom classification system that divides diatoms into two groups: oogamous centrics with radial symmetry and isogamous pennates with bilateral symmetry. Currently, the diatom phylogenetic and genomic studies use increasingly larger proportion of diatom diversity (Nakov et al., 2018; Nakov et al., 2019). However, the most common provisional classification that has also been adopted by Algaebase (Guiry & Guiry, 2023) still subdivides diatoms into three classes – Coscinodiscophyceae, Mediophyceae and Bacillariophyceae (Medlin, 2016). In this system, the class Coscinodiscophyceae includes mostly radiate centrics such as *Aulacoseira*, *Coscinodiscus* or *Melosira*. This class is considered a group with plesiomorphic characters and their representatives are well known since Mesozoic. The class Mediophyceae mainly contains the so called multipolar centrics (for example the genera *Biddulphia*, *Chaetoceros*, *Odontella*) but its monophyly is uncertain and it is probable that the structure of this group will be rearranged in future phylogenetic revisions. Finally, the class Bacillariophyceae comprises diatoms with primarily bilateral (biradial) valves including the ones with or without raphe. However, since the overall phylogenetic relationships of these deeply rooted diatom groups remain uncertain, the

traditional terms such as *centric* and *pennate* diatoms are still widely used to address these groups for descriptive purposes, regardless of their actual phylogenetic structure (Sims et al., 2006; Williams & Kociolek, 2007; Medlin, 2016).

Frustule morphology

The diatom frustule is composed of two overlapping *thecae*, each of which consists of a valve and an accompanying series of girdle bands (Fig. 1). Each frustule has an older part (epitheca) and a younger part (hypotheca) and can expand only in a pervalvar direction, usually via formation of new girdle bands (Round et al., 1990; Cox, 2012). The valves are characterized by their three-dimensional and hierarchical organization of porous plates and solid walls with pore diameters that range from nanometres to micrometres (Gordon et al, 2009). The variety of the patterns and shapes of this architecture is tremendous with no less diversified terminology. For better understanding of the structure and for more precise taxonomy, the character homology and ontogeny are being studied (Cox, 2012). In this text I will focus on those valve characters and features that are relevant to individual studies that constitute this thesis.

The pores vary in their size and spacing and they have been variously named depending on their dimensions and function. Their arrangement usually creates a pattern that tends to be either bilaterally or radially symmetric. Very small pores (*areolae*) that are almost undistinguishable by LM form linear patterns on the valve – *striae*, and they are common in the pennate diatoms (Round et al., 1990; Cox, 2011). Some pores are isolated and morphologically distinct and they are referred to as *stigmata* (sg. stigma). Most commonly, stigma appears in the central area of a valve and it is often positioned asymmetrically (Round et al., 1990; Cox, 2012), such as in the genus *Luticola* whose morphological variability was examined in the studies that are part of this thesis.

One lineage of pennate diatoms possesses a slit through the siliceous cell wall called raphe (Fig. 1). It is a system of one or two slits along the longitudinal axis of a valve and it functions in motility (Ruck & Theriot, 2011). Interestingly, members of *Eunotiaceae* which served as a model group in one of the studies included in this thesis, have an unusual short marginal raphe whose edges are positioned on the valve mantle. As a result of this morphology, raphe branches are visible in the girdle view. According to the fossil records, the eunotioid raphe was more developed in some ancient morphotypes and hypothetically the current state is a result of a progressive degradation (Siver & Wolfe, 2007). It is probable that raphe was originally located in the central part of the valve and recent lineages with marginal raphe (such as in *Eunotia*) are phylogenetically derived.

Valve morphogenesis

Silica deposition and new valve formation occurs inside the cell in the silica deposition vesicle (SDV). The shape of the SDV corresponds with the shape of the developing valve because it keeps pace with the silica deposition (Mann, 2006). Formation of the valve shape in SDV follows some basic rules as reviewed in Mann (2006): "*Different parts of the valve are laid down at different times: the centre first, the periphery later; an almost two-dimensional array of ribs and striae first, then any additional layers and structures external or internal to the first-formed layer; the outlines of the valve pores first, then any structures and occlusions within them*". New valves are formed within the old frustule in close contact (Pickett-Heaps et al., 1990; Cox, 2012) and, therefore, they are constrained by the margins of the parental frustule and also by the surface interaction with the sibling valve (Mann, 1981; Cox, 2012). When the new valve is complete, it is released to the exterior by fusion of the sillicalemma and plasmalemma (Schmid et al., 1981).

Valve morphogenesis is initiated from a pattern center outwards to the margins (Schmid et al., 1981). In centric diatoms, the pattern center is a small ring – an annulus with radiating ribs, in pennate diatoms it is a longitudinal rib called sternum (Mann, 1984). A special modification of the basic pennate plan is a raphe-sternum development in raphe-bearing diatoms. In this case, the pattern center consists of an axial rib which arises first and forms one side of the raphe, a central nodule, and a secondary axial rib that is formed by silicification from both poles and the center at the same time and forms the other side of the raphe (Fig. 2). Thus, every raphid diatom has valves that are bilaterally asymmetrical in their ontogeny. It is important to note that the eunotioid plan is a special exception to this, because their raphe is not integrated into the primary pattern-centre (Mann, 1984). When valve formation is complete, the points of connection on the secondary axial rib can be distinguished as Voigt discontinuities (Mann, 1984; Cox, 2012). Therefore, the primary and the secondary sides of a valve can be determined. Primary sides of two valves in one frustule can be on the same side of the cell or diagonally opposite (*cis*/*trans* arrangement). Sibling valves always have the same orientation and therefore, *cis* frustules produce either two *cis* or two *trans* siblings, while *trans* frustules produce always *cis* and *trans* siblings. Thus, the ratio of *cis* and *trans* frustules is usually 1:1 or 1:2 (such as in the genus *Pinnularia*). However, some species only form *cis* frustules, for example those having dorsiventral morphology, such as the genus *Eunotia* (Mann, 1983; Cox, 2012).

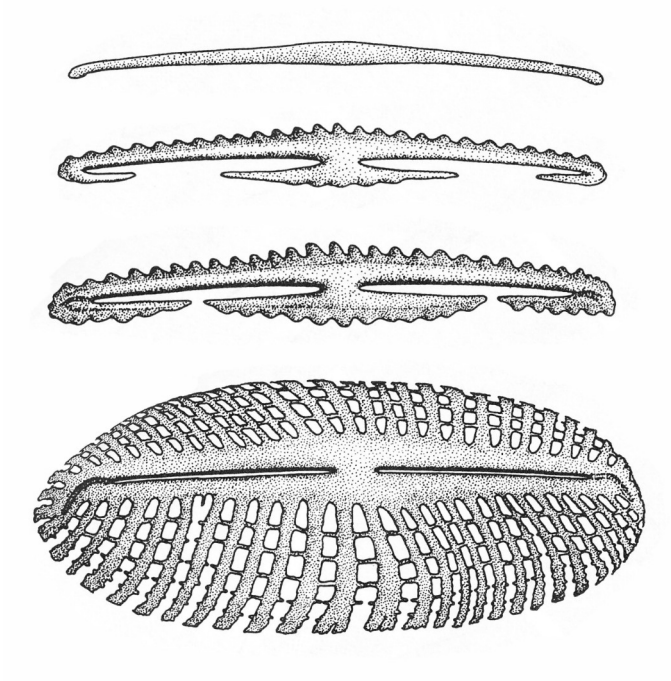

Figure 2. Side-oriented ontogenetic asymmetry of valves in naviculoid diatoms. The primary side is formed first and the secondary side is produced later by fusion of arms extending from both centre and poles. Voigt discontinuities often occur at fusion sites. Modified from Round et al. (1990).

Diatom life cycle and morphological allometry

Diatom cell wall structure is inevitably associated with its life cycle. The diatom frustule is formed of two complementary valves connected with a number of girdle bands. After each vegetative division, each daughter cell inherits one half-wall (*theca*) and forms a complementary half-wall (Round et al., 1990). Therefore, every diatom frustule is composed of two parts that are of a different age. Since the new thecas are formed within the frame of the parental ones, their size and shape is constrained. This phenomenon typically results in decrease of cell size in a clonal population over time (Round et al., 1990; Cox, 2012). When cells reach a threshold minimum size (so called "*first cardinal point*"; Geitler, 1932), they become sexually potent and sexual reproduction starts if external factors permit (Mann, 1999). Then, cell size is restored through an auxospore, a special zygote in which the initial *thecae* develop. These initial cells have rather different morphology than regular vegetative cells and after several divisions they disappear from the population (Edlund & Stoermer, 1997).

This peculiar cycle of cell size reduction and cell size restitution through sexual reproduction was first described by MacDonald (1869) and Pfitzer (1869). The so-called MacDonald-Pfitzer's hypothesis states, the cell size reduction in diatom populations is an inevitable result of the structure of the cell walls (Fig. 3).

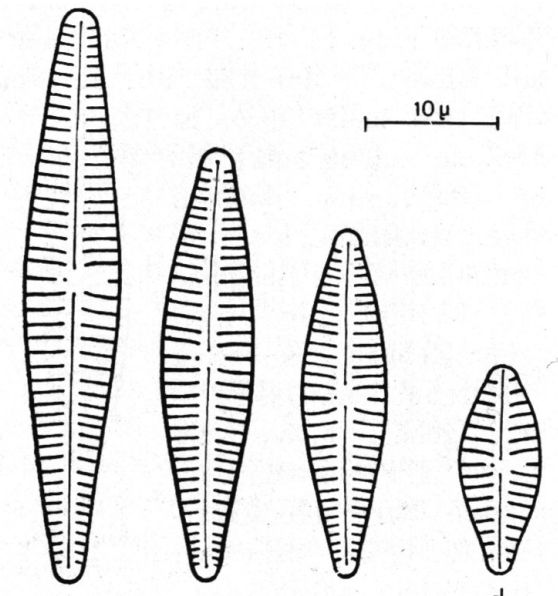

Fig. 19. *Gomphonema parvulum* var. *micropus*. Zellen (Schalen) aus einer Klonkulturreihe: a am 25. April, b am 1. Juli, c am 1. Oktober 1929, d am 12. Januar 1931.

Figure 3. One of the original size reduction series depicted by Geitler (1932), a founding work for diatom allometry research.

However, there are ways how to avoid cell size reduction (Lewis, 1984; Round et al., 1990; Edlund & Stoermer, 1997), although they are rare. More commonly, diatom populations in natural conditions seem to be able to prolong the vegetative phase of the life cycle for years, even for decades (Mann, 1988). Based on these findings, Lewis (1984) suggested that mechanisms that would avoid size reduction could be easily developed and instead, diatoms kept the size reduction phase as an adaptation that works for them as a timer for sexual reproduction. Some authors, however, doubt that these mechanisms could be "easily developed" because of the structural plan of the diatom frustule (Mann, 1988). Nevertheless, these hypotheses are difficult to test.

In laboratory conditions when cells are cultivated in stable room temperature and optimal nutrient and light levels, size reduction from largest to smallest cells can take several months (Geitler, 1932); however, in natural conditions such rapid progression is not probable because of the environmental limitations (Mann, 2011). In culture, populations can also lose their ability of sexual reproduction because they miss the size window and the population dies out; such case is referred to as closed life cycle (Mann & Chepurnov, 2004). In natural conditions, closed cycles have not been documented, however, cells that are smaller than the threshold are often found in nature (Mann, 2011). In general, life cycle length in nature is difficult to track and measure, because it is extremely challenging to follow the occurrence of sexual stages in the natural environment.

With decreasing cell size, the cell shape also changes. After the sexual reproduction, a new

initial cell forms *de novo* from an auxospore, than the period of mitotic divisions starts. During this phase, new frustules develop quite differently. Their valves are formed in close contact with the parental and sibling valves, and the whole development happens within the old frustule. Therefore, there is a physical inheritance of shape – the shape of one cell determines the shape of its progeny (Mann, 1994). This author notes, that this is in contrast with the development of shape *de novo,* as it occurs in *Micrasterias*, another unicelular alga with two cell halves of a different age, whose new semicells develop in minimal contact to the old semicells and therefore, they are rather independent units. However, despite the physical inheritance during the mitotic phase in diatom life cycle, the shape of the frustules does not stay the same. The new smaller valves are more rounded, they can lose capitate apices, long straight valves generate oval shaped valves (Geitler, 1932; Round et al., 1990; Mann, 1994; Edlund & Stoermer, 1997; Chapter 2 of this thesis).

This shape change is directly related to the life cycle and size reduction, therefore, it can be referred to as ontogenetic allometry (English & Potapova, 2012; Chapter 2 of this thesis). If an organism grows or diminishes isometrically (i. e. the shape stays the same and the proportions do not change), the volume of such organism scales with the surface to the two-thirds power (McMahon & Bonner, 1983). Therefore, during growth, the volume increases faster than the surface area and, on the other hand, during size reduction, the volume decreases slower than the surface area. This inevitably affects the rates of energy and material exchange between an organism and its surroundings and thus also physiology, ecology and evolution (Okie, 2013). Consequently, organisms developed ways how to modify the SA:V ratio through shape (fractality, dissimilitude) and surface alterations (internalisation) (Okie, 2013).

Similarly, in diatoms, we can observe how their frustules become more globular during the size reduction which may be a way for them how to keep the SA:V ratio balanced (Chapter 2 of this thesis). Diatoms are also able to expand their vacuoles, which is a surface alteration that is suitable for organisms with rigid cell walls (Hansen & Visser, 2019). Despite these modifications, the SA:V ratio during the size diminution probably still increases, therefore, the physiology of a clone may significantly change as the mitotic size reduction phase of the life cycle proceeds (Mann, 1994; Amato et al., 2005). Subsequently, SA:V ratio dynamics might be associated with environmental conditions, such as in *Diatoma moniliformis*, whose changes in cell proportions during the life cycle fit well with annual growth cycles (Potapova & Snoeijs, 1997).

Besides the shape changes that are predictable and follow some basic patterns, there are also slight irregularities on the frustules that rise during the cell division. These aberrations can be passed on to the new generations and they can affect the course of shape change and bring long term effects (Mann, 1994). According to Schmid (1994), "*the ratio of the volume of the nucleus, cy-*

toplasm, and vacuole also changes, leading to the physiological and subsequently the morphological heterogeneity of a clonal population". Due to this phenomenon, the shape variability in clonal populations can increase throughout the mitotic phase of the life cycle (Chapter 2 of this thesis).

The proportional changes and shifts in the frustule shape can be connected to a loss of taxonomically important characteristics (Schmid, 1994), and this can complicate species identification (Rhode et al., 2001; Pappas & Stoermer, 2003; Fránková et al., 2009). Populations at different size reduction stages in the mitotic part of the life cycle can also be misinterpreted as different species (Cox, 1986; Rose & Cox, 2014). In these cases, geometric morphometrics can be a useful tool for studying ontogenetic allometric trends and their taxonomic consequences (Veselá et al., 2009; English & Potapova, 2012; Edgar et al., 2015). According to Mann (1994), each gamodeme (deme composed of individuals that can interbreed) varies in shape and size during its life cycle but the multidimensional pattern of shape variation does not overlap the shape variation shown by either of the other gamodemes. The variability of such multidimensional pattern can be captured by quantitative analysis of allometric space (Neustupa, 2016). Using such analysis, it is possible to follow similarities of the course of shape changes throughout the vegetative size reduction phase and compare the ontogenetic allometric trends between or within more or less related species. In diatomology, this approach has not been applied yet but in this thesis, I used this concept in an analysis of a model dataset of 70 *Eunotia* species and their size reduction series (Chapter 5 of this thesis).

Symmetry and teratology of diatom frustules

Diatom frustules manifest high levels of rotational or reflective symmetry that is related to the ontogenetic trajectory starting either with an annulus for centrics or a sternum for pennates (Pappas at al., 2021). However, diatom shape and symmetry have probably undergone convergent and parallel evolution and they cannot be used as unambiguous indicators of relationships at generic or higher taxonomic levels (Mann, 1994; Kooistra et al., 2003; Alverson et al., 2006; Cox, 2014; Nakov et al., 2018). Studies that are based on cladistic analysis of morphological characters (Kociolek & Stoermer, 1988) or studies based on analyses of theoretical morphospace (Pappas, 2005; 2008) suggested that strongly asymmetric forms may have evolved from symmetric ancestors; nevertheless, molecular phylogenetic research did not conclusively support these hypotheses (Theriot et al., 2010; Nakov et al., 2019).

Biradial symmetry of the valves is one of the fundamental properties of raphid pennate diatoms. This pattern is characteristic of two axes of symmetry across the apical and transapical axis

of the valves and it may be phylogenetically ancestral (Sims et al., 2006; Cox, 2012). On the other hand, all raphid pennate diatoms are cryptically asymmetric. This asymmetry is based upon the above-mentioned manner of formation of the raphe-sternum during the valve ontogenesis (Mann, 1984). Therefore, even lineages with biradially symmetric frustule outlines have features that are intrinsically bound up with either primary or secondary valve side, such as Voigt discontinuities, stigmata, or raphe fissures. This is also the case of *Luticola poulickovae* that was used as a model system in the study of signed asymmetry of the valve outlines (Chapter 3 of this thesis).

In the evolution of raphid pennate diatoms, ancestral biradial symmetry of the valve outlines was broken several times in unrelated lineages resulting in distinctly asymmetric valves along the apical, transapical or both axes at the same time (Round et al., 1990). Symmetry breaking along the transapical axis results in heteropolar morphology that is often characteristic for epiphytic diatoms attached to surfaces with one pole of their frustules. Thus, the opposite poles (apices) of these cells are morphologically differentiated, which is evolutionarily related to the sessile way of life (Round et al., 1990). For example, this type of morphology is common in the genera *Gomphoneis* or *Gomphonema*. Interestingly, it was found that in isopolar genera such as *Pinnularia*, there is a constant polarity in the protoplast, which could hypothetically be the basis for the eventual future symmetry breaking and development of structural heteropolarity (Poulíčková et al., 2007; Cox, 2012).

On the other hand, in the genera such as *Cymbella* or *Encyonema* the symmetry is broken along the apical axis which led to the arcuate, dorsiventral morphology. The shape of such cells is distinctly curved – the ventral valve margins are concave and the dorsal margins are convex. Studied in more detail, it was recorded that some dorsiventral genera have wider secondary sides (*Cymbella*, *Cymbopleura*, *Gomphocymbella*) while some genera (*Encyonema*, *Reimeria*) have wider primary sides (Cox, 2012). Symmetry breaking across both axes of symmetry led to development of sigmoid forms such as for example *Gyrosigma*. It is assumed that sigmoid forms could have evolved from isopolar ancestors and this hypothesis has also been supported by the fact that a few biradially symmetric naviculoid genera bear raphe fissures that are curved in opposite directions (Cox, 2012). On a more subtle level, we can recognize yet another symmetry category, such as *cis* and *trans* cells, according to the position of primary and secondary valve sides in one frustule (Mann, 1983; Cox, 2012), which was mentioned above.

Besides these systematic symmetry breakings that are characteristic for the entire lineages, there are also subtle asymmetric deviations from the ideal *bauplan* of the diatom frustules. These deviations may occur in connection to the external factors and environmental pollution that can affect the frustule morphogenesis (Falasco et al., 2009; 2021). In fact, quite a few authors illustrated

frustule deformations in natural populations since the end of the 19th century (Cox, 1890; Falasco, 2021). These teratological forms, i. e. abnormalities in outline and striation patterns (Fig. 4), have been well documented in number of studies in relation to different stress factors, such as increased sublethal concentrations of heavy metals, acidification, radioactivity etc. (Falasco et al., 2021). Many research articles pointed out especially the connection of teratologies in frustule outlines and increased concentrations of heavy metals (Morin et al., 2008; Tapia, 2008; Falasco et al., 2009a, b; Lavoie et al., 2012). Moreover, diatom frustules are often well preserved in sediments and, therefore, frequence and severity of deformations may be used as an environmental proxy in palaeoecological research. For example, proportion of deformed frustules in fossil records was linked to water quality and pollution pulses leading to acidification and heavy metals release in long time periods (Dickman, 1998; Cooper et al., 2003; Sienkiewicz & Gasiorowski 2016).

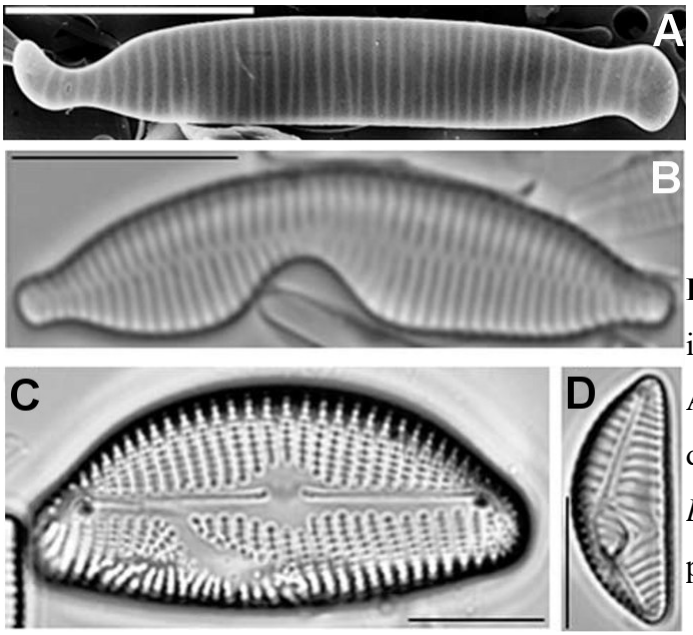

Figure 4. Examples of environmentally induced teratogenic deformations of frustules. A, B: *Diatoma ehrenbergii*, outline deviations. D: *Encyonema prostratum*, E: *Encyonema silesiacum*, abnormal striation patterns. Modified from Falasco et al. (2009).

Most of the studies assessed the occurrence of deformations as a binary character of individual frustules, for example as a proportion deformed individuals in populations (Cattaneo, 2004; Furey et al., 2009; Fernández et al., 2018). Some studies characterized the degree of deformation using semiquanitative criteria; however, even in this case the deformation assessment was based on subjective observations (Furey et al., 2009; Fernández et al., 2018). Recently, several studies assessed the degree of teratological deformations of individual frustules within the Euclidean shape space (Olenici et al., 2017, 2020; Cerisier et al., 2019). These studies have in one way or another applied the methodological framework of geometric morphometrics in quantification of deformations.

Interestingly, when quantifying frustule outline deformities, from the theoretical point of

view it is basically an analysis of symmetry group of a structure with bilateral or biradial symmetry. In current biological shape analysis, the framework of geometric morphometrics of symmetry is the one most commonly used in the analysis of such structures (Klingenberg et al., 2002; Savriama et al., 2010; Savriama & Klingenberg, 2011; Klingenberg 2015). In this thesis, I used this approach to study symmetry and asymmetry of frustules in relation to their allometric variability, patterns of frustule formation, and evaluation of teratogenic deviations (Chapters 3 and 5 of this thesis). In general, methodology of these analyses that are described in detail in the chapters 2 and 4 used symmetric transformations of frustule outline shapes across their apical axis or across both axes depending on the particular study system. Shape analysis of geometric transformations of individual symmetry groups enables to include them into unified multidimensional space (morphospace) in which we can explore, illustrate and quantify individual asymmetric patterns, teratogenic deviations both for individuals and populations. I believe that this approach represents a strong methodological framework for capturing this variability and interpretation of these patterns in ecological or ontogenetic contexts.

In the context of diatom research it is important to note that the size differences due to size reduction cycles and their impact on frustule shapes are the dominant parts of the observed variability. Both this allometric variability and the symmetry of frustules are unique features of diatom phenotypes and they provide an intriguing field of research for biological shape analysis. Therefore, in this thesis I studied allometric variability associated with size diminution dynamics (Chapters 2 and 5 of this thesis) and symmetric and asymmetric patterns related to frustule ontogeny and diatom life cycle (Chapters 3 and 4 of this thesis).

The thesis uses raphid diatoms as study systems to investigate the allometric and shape phenomena described above. Specifically, I studied the genera *Eunotia* Ehrenberg, *Luticola* D.G.Mann, *Navicula* Bory, and *Sellaphora* Mereschkowsky. The species *Luticola poulickovae* Levkov, Metzeltin & A.Pavlov, *Navicula cryptocephala* Kützing, *Sellaphora pupula* (Kützing) Mereschkowsky were studied in clonal cultures. Allometric spaces in the genus *Eunotia* were constructed using a meta-analysis of size reduction series published in Lange-Bertalot et al. (2011). In addition, asymmetric patterns in *Eunotia bilunaris* (Ehrenberg) Schaarschmidt were explored using natural populations from Central European mountain peatlands.

List of references

Adams, G. L.; Pichler, D. E.; Cox, E. J.; O'Gorman, E. J.; Seeney, A.; Woodward, G. & Reuman, D. C. (2013). Diatoms can be an important exception to temperature – size rules at species and community levels of organization. Global Change Biology, 19: 3540-3552.

Alverson, A. J.; Cannone, J. J.; Gutell, R. R. & Theriot, E. C. (2006). The evolution of elongate shape in diatoms. Journal of Phycology, 42: 655-668.

Amato, A.; Orsini, L.; D'Alelio, D. & Montresor, M. (2005). Life cycle, size reduction patterns, and ultrastructure of the pennate planktonic diatom Pseudo-nitzschia delicatissima (Bacillariophyceae). Journal of Phycology, 41: 542-556.

Bookstein, F. L. (2013). The measurement of biological shape and shape change. Springer Berlin, Heidelberg, 191 pp.

Bookstein, F. L. (2019). Reflections on a Biometrics of Organismal Form. Biological Theory, 14:177-211.

Cattaneo, A.; Couillard, Y.; Wunsam, S. & Courcelles, M. (2004). Diatom taxonomic and morphological changes as indicators of metal pollution and recovery in Lac Dufault (Québec, Canada). Journal of Paleolimnology, 32: 163-175.

Cerisier, A.; Vedrenne, J.; Lavoie, I.; Morin, S. (2019). Assessing the Severity of Diatom Deformities using Geometric Morphometry. Botany Letters, 166: 32–40.

Cooke, S. B. & Terhune, C. E. (2015). Form, function, and geometric morphometrics. The Anatomical Record, 298: 5-28.

Cox, J. D. (1890). Deformed diatoms. Proceedings of the American Society of Microscopists, 12: 178-183.

Cox, E. J. (1986). Some taxonomic and ecological considerations of morphological variation within natural populations of benthic diatoms lles. In: Ricard, M. (ed.). Proceedings of the 8th Diatom Symposium, Paris 1984, pp. 163–172. O. Koeltz, Koenigstein.

Cox, E. J. (2011). Morphology, cell wall, cytology, ultrastructure and morphogenetic studies. In: Seckbach, J. & Kociolek, P. (eds.). The diatom world, pp. 21-45. Springer, Dordrecht.

Cox, E. J. (2012). Ontogeny, homology, and terminology - wall morphogenesis as an aid to

character recognition and character state definition for pennate diatom systematics *Journal of Phycology, 48: 1-3*1.

Cox, E. J. (2014). Diatom identification in the face of changing species concepts and evidence of phenotypic plasticity. Journal of Micropalaeontology, 33: 111-120.

Dickman, M. D. (1998). Benthic marine diatom deformities associated with contaminated sediments in Hong Kong. Environment International, 24: 749-759.

Edgar, R. K.; Salech, A. L. & Edgar, S. M. (2015). A morphometric diagnosis using continuous characters of *Pinnunavis edkuensis*, sp. nov. (Bacillariophyta: Bacillariophyceae), a brackish-marine species from Egypt. Phytotaxa, 212: 1–56.

Edlund M. B. & Stoermer E. F. (1997). Ecological, evolutionary, and systematic significance of diatom life history. Journal of Phycology, 33: 897-918.

English, J. D. & Potapova, M. G. (2012). Ontogenetic and interspecific valve shape variation in the Pinnatae group of the genus *Surirella* and the description of *S. lacrimula* sp. nov. Diatom Research, 27: 9-27.

Falasco, E.; Bona, F.; Badino, G.; Hoffmann, L. & Ector, L. (2009). Diatom teratological forms and environmental alterations: a review. Hydrobiologia, 623: 1-35.

Falasco, E.; Ector, L.; Wetzel, C. E.; Badino, G. & Bona, F. (2021). Looking back, looking forward: a review of the new literature on diatom teratological forms (2010–2020). Hydrobiologia, 848: 1675-1753.

Fernández, M. R.; Martín, G.; Corzo, J.; De La Linde, A.; García, E.; López, M. & Sousa, M. (2018). Design and Testing of a New Diatom-based Index for Heavy Metal Pollution. Archives of Environmental Contamination and Toxicology 74: 170-192.

Fránková, M.; Poulíčková, A.; Neustupa, J.; Pichrtová, M. & Marvan, P. (2009). Geometric morphometrics – a sensitive method to distinguish diatom morphospecies: a case study on the sympatric populations of *Reimeria sinuata* and *Gomphonema tergestinum* (Bacillariophyceae) from the River Bečva, Czech Republic. Nova Hedwigia, 88: 81-95.

Furey, P. C.; Lowe, R. L. & Johansen, J. R. (2009). Teratology in *Eunotia* Taxa in the Great Smoky Mountains National Park and Description of *Eunotia macroglossa* sp. nov. Diatom Research, 24: 273-290.

Geitler, L. (1932). Der Formwechsel der pennaten Diatomeen (Kieselalgen). Archiv für Protistenkunde, 78: 1-226.

Gordon, R.; Losic, D.; Tiffany, M. A.; Nagy, S. S. & Sterrenburg, F. A. (2009). The Glass Menagerie: diatoms for novel applications in nanotechnology. Trends in Biotechnology, 27: 116-127.

Guiry, M. D. & Guiry, G. M. (2023). AlgaeBase. World-wide electronic publication, National University of Ireland, Galway. https://www.algaebase.org

Hansen, A. N. & Visser, A. W. (2019). The seasonal succession of optimal diatom traits. Limnology and Oceanography, 64: 1442-1457.

Klingenberg, C. P. (2002). Morphometrics and the role of the phenotype in studies of the evolution of developmental mechanisms. Gene, 287: 3-10.

Klingenberg, C. P. (2015). Analyzing fluctuating asymmetry with geometric morphometrics: concepts, methods, and applications. Symmetry, 7: 843-934.

Kociolek, J. P. & Stoermer, E. F. (1988). A preliminary investigation of the phylogenetic relationships among the freshwater, apical pore field-baring Cymbelloid and Gomphonemoid diatoms (Bacillariophyceae). Journal of Phycology, 24: 377-385.

Kooistra, W. H. C. F.; Gersonde, R.; Medlin L. F. & Mann, D. G. (2007). The Origin and Evolution of the Diatoms: Their Adaptation to a Planktonic Existence. In: Falkowski, P. G. & Knoll, A. H. (eds.). Evolution of Primary Producers in the Sea, pp. 207-249. Acad. Press, New York.

Kooistra, W. H. C. F.; Stefano, M. D.; Mann, D. G. & Medlin, K. (2003). The phylogeny of the diatoms. In: Müller, W. E. G. (ed.). Silicon Biomineralization, pp. 59-97. Springer Berlin, Heidelberg.

Lange-Bertalot, Y.; Bąk, M.; Witkowski, A. & Tagliaventi, N. (2011). Diatoms of Europe: Diatoms of the European Inland Waters and Comparable Habitats. Volume 6. A.R.G. Gantner Verl., Wien.

Lavoie, I.; Hamilton, P. B.; Morin, S.; Tiam, S. K.; Kahlert, M.; Gonçalves, S.; Falasco, E.; Fortin, C.; Gontero, B.; Heudre, D.; Kahlert, M.; Kojadinovic-Sirinelli, M.; Manoylov, K.; Pandey, L. K. & Taylor, J. C. (2017). Diatom teratologies as biomarkers of contamination: are all deformities ecologically meaningful? Ecological Indicators, 82: 539-550.

Lewis W. M. Jr. (1984). The diatom sex clock and its evolutionary significance. The American Naturalist, 123: 73–80.

MacDonald J. D. (1869). On the structure of diatomaceous frustule, and its genetic cycle. Annals

and Magazine of Natural History, 3: 1-8.

Mann, D. G. (1981). A note on valve formation and homology in the diatom genus *Cymbella*. Annals of Botany 47: 267-269.

Mann, D. G. (1983). Symmetry and cell division in raphid diatoms. Annals of Botany, 52: 573-581.

Mann, D. G. (1984). An ontogenetic approach to diatom systematics. In: Mann, D. G. (ed.). Proceedings of the 7th International Diatom Symposium, pp. 113-144. O. Koeltz, Koenigstein.

Mann, D. G. (1994). The origins of shape and form in diatoms: the interplay between morphometric studies and systematics. In: Ingram, D. & Hudson, A. (eds.). Shape and Form in Plants and Fungi, pp. 17-38. Academic Press, New York.

Mann, D. G. (1999). The species concept in diatoms. Phycologia, 38: 437-495.

Mann, D. G. (2006). Specifying a morphogenetic model for diatoms: an analysis of pattern faults in the Voigt zone. Nova Hedwigia Beiheft, 130: 97-118.

Mann D. G. (2011). Size and sex. In: Seckbach, J. & Kociolek, P. (eds.). The diatom world, pp. 145-166. Springer, Dordrecht.

Mann, D. G. & Chepurnov, V. A. (2004). What have the Romans ever done for us? The past and future contribution of culture studies to diatom systematics. Nova Hedwigia, 79: 237-291.

Mann, D. G. & Round, F. (1988). Why didn't Lund see sex in *Asterionella*? A discussion of the diatom life cycle in nature. Algae and the Aquatic Environment, 29: 385-412.

Mann, D. G. & Vanormelingen, P. (2013). An inordinate fondness? The number, distributions, and origins of diatom species. Journal of Eukaryotic Microbiology, 60: 414-420.

McMahon, T. A. & Bonner, J. T. (1983). On size and life. Scientific American Library, New York.

Medlin, L. K. (2016). Evolution of the diatoms: major steps in their evolution and a review of the supporting molecular and morphological evidence. Phycologia, 55: 79-103.

Morin, S.; Duong, T. T.; Dabrin, A.; Coynel, A.; Herlory, O.; Baudrimont, M., Delmas, F.; Durrieu, G.; Schäfer, J.; Winterton, P.; Banc, G. & Coste, M. (2008). Long-term survey of heavy-metal pollution, biofilm contamination and diatom community structure in the Riou Mort watershed, South-West France. Environmental Pollution, 151: 532-542.

Nakov, T.; Beaulieu, J. M. & Alverson, A. J. (2018). Insights into global planktonic diatom diversity: the importance of comparisons between phylogenetically equivalent units that account for time. The ISME Journal, 12: 2807-2810.

Nakov, T.; Beaulieu, J. M. & Alverson, A. J. (2019). Diatoms diversify and turn over faster in freshwater than marine environments. Evolution, 73: 2497-2511.

Neustupa, J. (2016): Static allometry of unicellular green algae: scaling of cellular surface area and volume in the genus *Micrasterias* (Desmidiales). Journal of Evolutionary Biology, 29: 292-305.

Okie, J. G. (2013). General models for the spectra of surface area scaling strategies of cells and organisms: fractality, geometric dissimilitude, and internalization. The American Naturalist, 181: 421-439.

Olenici, A.; Baciu, C.; Blanco, S.; Morin, S. (2020). Naturally and Environmentally Driven Variations in Diatom Morphology: Implications for Diatom-based Assessment of Water Quality. In: Cristóbal, G.; Blanco, S. & Bueno, G. (eds). Modern Trends in Diatom Identification. Fundamentals and Applications, pp. 39–52. Springer, Cham.

Pappas, J. L. (2005). Theoretical morphospace and its relation to freshwater gomphonemoid–cymbelloid diatom (Bacillariophyta) lineages. Journal of Biological Systems, 13: 385-398.

Pappas, J. L. (2008). More on theoretical morphospace and its relation to freshwater gomphonemoid-cymbelloid diatom (Bacillariophyta) lineages. Journal of Biological Systems, 16: 119-137.

Pappas, J.; Kociolek, P. & Stoermer, E. F. (2014). Quantitative morphometric methods in diatom research. Nova Hedwigia Beiheft, 143: 281–306.

Pappas, J. L. & Stoermer, E. F. (2003). Legendre shape descriptors and shape group determination of specimens in the *Cymbella cistula* species complex. Phycologia, 42: 90-97.

Pappas, J. L., Tiffany, M. A. & Gordon, R. (2021). The uncanny symmetry of some diatoms and not of others: A multi-scale morphological characteristic and a puzzle for morphogenesis. In: Annenkov, V.; Seckback, J. & Gordon, J. (eds). Diatom Morphogenesis, pp. 19-67. Scrivener Publ. LLC, Beverly.

Pfitzer, E. (1869). Über den Bau und die Zellteilung der Diatomeen. Botanische Zeitung, 27: 774-776.

Pickett-Heaps, J. D.; Schmid, A. M. M. & Edgar, L. A. (1990). The cell biology of diatom valve formation. In: Round, F. E. & Chapman, D. J. (eds.). Progress in Phycological Research, pp. 1-168. Biopress Ltd., Bristol.

Potapova, M. & Snoeijs, P. (1997). The natural life cycle in wild populations of *Diatoma moniliformis* (Bacillariophyceae) and its disruption in an aberrant environment. Journal of Phycology, 33: 924-937.

Poulíčková, A.; Mayama, S.; Chepurnov, V. A. & Mann, D. G. (2007). Heterothallic auxosporulation, incunabula and perizonium in *Pinnularia* (Bacillariophyceae). European Journal of Phycology, 42: 367-390.

Rhode, K. M.; Pappas, J. L. & Stoermer, E. F. (2001). Quantitative analysis of shape variation in type and modern populations of *Meridion* (Bacillariophyceae). Journal of Phycology, 37: 175-183.

Rose, D. T. & Cox, E. J. (2014). What constitutes *Gomphonema parvulum*? Long-term culture studies show that some varieties of *G. parvulum* belong to other *Gomphonema* species. Plant Ecology and Evolution, 147: 366-373.

Round, F. E.; Crawford, R. M. & Mann, D. G. (1990). Diatoms: Biology and Morphology of the Genera. Cambridge Univ. Press, Cambridge, 747 pp.

Ruck, E. C. & Theriot, E. C. (2011). Origin and evolution of the canal raphe system in diatoms. Protist, 162: 723-737.

Savriama, Y.; Klingenberg, C. P. (2011). Beyond Bilateral Symmetry: Geometric Morphometric Methods for any Type of Symmetry. BMC Evolutionary Biology, 11: 280.

Savriama, Y.; Neustupa, J.; Klingenberg, C. P. (2010). Geometric morphometrics of symmetry and allometry in *Micrasterias rotata* (Zygnemophyceae, Viridiplantae). Nova Hedwigia Beiheft, 136: 43–54.

Schmid, A. M. M. (1994). Aspects of morphogenesis and function of diatom cell walls with implications for taxonomy. Protoplasma, 181: 43-60.

Schmid, A. M. M.; Borowitzka, M. A. & Volcani, B. E. (1981). Morphogenesis and biochemistry of diatom cell walls. In: Kiermaier, O. (ed.). Cytomorphogenesis in Plants, pp. 63–97. The Academy of Natural Sciences, Philadephia.

Sienkiewicz, E. & Gąsiorowski, M. (2016). The evolution of a mining lake - from acidity to natural neutralization. Science of the Total Environment, 557: 343-354.

Sims, P. A.; Mann, D. G. & Medlin, L. K. (2006). Evolution of the diatoms: insights from fossil, biological and molecular data. Phycologia, 45: 361-402.

Siver, P. A. & Wolfe, A. P. (2007). *Eunotia* spp. (Bacillariophyceae) from Middle Eocene lake sediments and comments on the origin of the diatom raphe. Botany, 85: 83-90.

Smetacek, V. (1999). Diatoms and the ocean carbon cycle. Protist, 150: 25-32.

Tapia, P. M. (2008). Diatoms as bioindicators of pollution in the Mantaro River, Central Andes, Peru. International Journal of Environment and Health, 2: 82-91.

Theriot, E. C.; Ashworth, M.; Ruck, E.; Nakov, T. & Jansen, R. K. (2010). A preliminary multigene phylogeny of the diatoms (Bacillariophyta): challenges for future research. Plant Ecology and Evolution, 143: 278-296.

Thompson, D. W. (1942). On Growth and Form. Cambridge Univ. Press, Cambridge, 470 pp.

Veselá, J.; Neustupa, J.; Pichrtová, M. & Poulíčková, A. (2009). Morphometric study of *Navicula* morphospecies (Bacillariophyta) with respect to diatom life cycle. Fottea, 9:307-316.

2. Morphometric allometry of representatives of three naviculoid genera throughout their life cycle

[published as Woodard, K.; Kulichová, J.; Poláčková, T. & Neustupa, J. (2016). Morphometric allometry of representatives of three naviculoid genera throughout their life cycle. Diatom Research, 31: 231–242.]

Abstract

The frustule architecture of diatoms and the nature of the vegetative cell division phase of their life cycle constrain cell size and shape. For decades, diatomists have observed that size diminution is accompanied by valve shape changes. However, allometric shape changes have rarely been assessed using quantitative statistical tools. In the present study, we employed geometric morphometrics to examine the shape dynamics of raphid diatom frustules. An investigation was carried out to explore whether shape characteristics, such as circularity or asymmetry, and variation of valve outline, increase with decreasing cell size. Four monoclonal strains (*Luticola dismutica* strain 1, *L. dismutica* strain 2, *Navicula cryptocephala*, and *Sellaphora pupula*) were cultivated under stable conditions for two years in order to capture the complete range of cell sizes from initial to sexually competent cells. Shape changes and the pattern of shape change relative to size were quantified using geometric morphometrics. A quantitative shape analysis revealed similar allometric trends among the different strains and genera. With decreasing cell size, circularity of the valve outlines increased, that is, the complexity of the valves decreased. However, shape variation of valves within the populations increased with decreasing cell size. The levels of asymmetry did not change consistently throughout the size diminution phase. In two out of four strains, horizontal (dorsiventral) asymmetry was significantly lower than vertical (heteropolar) and transversal (sigmoid) asymmetries. The increasing morphological variation in clonal strains was likely caused by an accumulation of structural deviations during morphogenesis. In this respect, this is a specific example of the structural inheritance of morphological characteristics, which is naturally related to the peculiar vegetative life cycle of the diatoms.

Keywords: *allometry, geometric morphometrics, life cycle, raphid diatoms, plasticity*

Introduction

Diatoms are ubiquitous unicellular algae with a unique morphology. The siliceous cell wall (frustule) of diatoms consists of two complementary valves. In simple terms, the epivalve fits over the hypovalve in the same way as a lid fits over a bottom of a Petri dish. When the cell divides, new valves and bands develop inside the original valves. Therefore, the old hypovalve becomes the epivalve of the new frustule. It is apparent that, over time, this process leads to mean cell size diminution in a clonal population. MacDonald (1869) and Pfitzer (1869) each independently described this peculiarity, and it is now known as the MacDonald–Pfitzer hypothesis (Kociolek & Stoermer 2010). Even though there are mechanisms to avoid it (Lewis 1984, Edlund & Stoermer 1997), most diatom species appear to break out of the size diminu-tion via sexual reproduction. According to Geitler (1932), the condition necessary for initiating the sexual process is reaching a minimum cell size. This so-called *first cardinal point* of the diatom life cycle is defined as a size at which the cells can be induced to become gametangia. In pennate diatoms, this is typically when cell size is around 30–40% of the maximum size (Drebes 1977). The *second cardinal point* is reached after sexual reproduction occurs (Geitler 1932). At this point, cells restore themselves to the largest size they can achieve during their life cycle. Enlargement occurs through auxospore formation, a special zygote in which the initial epivalve and hypovalve develop. The new valves are formed below the surface of the auxospore. Therefore, initial cells have a rather differ-ent morphology to typical vegetative cells. Interestingly, cells that contain initial valves discontinue dividing after a few divisions and disappear from the population (Edlund & Stoermer 1997). The vegetative cell division phase of a population can take several years or even decades (Round et al. 1990). As the population mean approaches the minimum cell size, some cells miss the opportunity for sexual reproduction and continue to divide vegetatively, and, as a result, continue to diminish in size. These extremely small cells are often teratological and their pervalvar axis is several times greater than that in the normal vegetative cells (Geitler 1932). They are not viable under natural conditions but they can survive for a while in culture (Geitler 1932).

The unique characteristic of the diatom life cycle is that, unlike other organisms, their mean body (cell) size (in a clone) decreases over time. During this period, non-proportional shape change of the diatom frustule outline has been described (Geitler 1932, Tropper 1975, Theriot & Ladewski 1986, Cox 1993, Schmid 1994, Edlund & Stoermer 1997, Mann & Chepurnov 2005, Veselá et al. 2009, English & Potapova 2012). As the number of cell divisions increases, cells of a number of species lose undulations and their outlines become more elliptical. In centric diatoms, the ratios of various elements change as the cell diameter changes (Theriot et al. 1988). These shifts can be con-

nected to a loss of taxonomically important characteristics (Schmid 1994), and species determination may be difficult (Rhode et al. 2001, Pappas & Stoermer 2003, Fránková et al. 2009). Populations at different size diminution stages in the life cycle can also be misinterpreted as different species (Cox 1986, Rose & Cox 2014). The size diminution during the vegetative phase of the life cycle presumably affects the metabolism of the cells. Geitler (1932) proposed that the size influences protoplast organization. According to Schmid (1994), 'the ratio of the volume of the nucleus, cytoplasm, and vacuole also changes, leading to the physiological and subsequently the morphological heterogeneity of a clonal population' (Schmid 1994). Schmid (1994) also noted that 'during the vegetative cell division phase, the epivalves serve as a mold for the newly synthetized hypo-valves'. Therefore, some inaccuracies that arise during morphogenesis can be passed on to the next generation.

In past decades, numerous diatomists have focused on this phenomenon. Geitler's monograph (1932) contains comprehensive, qualitative observations of the diatom life cycle in both natural and laboratory conditions, and is a pioneering study in the field. More recently, researchers have used various quantitative methods for capturing the shape dynamics of diatom valves, such as the regression of the width and length (Tropper 1975), the Legendre shape analysis (Theriot & Ladewski 1986, Rhode et al. 2001, Pappas & Stoermer 2003, Mann et al. 2004), and the Fourier analysis (Mou & Stoermer 1992, Pappas et al. 2001). Landmark-based geometric morphometrics were found to be inadequate for diatoms at first, because they lack homologous points (Mou & Stoermer 1992). For studying landmark-poor outlines, Bookstein (1997) introduced a sliding semi-landmark method. After the usual translating, scaling, and rotating landmarks, the semi-landmarks are slid along the outline until they match the curve between two corresponding points as accurately as they can (Adams et al. 2004). The Procrustes superimposition, based on semi-landmarks, has been established in a wide range of biological studies. With respect to diatoms, the semi-landmark method was used to explore morphological variability within the *Achnanthidium minutissimum* species complex (Potapova & Hamilton 2007). The landmark-based shape analysis was employed to study the morphology and ontogenetic allometric trends of several taxa in the genus *Surirella* (English & Potapova 2012). Recently, it was also used to compare the ontogenetic allometric trajectories of valve outline and several other continuous variables with respect to the diagnoses of three species of *Pinnunavis*, a raphid genus allied to *Pinnularia* and *Navicula* (Edgar et al. 2015).

In the present study, landmark-based geometric morphometrics are used for exploring the patterns of shape variability and for the quantification of allometric and non-allometric shape changes of raphid diatoms cultivated under laboratory conditions. Our aim was to describe and quantify the general patterns of the shape dynamics connected to the diatom life cycle. In this sense,

our study continues Geitler's (1932) approach, except that we used modern methods of quantitative shape analysis that were unavailable in his time. According to qualitative observations (Round et al. 1990, Mann 1999), the valve outline becomes simpler with the increasing number of vegetative cell divisions, and so our aim was to quantify the relation-ship of valve complexity and valve size. Our hypothesis was that, throughout the asexual life cycle, valve complexity decreases as valve size decreases. We assumed that the morphological variation within populations and the asymmetry of valves would increase due to the gradual accumulation of developmental inaccuracies during valve morphogenesis. We measured the complexity, dis-parity, and asymmetry of the valves within clonal popula-tions in relation to valve size. Rather than species-specific patterns, we attempted to look for trends that are similar across different genera of commonly occurring raphid diatoms, in order to identify the general laws involved in the morphological dynamics of the diatom valve.

Materials and methods

Cultivation and microscopy

Four monoclonal strains of raphid diatoms, obtained from Prof. A. Poulíčková, Palacký University Olomouc, were used in this study. The strains examined were *Luti-cola dismutica* (Hustedt) D. G. Mann (strains LUTM 59 and LUTM 48, [Poulíčková 2008]), *Navicula cryptocephala* Kützing, and *Sellaphora pupula* (Kützing) Mereschkowsky. All the strains were homothallic, so they undergo sexual reproduction within a monoclonal culture.

All four strains were cultivated from November 2009 to October 2011 to capture the entire size range of the cells throughout the life cycle. The strains were cultivated in liquid WC medium (Andersen 2005), at 18°C in 7 cm diameter Petri dishes, illuminated at 40 μmol m^{-2} s^{-1} from 18 W cool fluorescent tubes (Phillips TLD 18W/33). The medium was replaced every week in order to avoid exhaustion of nutrients. Once every month, approximately 10% of the cells were transplanted to new Petri dishes in order to avoid overcrowding of cells. Every two months, samples were taken from the cultures and processed for the light microscopy analysis. The valves were cleaned in beakers by oxidation with 35% hydrogen peroxide and several crystals of potassium dichromate for 15 minutes, fol-lowed by several washings with distilled water (Poulíčková 2008). The clean valves were then mounted in Naphrax, as described in Poulíčková & Mann (2006). The cultures were sampled until the complete range of valve sizes was captured and the auxosporulation and size restoration were observed.

Micrographs of 50 valves from each permanent slide (i.e. a sample corresponding to a certain life-cycle stage in a culture) were obtained using an Olympus BX-51 light microscope fitted with an Olympus Z5060 digital camera. The digital micrographs were compiled in Adobe Photoshop CS3 ver. 10.0 and a number of valves were randomly chosen for statistical analyses. Size groups were used only for the analysis of partial disparity (i.e. morphological variability) in different stages of the life cycle and were determined based on the intervals of 10% of the maximal valve length (Table 1).

Strain	Size group % from the biggest cell length	Size group designation	Number of specimens	Size range (µm)
Luticola 1	100–90%	1	25	41.0–36.9
	90–80%	2	25	36.8–32.8
	80–70%	3	25	32.7–28.7
	70–60%	4	25	28.6–24.6
	60–50%	5	24	24.5–20.5
	50–40%	6	25	20.4–16.4
Luticola 2	100–90%	1	20	38.9–35.0
	90–80%	2	25	34.9–31.2
	80–70%	3	25	31.1–27.3
	70–60%	4	25	27.2–23.4
	60–50%	5	25	23.3–19.5
	50–40%	6	24	19.4–15.6
	40–30%	7	25	15.5–11.7
Navicula	100–90%	1	25	46.6–42.0
	90–80%	2	25	41.9–37.3
	80–70%	3	25	37.2–32.6
	70–60%	4	25	32.5–27.9
	60–50%	5	25	27.8–23.6
Sellaphora	100–90%	1	25	38.7–34.8
	90–80%	2	25	34.7–30.9
	80–70%	3	25	30.8–27.1
	70–60%	4	25	27.0–23.2
	60–50%	5	25	23.1–19.3

Table 1. The size group delimitation, designation of size groups, number of specimens in size groups, and a size range of size groups in µm.

Statistical analysis

Geometric morphometric analyses were performed using the TPS-series software (Rohlf 2013). The shapes of the valves were registered in TpsDig, ver. 1.45. In total, 32 landmarks were positioned along the valve outline. Four landmarks were in fixed positions (nos 1–4: intersection of the valve outline with the apical and transapical axes) and the remaining 28 landmarks were allowed to slide along the outline between the fixed landmarks (5–11; 12–18; 19–25; and 26–32).

The valves of all four strains were symmetrized along both the apical and the transapical axes. This was because left–right valve orientation could not be clearly determined from the micrographs, which focused primarily on the valve outline. Due to the symmetrization, the asymmetric component of shape variation was eliminated from the data, and except for the decomposition of the symmetric and asymmetric components of the shape variability, subsequent analyses were performed on symmetric configurations (Klingenberg et al. 2002).

The Procrustes superimposition was conducted in TpsRelw, ver. 1.46. Following that, the thin-plate spline analysis, based on tangent space projections (Bookstein 1997, Zelditch et al. 2004), was performed. Principal component analysis (also called the relative warp analysis) of partial warps and uniform components was conducted for each strain separately in TpsRelw, ver. 1.46. The first two relative warps were plotted against each other in order to illustrate the shape changes among cells in the individual strains. Deformation grids based on the thin-plate spline interpolation (Zelditch et al. 2004) represented the margins of the realized morphospace on a particular warp in each strain. To capture the size-to-shape patterns of individual strains, we conducted multiple regressions of shape coordinates using a quarter of the symmetric coordinates (landmarks 1; 3; 5–11) on centroid size (Klingenberg 1996) in TpsRegr, ver. 1.36.

The complexity of 2D valve outlines was expressed as 1-circularity. In other words, the more the outline deviated from the shape of a circle, the lower the value of circularity (Osserman 1978). The isoperimetric quotient, evaluating circularity of outlines, is defined as $Q = 4\pi A/P^2$, where A is area enclosed by perimeter P. Thus, Q may be maximally equal to 1.0, attained when the shape is a circle (Osserman 1978). Perimeter (P) was counted as a sum of Euclidean distances between neighbouring landmarks along the out-line in the configurations of 32 landmarks and A was then estimated as an area of a polygon formed by the landmarks. The relationship between circularity and valve size (centroid size) was tested using polynomial regression analysis in PAST, ver. 2.17c (Hammer et al. 2001).

To analyze morphological variability (disparity) of the valves, the Procrustes distances of individual objects from the reference forms were computed from landmark configurations (Foote 1993). The Procrustes distances were summed for each size group and in each strain separately using TpsSmall, ver. 1.20. The relationship between dis-parity and valve size (centroid size) was tested using polynomial regression analysis in PAST, ver. 2.17c (Hammer et al. 2001).

The following analyses were conducted in order to decompose the symmetric and asymmetric components of the shape variability. We applied the method described by Savriama & Klingenberg (2011) using nonsymmetrized landmark configurations. Valve outlines of the studied strains are symmetrical across two orthogonal axes, thus they are designated biradially symmetric.

Two perpendicular axes of symmetry were used to partition the configuration into four parts. The studied dataset consisted of the original configurations and the relabelled configurations reflected along the transapical axis, apical axis and the transapical + apical axes (Savriama et al. 2010, Neustupa 2013). As a result, each specimen was characterized by four configurations and their average shape was perfectly symmetrical (Savriama & Klingenberg 2011). The combined dataset consisted of 4 × 149 = 596 *L. dismutica* 1 objects, 4 × 169 = 676 *L. dismutica* 2 objects, 4 × 125 = 500 *N. cryptocephala* objects, and 4 × 125 = 500 *S. pupula* objects. The principal component analysis (PCA) of the original and the rotated/relabelled configurations yields components that clearly separate individual segments of the asymmetric variation (Savriama & Klingenberg 2011). In objects with a biradially symmetric arrangement, the asymmetric variation can be decomposed into three components, namely asymmetry along the apical axis (vertical asymmetry, heteropolar cells), asymmetry along the transapical axis (horizontal asymmetry, dorsiventral cells) and asymmetry along the transversal axis (transversal asymmetry, sigmoid cells), (Fig. 1).

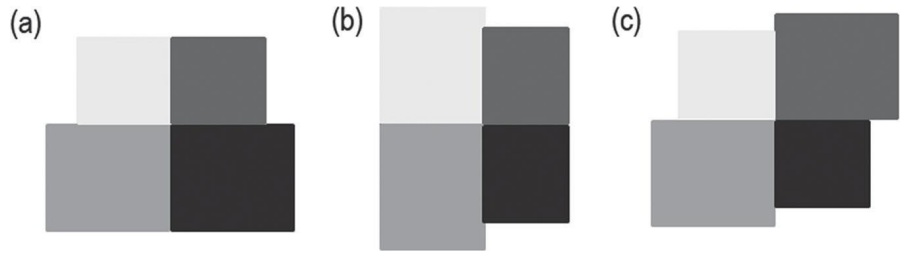

Figure 1. Symmetry transformations. (a) vertical (heteropolar) type; (b) horizontal (dorsiventral) type; (c) transversal (sigmoid) type. Apical axis of cells corresponds to the y-axis.

In this study, the quantities of asymmetry in individual asymmetric components were assessed by using a separate set of PCAs of the four configurations originating from each object (the original and the three reflected/relabelled configurations). PCAs were based on the variance–covariance matrices of the Procrustes aligned coordinates. Each PCA yielded three axes, illustrating three asymmetrical components. The absolute values of the scores of the original configuration on each of these three components were used as measurements of the asymmetrical variation in each cell. The generalized Procrustes analysis (GPA) and PCA were conducted in package *shapes* ver. 1.0.9 (Dryden & Mardia 1998) in R ver. 2.13.0 (R Development Core Team 2011). Separately, relative pro-portions of individual asymmetrical components in each cell were assessed as percentages of the explained variation spanned by the individual PC axes. The Friedman test and *post hoc* pairwise comparisons (Wilcoxon's test) were used to evaluate differences among values of asymmetrical components acquired from individual valve landmark configurations of individual strains. The

resulting data on the absolute and relative asymmetric variation, in all studied strains, were used to assess differences among the cells. The relationship between centroid size and asymmetry values was tested using the polynomial regression analysis in PAST, ver. 2.17 (Hammer et al. 2001).

Results

During the vegetative cell division phase of the life cycle, the valve sizes of all four strains changed significantly. The valve size in *Luticola* 1 decreased to 40–50%, in *Luticola* 2 to 30–40% (Fig. 2), in *Navicula* to 50–60%, and in *Sellaphora* to 50–60% from the original size (Table 1). The change in valve size was accompanied by a parallel change in the shape of the valves. The multi-variate regression analysis of the shape coordinates on centroid size revealed that size diminution accounted for the notable proportions of the overall shape variations present in all four strains (Table 2). The regression models explained 67% of the total variation in *Luticola* 1, 83% in *Luticola* 2, 66% in *Navicula* and 70% in *Sellaphora*, respectively.

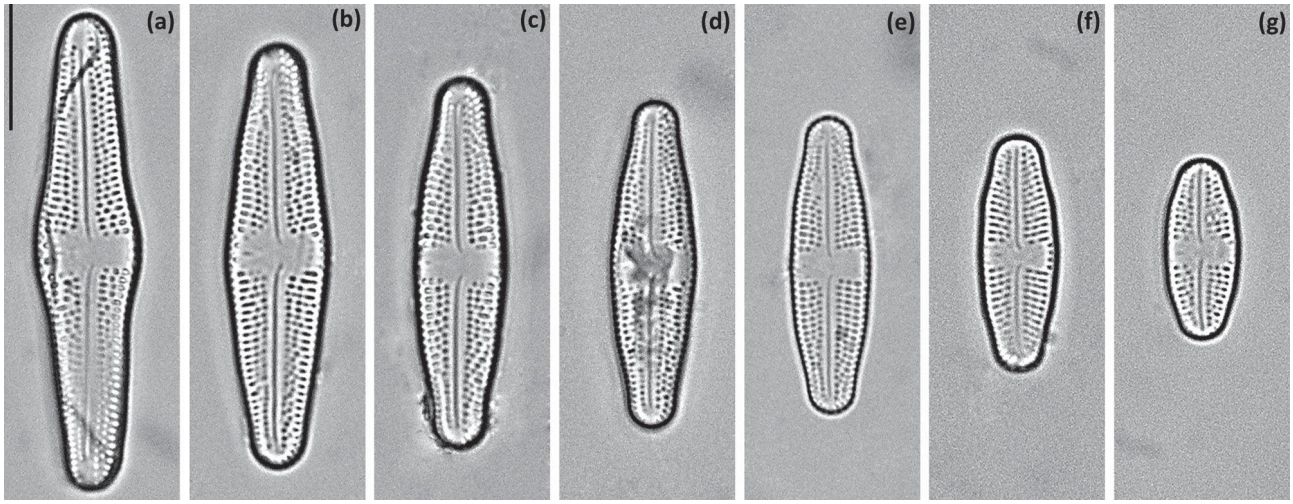

Figure 2. Representative cells in the size diminution series of *Luticola* 2 strain. Each cell falls into a single-size group (sg). (a) sg 1; (b) sg 2; (c) sg 3; (d) sg 4; (e) sg 5; (f) sg 6; and (g) sg 7. Scale bar = 10 μm.

Strain	RWA (% of explained variation by individual RWs)		Shape-size regression		
	RW1	RW2	% explained	Wilks' lambda	*p*-Value
Luticola 1	98.70	0.73	67.00	0.12	< .001
Luticola 2	99.04	0.57	83.00	0.06	< .001
Navicula	96.98	1.54	66.00	0.29	< .001
Sellaphora	99.25	0.40	70.00	0.11	< .001

Table 2. The relative warps analyses and the multivariate regression of shape coordinates on centroid size.

The RW1 scores of the cells from each strain represented the ontogenetic allometric trends throughout the vegetative cell division phase (Figs 3–6). RW 1 axes in all ordinations were strongly dominated with respect to described variation. They accounted for more than 95% of variability in all four strains. RW 1 corresponded to the roundness of the valves in all four strains, while the second relative warp (RW2) corresponded to the broadness and roundness of the poles relative to the whole valve. Despite these common characteristics, differing shape patterns were identified in each strain. The valve outline shape variability, along RW1 in both *Luticola* strains, varied between an elongated shape with a swollen central part and an elliptical shape with a tapered central part (Figs 3– 4). Along RW2, the valve outline varied between valves with rounded apical parts and swollen central part, and valves with a lanceolate shape. In the *Navicula* strain, RW1 corresponded to the width of valves and RW2 cor-responded to the width of the apical parts (Fig. 5). In the *Sellaphora* strain, the valve shape varied between an elongated elliptical shape and rounded shape along the RW. RW2 corresponded to the variability between valves with rounded apices and straight central parts, and elliptical valves with narrower apices and rather convex central parts (Fig. 6).

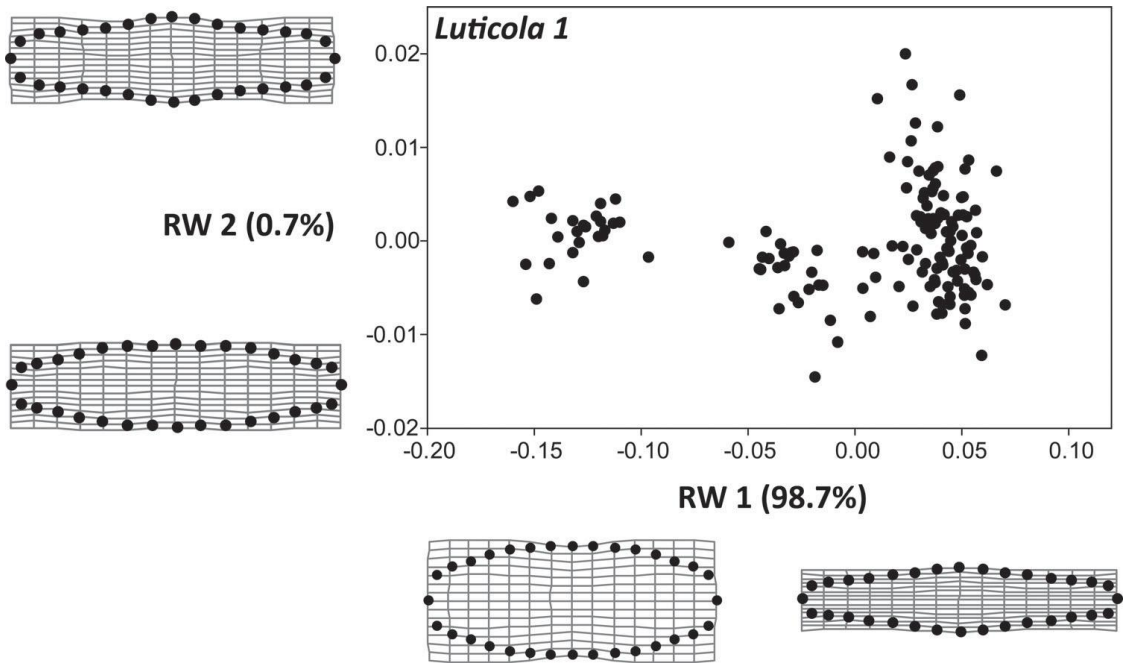

Figure 3. Ordination plot of the second (RW2) vs. first (RW1) relative warps in the strain *Luticola* 1 representing the shape differences between the valves. Thin-plate splines represent the margins of the realized morphospace on a particular warp.

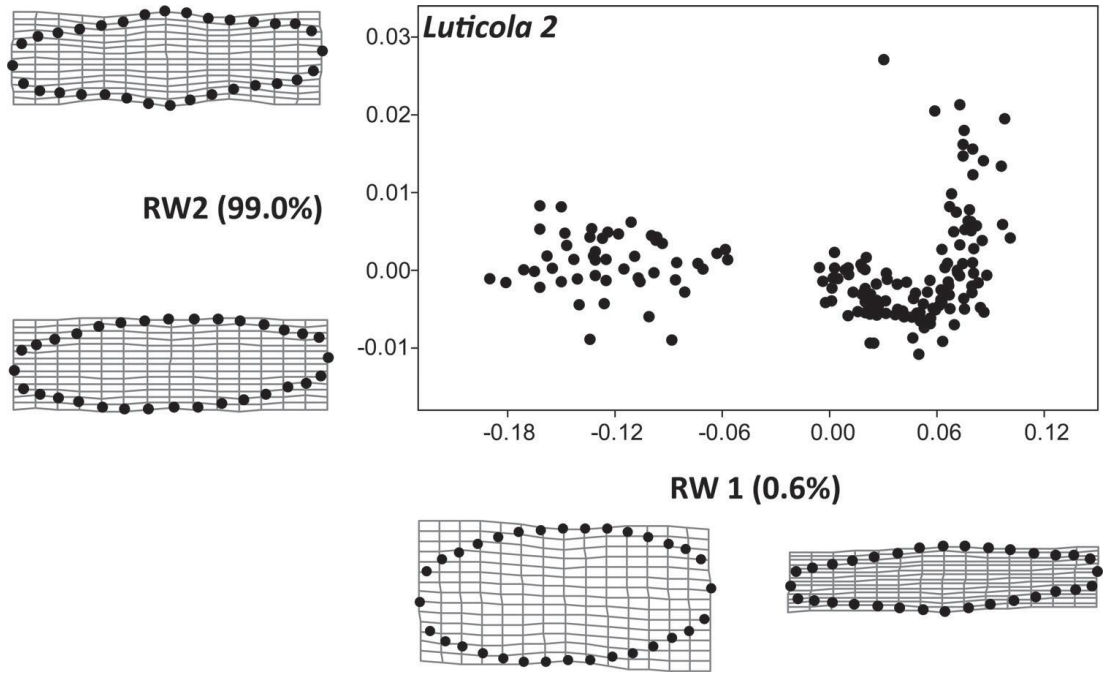

Figure 4. Ordination plot of the second (RW2) vs. first (RW1) relative warps in the strain *Luticola* 2 representing the shape differences between the valves. Thin-plate splines represent the margins of the realized morphospace on a particular warp.

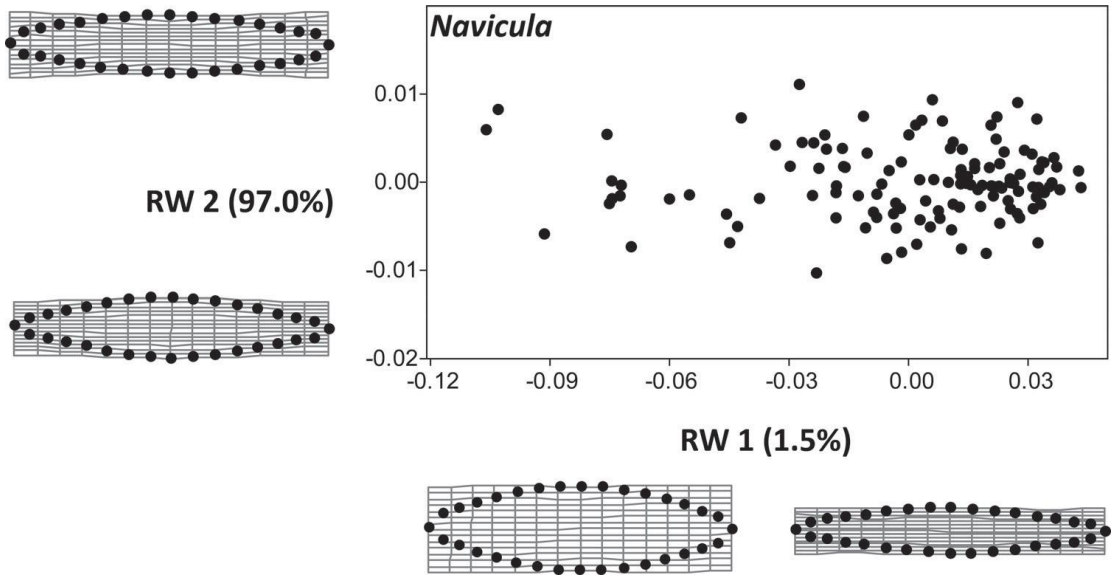

Figure 5. Ordination plot of the second (RW2) vs. first (RW1) relative warps in the strain *Navicula* representing the shape differences between the valves. Thin-plate splines represent the margins of the realized morphospace on a particular warp.

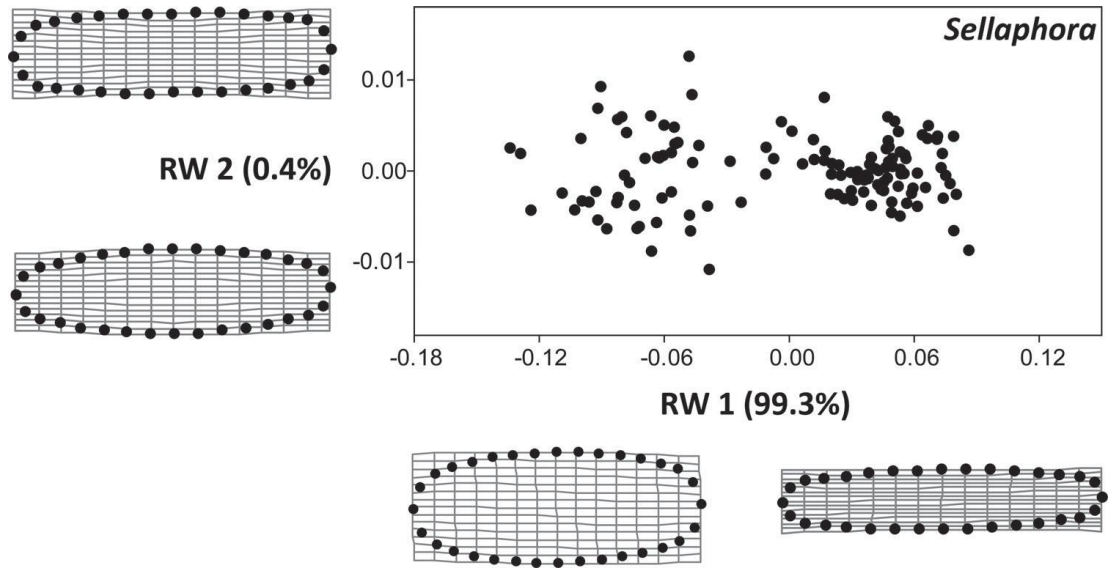

Figure 6. Ordination plot of the second (RW2) vs. first (RW1) relative warps in the strain *Sellaphora* representing the shape differences between the valves. Thin-plate splines represent the margins of the realized morphospace on a particular warp.

The analyses of circularity in all four strains favoured a second-order polynomial rather than a linear fit (Table 3). In all four strains, the circularity increased with decreasing size. In *Luticola* 2, *Navicula*, and *Sellaphora*, the minimum circularity values occurred in the biggest valves and the circularity then increased and the maximum values were reached in the smallest valves. However, in *Luticola* 1, circularity had the lowest values in the intermediate stages of the life cycle. Then, this parameter increased (i.e. frustule shape complexity increased) in smaller valves (Fig. 7). The *Sellaphora* strain presented the most gradual increase in circularity in comparison to the other strains.

The disparity analysis also favoured the second-order polynomial fit in all strains except *Luticola* 1, in which neither the linear nor the second-order polynomial regression models were significant. In the remaining three strains, the results of the second-order polynomial regression were significant (Table 3). In these three strains, the disparity increase reached its maximum in the smallest valves (Fig. 8).

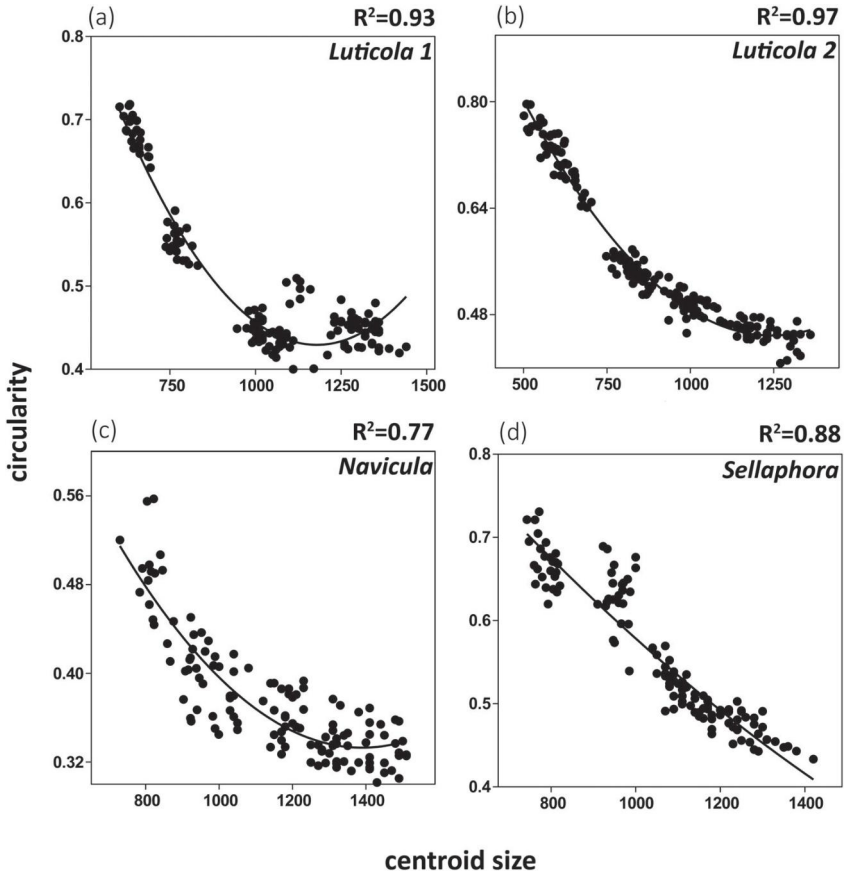

Figure 7. Jitter plot of second-order regression of circularity versus centroid size. Circularity increases with decreasing size in a nonlinear manner. (a) *Luticola* 1; (b) *Luticola* 2; (c) *Navicula*; and (d) *Sellaphora*.

Table 3. The regression analyses of asymmetry, disparity, and circularity versus centroid size.

		First-order regression			Second-order regression		
Strain	Type of analysis	R^2	p-Value	F	R^2	p-Value	F
Luticola 1	horizontal asymmetry	0.06	< .01	9.34	0.09	< .001	6.91
	vertical asymmetry	0.02	n.s.	3.68	0.02	n.s.	1.83
	transversal asymmetry	0.07	< .01	10.98	0.07	< .01	5.50
	disparity	0.0005	n.s.	0.08	0.0005	n.s.	0.04
	circularity	0.70	< .001	338.78	0.93	< .001	943.88
Luticola 2	horizontal asymmetry	0.001	n.s.	0.17	0.07	< .01	5.81
	vertical asymmetry	0.06	< .01	11.07	0.07	< .01	6.49
	transversal asymmetry	0.08	< .001	13.58	0.08	< .001	7.18
	disparity	0.16	< .001	32.47	0.25	< .001	27.05
	circularity	0.88	< .001	1160.9	0.97	< .001	2956
Navicula	horizontal asymmetry	0.04	< .05	5.26	0.05	n.s.	2.87
	vertical asymmetry	0.06	< .01	7.10	0.13	< .001	9.24
	transversal asymmetry	0.12	< .001	16.16	0.16	< .001	11.51
	disparity	0.30	< .001	50.89	0.35	< .001	32.73
	circularity	0.67	< .001	248.88	0.8	< .001	204.63
Sellaphora	horizontal asymmetry	0.07	< .01	9.10	0.10	< .01	6.56
	vertical asymmetry	0.13	< .001	18.86	0.13	< .001	9.36
	transversal asymmetry	0.08	< .01	10.19	0.08	< .01	5.19
	disparity	0.12	< .001	16.75	0.13	< .001	8.86
	circularity	0.87	< .001	856.57	0.88	< .001	433.31

The asymmetry of landmark configurations did not change explicitly in relation to valve size. The differences among the size groups typically described only small proportions of variation in the observed values of valve asymmetry. Nevertheless, several regression analyses of each component of asymmetric variability showed a non-random linear (vertical asymmetry in *Sellaphora*) or quadratic (vertical and transversal asymmetries in *Navicula* and horizontal asymmetry in *Luticola* 1 and 2) relation-ship with centroid size (Table 3). However, the coefficients of determination (R^2) were low, especially in comparison with analyses of the relationship of partial disparity or circularity and the size group rank, and the trends were not uniform, that is, some components of asymmetry increased and some decreased in relation to centroid size in the same strain. The Friedman tests of differences between the individual types of asymmetry within the strains were significant in *Luticola* 2 ($p < .05$) and *Sellaphora* ($p < .001$) strains. In both, the horizontal (dorsiventral) asymmetry component was significantly lower than both remaining components (Fig. 9). In the other two strains, the asymmetric patterns corresponding to heteropolar, dorsiventral, and sigmoid transformations of the ideally symmetric body plan were approximately equal.

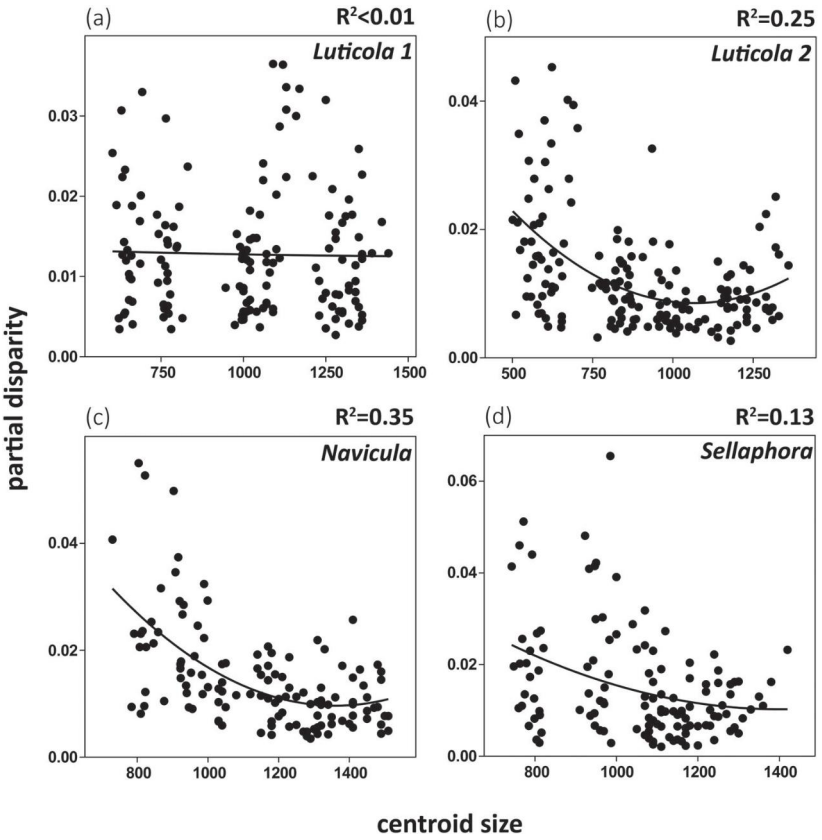

Figure 8. Jitter plot of second-order regression of tangent Procrustes distances of individual cells to centroids of their respective size groups versus centroid size. Shape variability (disparity) increases with decreasing size. (a) *Luticola* 1; (b) *Luticola* 2; (c) *Navicula*; and (d) *Sellaphora*.

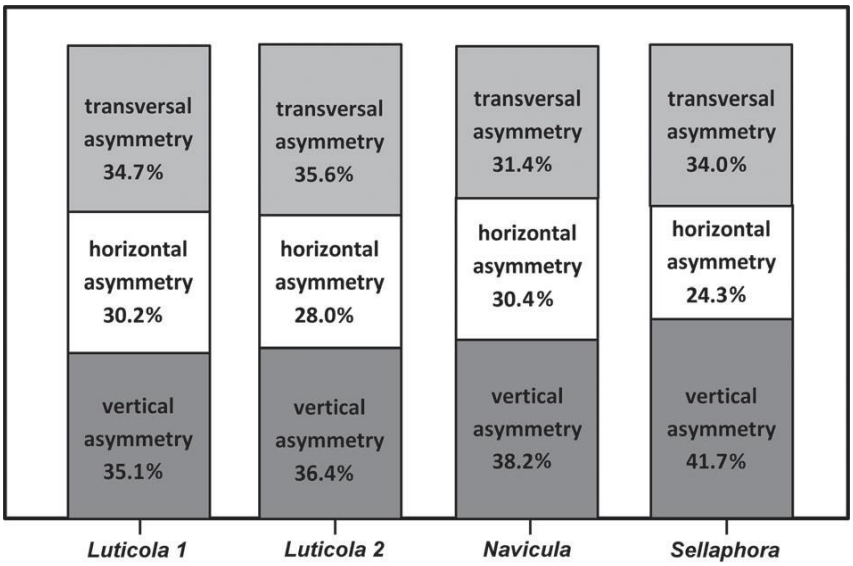

Figure 9. The proportions of individual types of asymmetry within the strains. Vertical asymmetry – heteropolar type; horizontal asymmetry – dorsiventral type; and transversal asymmetry – sigmoid type.

Discussion

A quantitative shape analysis revealed similar ontogenetic allometric trends among the different strains and genera. In all four strains, valve outline complexity decreased as the number of vegetative cell divisions increased and was at its lowest at the end of the vegetative cell division phase. In other words, the smaller the cells of the studied strains were, the more circular their outlines were. Although there were similarities between the strains, there were also differences in their life cycles and shape dynamics. In particular, both *Luticola* strains exhibited patterns different from the other strains. According to our observations, cell size restoration in *Navicula* and *Sellaphora* strains occurred when the cells reached 50–60% of their original size. However, both *Luticola* 1 and *Luticola* 2 initiated sexual reproduction when they reached 40–50% and 30–40% of their original sizes, respectively (Poulíčková & Mann 2006, Poulíčková 2008**)**. The initial cells of *Luticola* resemble the shape of their auxospores with a typical central swelling (Poulíčková 2008). These centrally swollen initial cells become narrower after a few divisions, as reported by Geitler (1932). The specific rounded shape of the initial cells may explain the high circularity that occurs in the biggest size group (Fig. 7). On the other hand, the initial and post-initial cells of the *Navicula* cells do not exhibit any swelling, despite their centrally swollen auxospore (Poulíčková & Mann 2006). Consequently, the circularity was the lowest in the biggest size group (Fig. 7). *Sellaphora* cells do not have any swelling of the auxospores or the initial cells (Mann 1989), and the circularity values in all five size groups were consistent with this.

It has been proposed that size can influence the physical conditions of a cell's internal environment and the organization of its organelles (Geitler 1932, Schmid 1994). As the space inside the frustule decreases, the viscosity, surface tension, and pressure increase (Geitler 1932). The surface-to-volume (S-to-V) ratio of isometrically scaled objects increases with decreasing size. In other words, the cell volume decreases more rapidly than the surface (Thompson 1917). However, the cell size diminution in pennate diatoms is accompanied by allometric shape changes of the cells (Geitler 1932). According to our results, cell shape simplifies with an increasing number of cell divisions, so the change in the S-to-V ratio is probably not that profound. The S-to-V ratio may be influenced by the possible changes in cingulum height throughout the vegetative cell division phase. Geitler (1932) mentioned that there is no strong correlation between cell length and cingulum height. According to his observation, cingulum height may even increase slightly as cell length decreases (Geitler 1932). Geitler's hypotheses are supported by a morphometric study of *Diatoma moniliformis* (Kützing) D. M. Williams populations in natural conditions (Potapova & Snoeijs 1997). According to the above-mentioned authors, a decrease in the apical axis is inevitable;

however, the transapical and pervalvar axes can be modified, especially because the diatom girdle is much more flexible than the thecae. Thus, we conclude that potential changes in cingulum height may contribute to a deceleration of the S-to-V ratio of the studied strains throughout the vegetative cell division phase.

Even though cell complexity of the populations decreased during the size diminution phase, disparity (shape variability) increased. Given the genetic homogeneity of our strains, this pattern could not be ascribed to any hypothetical shifts between different genotypes producing different morphologies during the vegetative cell division phase. Conversely, the observed disparity patterns within the clonal populations should be treated as specific examples of structural inheritance (Jablonka & Raz 2009). According to the qualitative observations based on light and electron microscopy, diatom parental cells serve as a mould for the circumferential outline of newly formed hypothecae during vegetative cell division. Consequently, some slight morphological deviations can be passed on to other generations (Crawford 1981, Schmid 1986, Schmid 1994). This could explain the pattern of increasing phenotypic plasticity in our strains, namely the accumulating inaccuracies resulting in shape variety within a population. We propose that the observed, consistent increase in morphological disparity of the studied populations might illustrate a more general pattern exhibited by diatom populations that results from their unique mechanism of cell wall morphogenesis and vegetative inheritance.

Our test of asymmetry components and their contribution to the overall asymmetry revealed that, in two out of four strains (*Luticola* 2 and *Sellaphora*), the horizontal (dorsiventral) asymmetry was significantly lower than the other components. In the remaining strains, the differences between the asymmetry components were not significant, that is, the asymmetric components in these strains were balanced. This is strikingly different from the pattern in desmids (Savriama et al. 2010, Neustupa 2013), another microalgal group with complex cellular symmetry. These charophyte algae possess cell halves (semi-cells) that form at different times and therefore can form under different environmental conditions. Thus, their asymmetric variation is dominated by upper–lower shape differences, which highlights the contrast between the semi-cells. The silica deposition process in diatoms is not simultaneous but sequential (Mann 1981). The raphe system is deposited first on one side of the valve (the primary side) and then on the other (the secondary side).When the last part of the raphe is defined, two discontinuities remain (Voigt discontinuities), (Mann 1981). Despite these irregularities, we did not detect any signal in our data that would indicate increased left–right asymmetry (i.e. differences between the primary and secondary sides of the valve).

During the vegetative cell division phase of the life cycle, the level of asymmetry remained rather constant. In contrast to increasing disparity, asymmetry did not change consistently in

relation to size. The slight asymmetry of the valves can therefore be considered an intrinsic property of diatom cell morphology, regardless of the number of preceding vegetative cell divisions. The decomposition of individual segments of asymmetry was conducted following a modified protocol based on Savriama et al. (2010) and Savriama & Klingenberg (2011). As in these studies, as well as in Neustupa (2013) and Savriama et al. (2015), it was based on the general Procrustes superimposition of the symmetry group formed by the transformations of the original configurations of the landmarks spanning the outline of the valves. Thus, in a biradially symmetric 2D object, such as the pennate diatom valve, there were four symmetry transformations forming the symmetry group (Klingenberg 2015).

However, our asymmetry analysis differed from those mentioned above because it always considered one con-figuration at a time. Thus, the Procrustes superimposition was conducted separately for each set of the original and the transformed configurations of the landmarks describing the shape properties of a single valve. This approach is very similar to general protocols described by Zabrodsky et al. (1992, 1995) and Graham et al. (2010) for the analysis of the amounts of continuous symmetry in configurations defined by a set of homologous points. Klingenberg (2015) pointed out that this approach, while mathematically correct, has no way of distinguishing fluctuating and directional asymmetry. However, in unicellular organisms with biradially symmetrical cells, the repeated parts are usually unsigned, that is, their left and right, or top and bottom cellular halves cannot be distinguished (Fránková et al. 2009, Savriama et al. 2010, Neustupa 2013). This is also the case for many diatoms and, therefore, our analysis was based on the decomposition of the total cellular asymmetry into three segments that correspond to the bending of the horizontal and vertical axes of valve symmetry. However, it did not use the concepts of fluctuating and directional asymmetry. Zabrodsky et al. (1992, 1995) used their methodology in chemistry, for the identification of the different types of symmetry optimally fitting a set of points, such as positions of individual atoms in a molecule. In fact, this is also applicable to diatom valves, as a way of looking for the best fitting form of valve asymmetry. Given different evolutionary or ecological hypotheses, an analysis of the proportions of the asymmetric variation corresponding to the heteropolar, dorsiventral, and sigmoid patterns in individual cells may be of interest.

Additionally, another difference between the one-by-one asymmetry decomposition used in this study and the joint Procrustes analysis of large sets of the original and the transformed configurations is the elimination of the entirely symmetric variation that typically describes the among-individual variances (Savriama et al. 2010, Neustupa 2013). The joint Procrustes approach typically assigns large proportions of the total variation to a variation that is identical in all repeated parts, but differs among the individuals. This segment of variation inherently increases in relation to

the size of the dataset and, thus, in relation to its total morphological variability. Therefore, the joint Procrustes approach would not allow for the quantitative comparison of the asymmetric variations among datasets with different numbers of individuals, such as those acquired in different studies or experimental designs.

As shown elsewhere (Potapova & Hamilton 2007, Veselá et al. 2009, English & Potapova 2012, Edgar et al. 2015), geometric morphometrics has a great potential for application in various areas of diatomology (for detailed review see Pappas et al. 2014). It enables a researcher to quantify and analyse slight morphological differences that cannot be captured by microscopic observation. The geometric morphometric techniques can reveal distinct differences between morphs in diatom samples that were traditionally assigned to single species (Van de Vijver et al. 2013). Traditional measurements may be biased by the omnipresent size diminution, which can outweigh the shape differences. On the other hand, geometric morphometrics studies size-free variation, and thus it is possible to discriminate between two species at different stages of their vegetative life cycle (Veselá et al. 2009). The shape changes related to size can even serve as a signal when exploring diatom species diversity because different species can have dissimilar allometric trajectories (English & Potapova 2012). As illustrated in this study, shape variability and dynamics in clonal populations can be used to explore phenotypic plasticity and its evolutionary implications. The morphological variation and asymmetry of diatom valves at the population level can be studied in relation to environmental conditions or stress factors (Potapova & Hamilton 2007). Thus, diatoms, with their rigid silica frustules, are ideal model organisms for quantitative morphometric studies focused on free-living cells.

Acknowledgements

The author is grateful to Prof. Aloisie Poulíčková for providing four strains of raphid diatoms used in this study. The author also thanks the anonymous reviewers of Diatom Research and the editor, Dr. Eileen J. Cox, for their critical comments on the manuscript that had led to significant improvements of the final text.

Funding

The study was funded by the Faculty of Science of the Charles University in Prague. The English language and style corrections were made by Editage.

References

ADAMS D.C., ROHLF F.J. & SLICE D.E. 2004. Geometric morphometrics: ten years of progress following the 'revolution'. *Italian Journal of Zoology* 71: 5–16.

ANDERSEN R.A. (Ed.). 2005. *Algal culturing techniques*. Elsevier Academic Press, London. 578 pp.

BOOKSTEIN F.L. 1997. *Morphometric tools for landmark data: geometry and biology*. Cambridge University Press, Cambridge. 436 pp.

COX E. J. 1986. Some Taxonomic and Ecological Considerations of Morphological Variation within Natural Populations of Benthic Diatoms Considérations taxonomiques et écologiques sur les variations morphologiques de diatomées benthiques en populations naturelles. In: *8th Diatom-Symposium*, *Paris 1984* (Ed. by M. Ricard), pp. 163-172. O. Koeltz, Koenigstein.

COX E. J. 1993. Diatom systematics—a review of past and present practice and a personal vision for future development. *Beihefte zur Nova Hedwigia* 106: 1-20.

CRAWFORD R.M. 1981. Some considerations of size reduction in diatom cell walls. In: *Proceedings of the 6th International Diatom Symposium* (Ed. by R. Ross), pp. 253–265. O. Koeltz, Koenig-stein.

DREBES G. 1977. Sexuality. In: *The biology of diatoms* (Ed. by D. Werner), pp. 250-283. University of California Press, Berkeley, California.

DRYDEN I.L. & MARDIA K.V. 1998. *Statistical analysis of shape.* John Wiley & Sons, New York. 347 pp.

EDGAR R. K., SALEH A. I. & EDGAR, S. M. 2015. A morphometric diagnosis using continuous characters of *Pinnunavis edkuensis*, *sp. nov.* (Bacillariophyta: Bacillariophyceae), a brackish-marine species from Egypt. *Phytotaxa* 212: 1-56.

EDLUND M.B. & STOERMER E.F. 1997. Ecological, evolutionary, and systematic significance of diatom life history. *Journal of Phycology* 33: 897–918.

ENGLISH J.D. & POTAPOVA M.G. 2012. Ontogenetic and interspecific valve shape variation in the Pinnatae group of the genus *Surirella* and the description of *S. lacrimula* sp. nov. *Diatom Research* 27: 9–27.

FOOTE M. 1993. Contributions of individual taxa to overall morphological disparity. *Paleobiology* 19: 403–419.

FRÁNKOVÁ M., POULÍČKOVÁ A., NEUSTUPA J., PICHRTOVÁ M. & MARVAN P. 2009. Geometric morphometrics – a sensitive method to distinguish diatom morphospecies: a case study on the sympatric populations of *Reimeria sinuata* and *Gomphonema tergestinum* (Bacillariophyceae) from the River Bečva, Czech Republic. *Nova Hedwigia* 88: 81–95.

GEITLER L. 1932. Der Formwechsel der pennaten Diatomeen (Kieselalgen). *Archiv fur Protistenkunde* 78: 1–226.

GRAHAM J. H., RAZ S., HEL-OR, H. & NEVO E. 2010. Fluctuating asymmetry: methods, theory, and applications. *Symmetry 2*: 466-540.

HAMMER O., HARPER D.A.T. & RYAN P.D. 2001. PAST: Paleontological statistics software package for education and data analysis. *Palaeontologia Electronica* 4: 9. http://palaeo-electronica.org/2001_1/past/issue1_01.htm

JABLONKA E. & RAZ G. 2009. Transgenerational epigenetic inheritance: prevalence, mechanisms, and implications for the study of heredity and evolution. *The Quarterly Review of Biology* 84: 131–176.

KLINGENBERG C. P. 1996. Multivariate allometry. In *Advances in Morphometrics* (Ed. by L. F. Marcus), pp. 23–49. Plenum Press, New York.

KLINGENBERG C. P. 2015. Analyzing fluctuating asymmetry with geometric morphometrics: concepts, methods, and applications. *Symmetry* 7: 843–934.

KLINGENBERG C.P., BARLUENGA M. & MEYER A. 2002. Shape analysis of symmetric structures: quantifying variation among individuals and asymmetry. *Evolution* 56: 1909–1920.

KOCIOLEK J.P. & STOERMER E.F. 2010. Variation and polymorphism in diatoms: the triple helix of development, genetics and environment. A review of the literature. *Vie et Milieu* 60: 75–87.

LEWIS JR. W.M. 1984. The diatom sex clock and its evolutionary significance. *American Naturalist* 123: 73–80.

MACDONALD J.D. 1869. On the structure of diatomaceous frustule, and its genetic cycle. *Annals and Magazine of Natural History* 3: 1–8.

MANN D.G. 1981. A note on valve formation and homology in the diatom genus *Cymbella*. *Annals of Botany* 47: 267–269.

MANN D.G. 1989. The diatom genus *Sellaphora*: separation from *Navicula*. *British Phycological Journal* 24: 1–20.

MANN D. G. 1999. The species concept in diatoms. *Phycologia* 38: 437–495.

MANN D.G., MCDONALD S.M., BAYER M.M., DROOP S.J.M., CHEPURNOV V.A., LOKE R.E., CIOBANU A. & DU BUF J.M.H. 2004. The *Sellaphora pupula* species complex (Bacillariophyceae): morphometric analysis, ultrastructure and mating data provide evidence for five new species. *Phycologia* 43: 459–482.

MANN D.G. & CHEPURNOV V.A. 2005. Auxosporulation, mating system, and reproductive system in *Neidium* (Bacillaiophyceae). *Phycologia* 44: 335–350.

MOU D. & STOERMER E.F. 1992. Separating *Tabellaria* (Bacillariophyceae) shape groups based on Fourier descriptors. *Journal of Phycology* 28: 386–395.

NEUSTUPA J. 2013. Patterns of symmetric and asymmetric morphological variation in unicellular green microalgae of the genus *Micrasterias* (Desmidiales, Viridiplantae). *Fottea* 13: 53–63.

OSSERMAN R. 1978. The isoperimetric inequality. *Bulletin of the American Mathematical Society* 84: 1182–1238.

PFITZER E. 1869. Über den Bau und die Zellteilung der Diatomeen. *Botanische Zeitung* 27: 774–776.

PAPPAS J.L., FOWLER G.W. & STOERMER E.F. 2001. Calculating shape descriptors from Fourier analysis: shape analysis of *Asterionella* (Heterokontophyta, Bacillariophyceae). *Phycologia* 40: 440–456.

PAPPAS J.L. & STOERMER E.F. 2003. Legendre shape descriptors and shape group determination of specimens in the *Cymbella cistula* species complex. *Phycologia* 42: 90–97.

PAPPAS J. L., KOCIOLEK J. P. & STOERMER E. F. (2014). Quantitative morphometric methods in diatom research. *Nova Hedwigia, Beiheft* 143: 281-306.

POTAPOVA M. & SNOEIJS P. 1997. The natural life cycle in wild populations of *Diatoma moniliformis* (Bacillariophyceae) and its disruption in an aberrant environment. *Journal of Phycology* 33: 924–937.

POTAPOVA M. & HAMILTON P.B. 2007. Morphological and ecological variation within the *Achnanthidium minutissimum* (Bacillariophyceae) species complex. *Journal of Phycology* 43: 561–575.

POULÍČKOVÁ A. 2008. Morphology, cytology and sexual reproduction in the aerophytic cave diatom *Luticola dismutica* (Bacillariophyceae). *Preslia* 80: 87–99.

POULÍČKOVÁ A. & MANN D.G. 2006. Sexual reproduction in *Navicula cryptocephala* (Bacillariophyceae). *Journal of Phycology* 42: 872–886.

R DEVELOPMENT CORE TEAM. 2011. R: A language and environment for statistical computing. R Foundation for Statistical Computing, Vienna. https://www.r-project.org/foundation/

RHODE K.M., PAPPAS J.L. & STOERMER E.F. 2001. Quantitative analysis of shape variation in type and modern populations of *Meridion* (Bacillariophyceae). *Journal of Phycology* 37: 175–183.

ROHLF F.J. 2013. *TPS software series*. Department of Ecology and Evolution, State University of New York, Stony Brook.

ROUND F.E., CRAWFORD R.M. & MANN D.G. 1990. *The Diatoms: Biology and Morphology of the Genera*. Cambridge University Press, Cambridge. 131 pp.

SAVRIAMA Y., NEUSTUPA J. & KLINGENBERG C.P. 2010. Geometric morphometrics of symmetry and allometry in *Micrasterias rotata* (Zygnemophyceae, Viridiplantae). *Nova Hedwigia* 136: 43–54.

SAVRIAMA Y. & KLINGENBERG C.P. 2011. Beyond bilateral symmetry: geometric morphometric methods for any type of symmetry. *BMC Evolutionary Biology* 11: 280.

SAVRIAMA Y., STIGE L. C., GERBER S., PÉREZ T., ALIBERT P. & DAVID B. 2015. Impact of sewage pollution on two species of sea urchins in the Mediterranean Sea (Cortiou, France): Radial asymmetry as a bioindicator of stress. *Ecological Indicators* 54: 39–47.

SCHMID A.M. 1986. Organization and function of cell structures in diatoms and their morphogenesis. *In: Proceedings of the 8th International Diatom Symposium* (Ed. by M. Ricard), pp. 271–292. O. Koeltz, Koenigstein.

SCHMID A.M. 1994. Aspects of morphogenesis and function of diatom cell walls with implications for taxonomy. *Protoplasma* 181: 43–60.

THOMPSON D'ARCY W. 1917. *On growth and form*. Cambridge University Press, Cambridge. 793 pp.

THERIOT E. & LADEWSKI T.B. 1986. Morphometric analysis of shape of specimens from the neotype of *Tabellaria flocculosa* (Bacillariophyceae). *American Journal of Botany* 73: 224–229.

THERIOT E., HÅKANSSON H. & STOERMER E.F. 1988. Morphometric analysis of *Stephanodiscus alpinus* (Bacillariophyceae) and its morphology as an indicator of lake trophic status. *Phycologia* 27: 485–493.

TROPPER C.B. 1975. Morphological variation of *Achnanthes hauckiana* (Bacillariophyceae) in the field. *Journal of Phycology* 11: 297–302.

VAN DE VIJVER B., MORAVCOVA A., KUSBER W.H. & NEUSTUPA, J. 2013. Analysis of the type material of *Pinnularia divergentissima* (Grunow in Van Heurck) Cleve (Bacillariophyceae). *Fottea* 13: 1-14.

VESELÁ J., NEUSTUPA J., PICHRTOVÁ M. & POULÍČKOVÁ A. 2009. Morphometric study of *Navicula* morphospecies (Bacillariophyta) with respect to diatom life cycle. *Fottea* 9: 307–316.

ZABRODSKY H., PELEG S. & AVNIR D. 1992. Continuous symmetry measures. *Journal of the American Chemical Society* 114: 7843–7851.

ZABRODSKY H., PELEG S. & AVNIR D. 1995. Symmetry as a continuous feature. *Pattern Analysis and Machine Intelligence, IEEE Transactions on* 17: 1154–1166.

ZELDITCH M.L., SWIDERSKI D.L., SHEETS H.D. & FINK W.L. 2004. *Geometric morphometrics for biologists*. Elsevier Academic Press, New York. 443 pp.

3. Morphometric Asymmetry of Frustule Outlines in the Pennate Diatom *Luticola poulickovae* (Bacillariophyceae)

[published as Woodard, K. & Neustupa, J. (2016). Morphometric asymmetry of frustule outlines in the pennate diatom *Luticola poulickovae* (Bacillariophyceae). Symmetry, 8: 150.]

Abstract

Side orientation of cells is usually ambiguous in unicellular organisms, making it impossible to separate components of directional asymmetry (DA) and fluctuating asymmetry (FA). However, frustules of the diatom *Luticola poulickovae* have biradially symmetric outlines, and their central areas bear ornamentation that is asymmetric across the apical axis. The goal of this study was to explore differentiation of morphometric asymmetry across the apical axis into DA and FA components. Is there detectable DA of the valve outlines of two *L. poulickovae* strains that may be related to the asymmetric central areas? Given that the life cycle of diatoms involves cell-size diminution, and cell shape is strongly affected by allometry, we also explored the question of whether asymmetry is correlated with cell size. The extent of symmetric variation among individuals in each strain, as well as DA and FA across the apical axis, were quantified using two Procrustes ANOVA models. The results revealed no correlation of either total asymmetry or FA with valve size. DA was significant and considerably more pronounced than FA in both strains, indicating that there is previously unknown systematic asymmetry of valve outlines of *L. poulickovae*, which may be related to the asymmetry of its central area.

Keywords: *biradial symmetry; fluctuating asymmetry; directional asymmetry; diatoms; frustule*

Introduction

Cellular shapes of algae often involve various complex types of morphological symmetry, which may include bilateral symmetry, such as in the two-dimensional projections of cells of the green algal genera *Pediastrum*, *Sorastrum*, and their relatives [1,2], or in the giant cells of the ulvophycean marine seaweeds of the genus *Halimeda* [3]. However, in most cases, the cells of unicellular algae and protists have multiple symmetric parts arranged along several axes of symmetry. A biradial arrangement of cells with two orthogonal axes of symmetry is typical for the desmids (i.e., members of the green algal order Desmidiales) such as the genera *Micrasterias*, *Euastrum*, and *Cosmarium* [4–6]. In addition, multiple rotational or translational symmetric arrangements are present in various filamentous microalgae, foraminiferan shells, and radiolarian skeletons [7].

One of the key attributes of symmetric morphologies exhibited by unicellular organisms is the ambiguity of their side orientation, such that the up/down and left/right sides are interchangeable, which renders fixed side assignment of individual symmetric parts impossible [1,6–9]. This makes most unicellular symmetric structures fundamentally different from those of multicellular organisms, such as animals and vascular plants. Morphometric analysis of symmetry and asymmetry of cells with side ambiguity, thus, cannot involve decomposition of asymmetric variation into directional asymmetry (DA) and fluctuating asymmetry (FA). DA represents the systematic difference of the shape coordinates between two sides of a structure (i.e., left/right, up/down), or in other words, it is constant deviation of one side compared to the other. FA refers to random individual shape differences between the sides after DA has been taken into account [10,11]; thus, DA is essentially a property of a sample, whereas FA can be quantified for each specimen under study. Separation of DA and FA is of great importance to the shape analysis of symmetric structures in clonal populations, as it is a key step that allows for distinction between systematic asymmetry, which is genetically fixed and heritable, and developmental instability [10,12]. In samples formed by clonal organisms, such as microalgal strains, FA inherently relates to non-genetic factors, such as environmental stressors, and could be directly linked to their disturbing effects on developmental processes.

Because of the impossibility of assigning sides across the symmetric axes, assessments of the morphological asymmetry of most unicellular organisms are restricted to methods that separate symmetry from the asymmetric components, but without further differentiation into DA and FA. A method of object symmetry has been developed for studies of bilaterally symmetric structures in which the axis of symmetry is included within the structure itself and separates left and right sides

as halves of a same structure. This method involves a joint morphospace comprising the original and reflected shape configurations that fill up the symmetry group constituted by the structure under study [11,12]. Individual axes of that morphospace (such as the principal components) then describe either entirely symmetric variation or individual patterns of asymmetry, which can, however, only be quantified as the total asymmetry of a particular type [5,12].

The diatoms (Bacillariophyceae) are a group of peculiar, mostly unicellular organisms with unusually complex patterns of morphological symmetry of their surface structures. A shell called the frustule, which is composed primarily of SiO_2 and consists of two halves (the epitheca and the hypotheca), surrounds the cell. The slightly smaller and younger half is formed following the vegetative binary division of a cell; during the formation of the younger half, the remaining epitheca serves as a mold for the synthesis of the new half [13]. In a series of successive vegetative divisions, this leads to a cell size reduction in a population. During this cell size diminution, the nucelar/cytoplasmic ratio changes, as well as the surface/volume ratio. This might influence the "cellular activity and developmental potential" [14,15] resulting in different cell division rates in different size classes and therefore nonlinear distribution of cell sizes in a population [14,15]. This cytological heterogeneity might also lead to subsequent morphological heterogeneity in a population [13]. Cells that attain a species-specific critical size as a result of numerous vegetative divisions typically transform into gametes and reproduce sexually. Vegetative cells that then begin a new cycle again are in the upper size range of the species-specific interval [16]. Size reduction is typically accompanied by a change in the shape of the frustules [17–20], which leads to pronounced morphological allometry, a process typical of nearly every diatom population in natural habitats or cultured strains. Pappas et al. [19] recently reported that variation in the empirical morphospace of most pennate diatom species relates to allometry as a result of the size reduction that occurs over successive vegetative cell divisions. Interestingly, these authors also suggested that the second most important variation pattern usually involves the asymmetry of valve outlines.

Pennate diatoms, which belong to the subclasses Bacillariophycideae and Fragilariophycideae, compose the bulk of diatom diversity, forming a monophyletic crown group of the class [21]. Although their valves (i.e., the upper planes of the frustules) are usually elongated and bilaterally symmetric across the longitudinal (apical) axis [16], the basic outline of the valves is typically biradial, with a second, transapical axis of symmetry orthogonal to the apical axis. The most species-rich subclass, Bacillariophycideae, includes diatoms with raphe, a pair of fissures that typically run along the longitudinal axis of valves. In some genera—such as *Frustulia, Cavinula*, and *Mastogloia*—the raphe is generally straight and there are no visible departures from the biradial symmetry of the valve shape [22]. Conversely, there are several genera, such as *Cymbella* or

Encyonema, that feature distinctly curved, crescent-like valve outlines, and thus, in these genera there is a pronounced DA of the frustule outline across the longitudinal axis. Likewise, there are several genera with distinct DA across the transapical axis, such as *Gomphonema, Gomphoneis*, and *Didymosphaenia* [16]. In addition to asymmetry in valve outline, there may also be additional structures on the valve surface that further emphasize the pronounced DA in these diatom taxa; for instance, there are often one or several distinct isolated and asymmetrically located points, called stigmata, in the central area of the valves, the asymmetric position of which invariably corresponds to the asymmetry of the valve outline. Notably, there are also diatom genera with valve outlines that have traditionally been considered biradially symmetrical but with distinctly asymmetric internal structures, such as raphe endings and stigmata. These intriguing genera include *Sellaphora* and *Pseudofallacia*, the species of which are characterized by unilateral deflection of the distal raphe ends [22]. Likewise, the proximal raphe ends are unilaterally bent in species of the genera *Pinnularia* and *Muelleria* [22]. In addition, an asymmetric pair of stigmata is common to species within the genus *Placoneis*, and an asymmetrically positioned isolated punctum is typical of species of *Geissleria* [22]. On the other hand, the valves of *Neidium* have straight raphe but contain an asymmetric structure called the Voigt discontinuity that occurs always on the secondary valve side, which allows for differentiation between both sides of the valve across the apical axis. Species of the genus *Luticola* are typified by the presence of both unilateral deflection of the proximal raphe ends and by asymmetric stigma in the central area of the valves (Figure 1), features that unambiguously denote two sides of *Luticola* valve outlines across the longitudinal axis. The valves of the *Luticola*, as well as of the other above-mentioned genera, represent relatively rare examples of morphological symmetry with clearly assigned sides in unicellular organisms. As such, analyses of symmetric and asymmetric variation similar to those conducted for multicellular organisms may be possible by using these structures. Because of the consistently asymmetric position of stigma and proximal raphe ends, the "side" factor can be included as a fixed effect in a Procrustes ANOVA model and the asymmetric variation can then decomposed into components of DA and FA. Klingenberg [9], in a recent review of quantitative morphometric studies focusing on biological symmetry, demonstrated that slight but significant DA in shape has been detected in most multicellular model systems. Although the functional or evolutionary adaptive significance of DA in multicellular organisms remains unclear, it may be a non-adaptive byproduct of the distinctive DA of their internal morphology. This pattern may not be easily applicable to unicellular structures, such as the inorganic shells of diatoms that surround cells of several successive vegetative generations, but in diatoms with distinct DA of the central area of valves, such as species of

Luticola, the entire valve outline may also be systematically asymmetric in relation to the pattern of their central area.

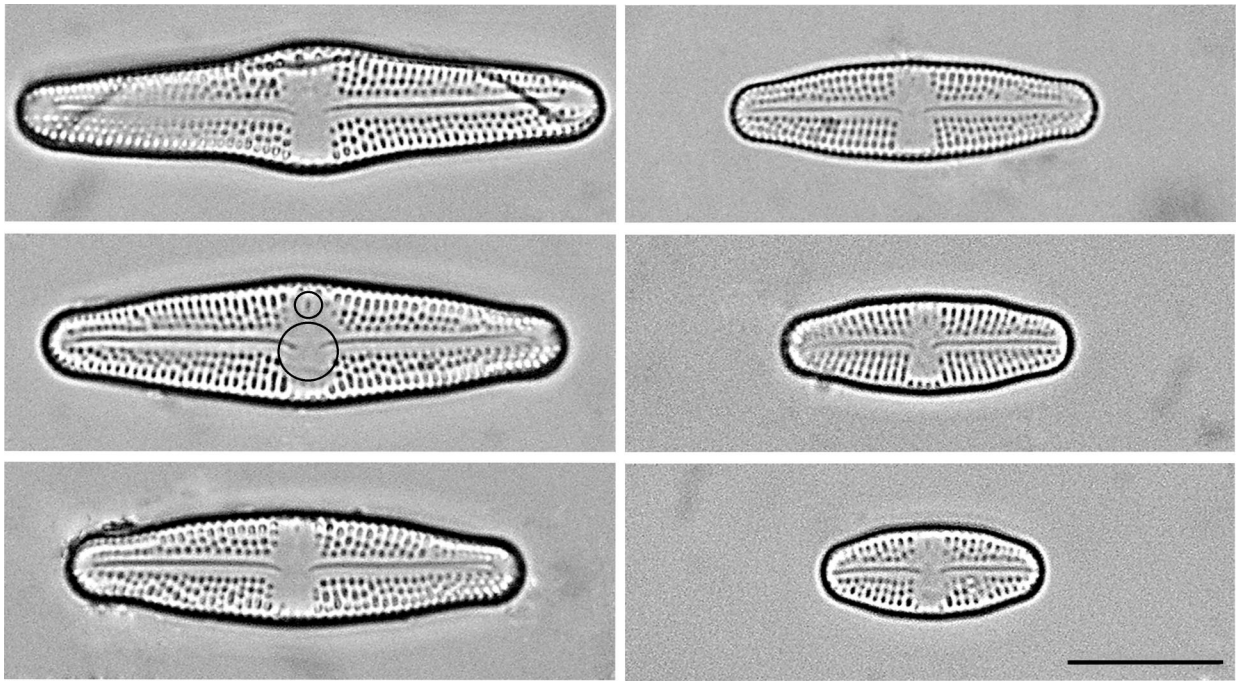

Figure 1. Representative cells in the size diminution series of *Luticola* 2 strain. Note the unilateral deflection of the proximal raphe ends and the asymmetrically positioned stigma in the central area of the valves (designated by circles). Scale bar for all figures = 10 μm.

To the best of our knowledge, FA and DA of diatom valve outline shapes have never been explicitly evaluated. Our study focused on the genus *Luticola*, and we asked the basic question of whether there is detectable DA of valve outline shape across the longitudinal axis with sides designated by the position of stigma and proximal raphe ends; if such asymmetry is detectable, it may suggest that the valve outline is morphogenetically related to the arrangement of the internal structures of frustules and cells. We also evaluated the degree of FA in valve shape across the longitudinal axis, to ascertain whether FA is significant when tested against the measurement error (ME), and how prominent this segment of asymmetry may be in relation to DA.

Shape variation of pennate diatoms is predominantly determined by allometric changes relating to size diminution of frustules [19,23], and therefore, we also examined the relationship between the DA and FA of valve outlines across the longitudinal axis and cell size. Does FA (or even DA) increase during successive vegetative divisions, thereby resulting in accumulating irregularities in the shape of the siliceous frustules? It has been shown that teratogenic

morphological asymmetry of diatom frustules in natural habitats is often related to chemical contamination, as well as resulting from physical stress factors [24], features that have been used in various biomonitoring and ecological surveys of freshwater and marine ecosystems [24–26]. Separation and quantification of FA, which is directly related to developmental instabilities from DA, which represents the systematic asymmetry of populations, might therefore be useful in environmental applications of diatom morphology.

Materials and Methods

Culturing and Data Acquisition

Two monoclonal strains of the raphid diatom *Luticola poulickovae* Levkov, Metzeltin & A. Pavlov (strains LUTM 59: Luticola 1; and LUTM 48: Luticola 2 [27]) were used in this study. Both strains were cultivated for over a year to capture the entire size range of the cells throughout the life cycle, as described in our previous study [23]. The strains were cultivated in liquid WC medium [28] at 18 °C in 7 cm diameter Petri dishes and illuminated by 18-W cool fluorescent tubes (Phillips TLD 18W/33, Amsterdam, The Netherlands). The medium was exchanged weekly to avoid nutrient depletion, and approximately 10% of the cells were transplanted to new Petri dishes monthly in order to avoid overcrowding. Samples were collected from the cultures and processed for light microscopy analysis every second month [23]. Permanent slides were made from the samples [27,29], with micrographs of 50 valves captured from each permanent slide (i.e., a sample corresponding to a certain life-cycle stage in a culture) using an Olympus BX-51 light microscope (Olympus Corporation, Tokyo, Japan) fitted with an Olympus Z5060 digital camera. The digital micrographs were compiled in Adobe Photoshop CS3 version 10.0 (Adobe Adobe Systems Incorporated, San Jose, CA, USA), and mixed together resulting in one set of micrographs for each strain containing a whole size range of the population. Then, valves were randomly chosen for statistical analyses (75 valves of *Luticola* 1, 72 valves of *Luticola* 2). The shapes of the valves were registered in TpsDig, version 2.26 [30]. In total, 100 landmarks were positioned along the valve outline. Two landmarks were in fixed positions (numbers 1 and 51: intersection of the valve outline with the apical axis), with the remaining 98 landmarks allowed to slide along the outline between the fixed landmarks (2–50; 52–100), (Figure 2).

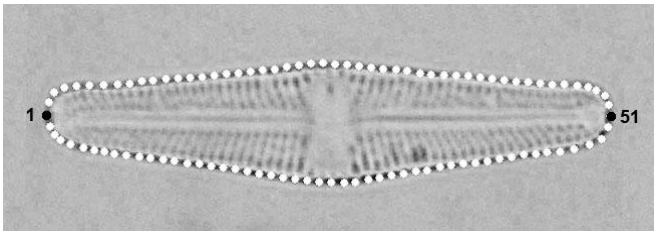

Figure 2. Position of landmarks. Two landmarks were in fixed positions (numbers1 and 51: intersection of the valve outline with the apical axis), with the remaining 98 landmarks allowed to slide along the outline between the fixed landmarks.

Geometric Morphometrics

The valves of *L. poulickovae* are symmetric according to two orthogonal axes, the longitudinal (apical) axis and the transapical axis. Asymmetry across the transapical axis, which was not examined in this study, was removed from the dataset by averaging the landmark and semi-landmark coordinates of the original and reflected/relabeled configurations [10]. Generalized Procrustes analysis (GPA) of this combined dataset also involved sliding the semi-landmarks depicting the outline shape of the valves. The locations of the individual semi-landmarks were optimized by minimizing the bending energy between the reference and target specimens [31], and empirical morphospaces of the averaged configurations in each strain were visualized using relative warps analysis with alpha set to zero, which yielded relative warps equivalent to the principal components of the principal component analysis (PCA) based on the tangent Procrustes coordinates. These analyses were conducted in TpsRelw, ver. 1.42 [30].

For the analysis of asymmetry across the longitudinal axis, we prepared the dataset of the original configurations, as well as those reflected across the symmetry axis of interest, and relabeled them accordingly. Amounts of symmetric variation among individuals, and the DA and FA in both datasets, were quantified and evaluated in two multivariate non-parametric Procrustes ANOVA models. The function "bilat.symmetry", implemented in package "geomorph" version 3.0.0 [32], was used in R 3.2.3 [33]. This function performed the Procrustes ANOVA of morphological symmetry; that is, the multivariate analysis of variance based on a matrix of tangent Procrustes distances among the original and reflected/relabeled configurations. In this analysis, variation was partitioned into several sources and designated as "individual", spanning shape differences among the valves; ‘side’, signifying DA, or the differences in the shapes of both symmetric halves across the longitudinal axis in each valve; their interaction "individual × side", which denoted FA, or the random fluctuations around the asymmetric mean in each valve; and ‘measurement error’, which illustrated the amount of variation spanned by digitization imprecision [10,34]. Contrary to the original description of Procrustes ANOVA of object symmetry spanned by the geometric

morphometric data, the number of degrees of freedom (*df*) is not obtained via multiplication of the number of landmarks and dimensions subtracted by those lost during GPA [32], as the distance-based Procrustes ANOVA implemented in the 'geomorph' package involves computation of *df* based on the actual number of observations instead; as such, variation is partitioned from the matrix of tangent Procrustes distances among the configurations. One advantage of this approach is that there are no limitations on using semilandmarks, which would otherwise yield incorrect *df* in the model. The *p*-values denoting the level of significance of the effects in the model are established by comparing the *F*-values for each factor to those obtained by 999 random permutation of the shape data (i.e., the rows of the data matrix) [32,35]. In addition, the *Z*-scores, defined as F_{obs}/σ_{Frand}, depict the effect sizes for each term of the model. The shape changes in valve outlines, corresponding to of DA and FA, were visualized by thin-plate splines in TpsRelw, ver. 1.42 and TpsSplin, ver. 1.20 [30]. The initial TPS grids were square in order to clearly illustrate the deformations [36]. For FA, the deformations of thin-plate splines were magnified four times, and for DA, the deformations were magnified 10 times.

Total asymmetry of individual valves across the longitudinal axis was computed as follows: the original and reflected/relabeled configurations were subjected to a joint PCA that yielded principal components that differentiated between the symmetric and asymmetric variation [5,12]. Then, total asymmetry of individual valves was computed as a sum of the absolute values of their scores on all the asymmetric principal components. Likewise, the amount of FA for each specimen was computed as the sum of the absolute values of scores on the principal components yielded by PCA of the FA shape coordinates resulting from the Procrustes ANOVA. These values were related to the centroid sizes of individual valves via linear correlation analyses in PAST ver. 2.17 [37].

Results

The RW 1 axes (Figures 3 and 4) accounted for more than 98% of variability in both strains. The valve shape along the RW 1 axis varied between narrow valve outlines with a broad, rounded central area and round outlines with less pronounced undulations, a trend that was similar in both strains. At the same time, the shape variation of the examined strains, described by RW2 and RW3, differed slightly; in *Luticola* 1, RW 2 (Figure 5) corresponded to asymmetry along the apical axis of the valves, whereas in *Luticola* 2 (Figure 6), this asymmetry was also accompanied by broadness of the central area of the valves. In *Luticola* 1, RW3 represented the variability of valve outlines with broad central areas, and outlines with relatively narrow central areas and round apical parts,

whereas in *Luticola* 2, the shape along RW 3 varied between valve outlines with broad and round central areas with relatively wide apical parts and outlines with straight, almost tapered central areas.

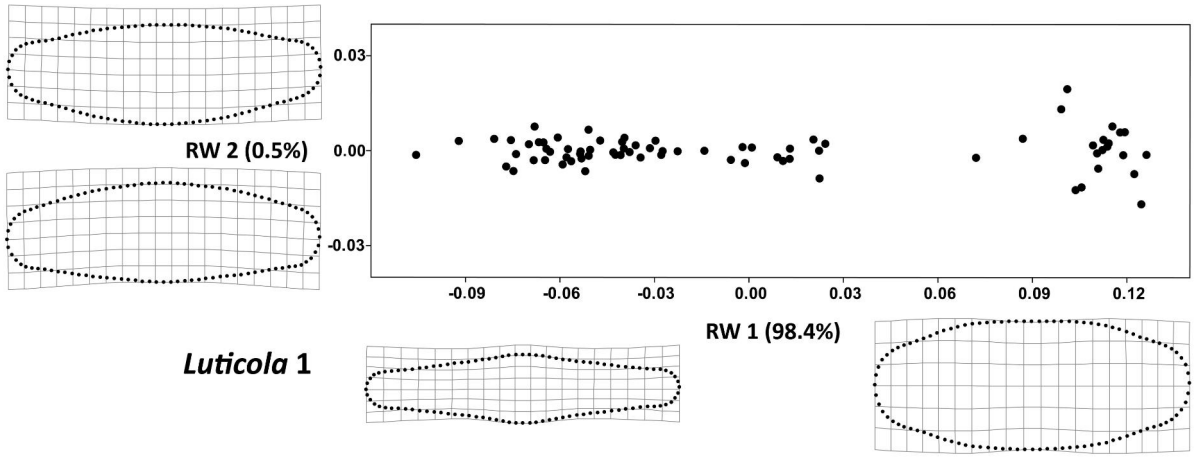

Figure 3. Total shape variability in the strain *Luticola* 1 during the size diminution phase of the life cycle represented by ordination plot of the first (RW 2) vs. second (RW 1) relative warp. Thin-plate splines represent the margins of the realized morphospace on a particular warp.

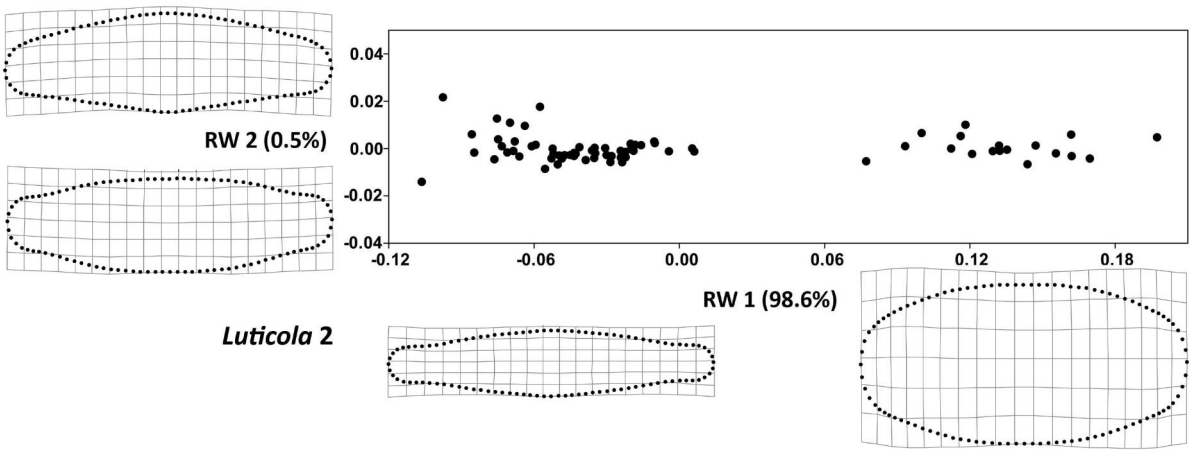

Figure 4. Total shape variability in the strain *Luticola* 2 during the size diminution phase of the life cycle represented by ordination plot of the first (RW 2) vs. second (RW 1) relative warp. Thin-plate splines represent the margins of the realized morphospace on a particular warp.

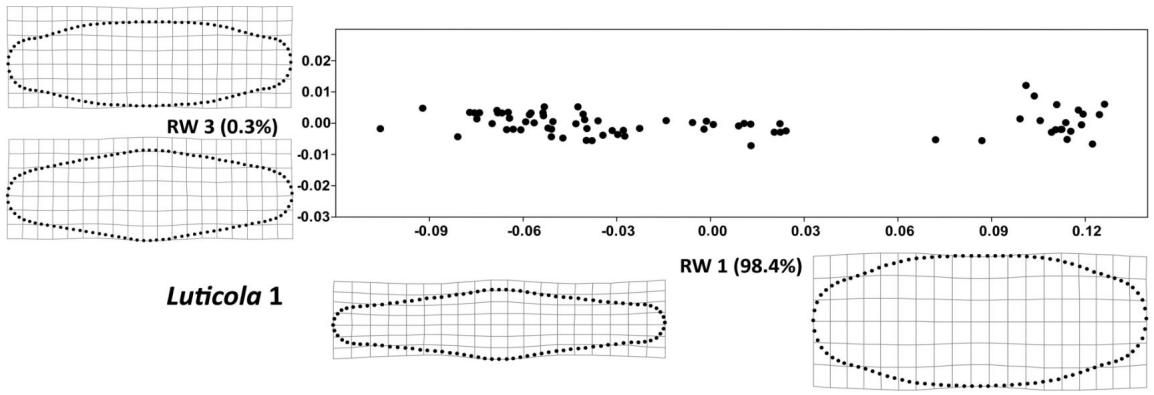

Figure 5. Total shape variability in the strain 1 during the size diminution phase of the life cycle represented by ordination plot of the RW3) second (RW1) relative warp. Thin-plate splines represent the margins of the realized a particular warp.

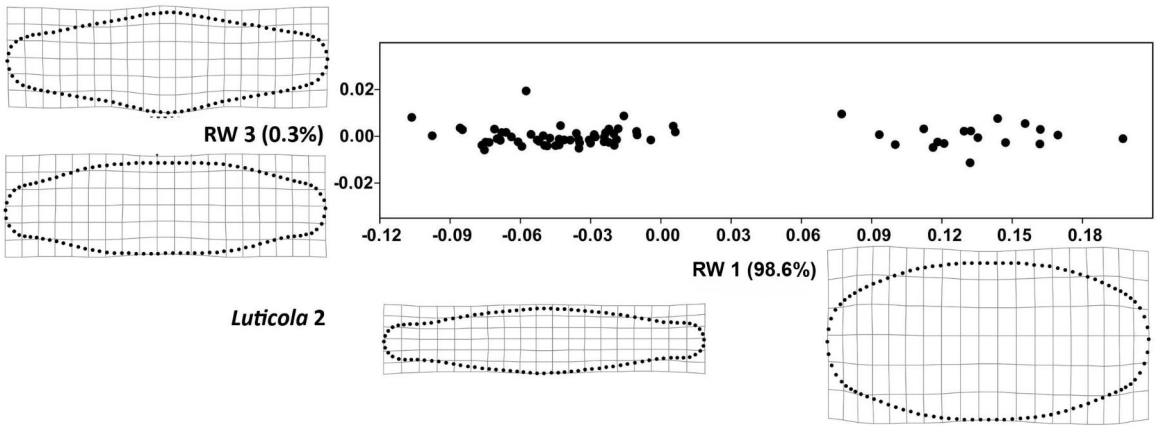

Figure 6. Total shape variability in the strain *Luticola* 2 during the size diminution phase of the life cycle represented by ordination plot of the third (RW3) vs. second (RW1) relative warp. Thin-plate splines represent the margins of the realized morphospace on a particular warp.

Both Procrustes ANOVA models yielded strikingly similar results (Table 1 and 2). The shape differences among individual valves were strongly significant and - by looking at the mean squares of individual effects - they were approximately 10 times larger than the asymmetry between both sides of the valves. However, DA still proved to be highly significant and considerably larger than the FA, spanned by the individual × side interaction. FA was relatively subtle, with mean squares about 11 and 19 times lower than for DA, and *Z*-scores approximately 7 and 11 times lower than for DA. In addition, FA was, on average, only ~2.7 times higher than ME, yet still yielded weakly significant random distributions of F-ratios, with *p*-values between 0.02 and 0.03. The FA shape trends were represented by magnified thin-plate splines. In *Luticola* 1, RW 1 represented curved valve outlines and RW 2 represented valves with undulated sides and broad apical parts. In

Luticola 2, the trends were similar, except that the undulation of the valves was more pronounced on the secondary valve side (with a stigma) and the apical parts were slightly curved (Figure 7).

Table 1. Results of Procrustes ANOVA evaluating symmetric and asymmetric variation in the strain *Luticola* 1.

Source	*df*	SS	MS	*F*	*Z*	*p*-Value
Individual	74	0.7385	0.009980	152.74	1.69	0.001
Side	1	0.0008	0.000749	11.47	8.39	0.001
Individual:Side	74	0.0048	0.000065	2.76	1.17	0.020
Measurement error	150	0.0036	0.000024	-	-	-
Total	299	0.7477	-	-	-	-

Table 2. Results of Procrustes ANOVA evaluating symmetric and asymmetric variation in the strain *Luticola* 2.

Source	*df*	SS	MS	*F*	*Z*	*p*-Value
Individual	71	0.9058	0.012757	184.88	1.68	0.002
Side	1	0.0013	0.001317	19.08	12.58	0.001
Individual:Side	71	0.0049	0.000069	2.72	1.16	0.027
Measurement error	144	0.0037	0.000025	-	-	-
Total	287	0.9157	-	-	-	-

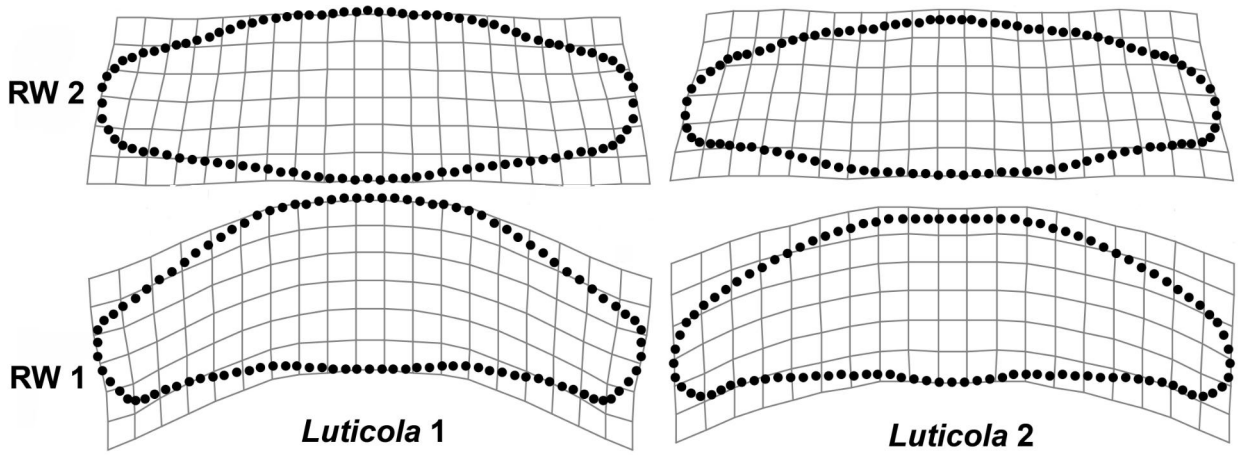

Figure 7. FA shape trends in the strains *Luticola* 1 and *Luticola* 2 represented by four times magnified thin-plate splines.

Systematic asymmetry of valve outlines, spanned by the DA effect in the Procrustes ANOVA models, was relatively similar in both populations. The actual shape trends were generally too subtle to be visible on the micrographs alone, but the magnified thin-plate splines showed that the central parts of the valves were asymmetrically bulged on the side of the proximal raphe ends deflection (Figure 8); moreover, the apical parts of the valves were slightly bent in the same direction, but this trend was rather less conspicuous in *Luticola* 1 than in *Luticola* 2. The opposite side of the valve outlines was straighter, and did not exhibit any distinctive bulges.

There were profound size variations within both datasets—the centroid size of the valves was reduced by 2.6 times in *Luticola* 1 and by 2.8 times in *Luticola* 2. This was mirrored by pronounced shape allometry, spanned by the first principal components of both PCAs of the original datasets. However, valve size was not significantly correlated with either total asymmetry or FA (Table 3). In *Luticola* 1, the relationship between centroid size and total asymmetry yielded a *p*-value only slightly above 0.05, but this analysis included a single outlying valve with a large centroid-size and total asymmetry values.

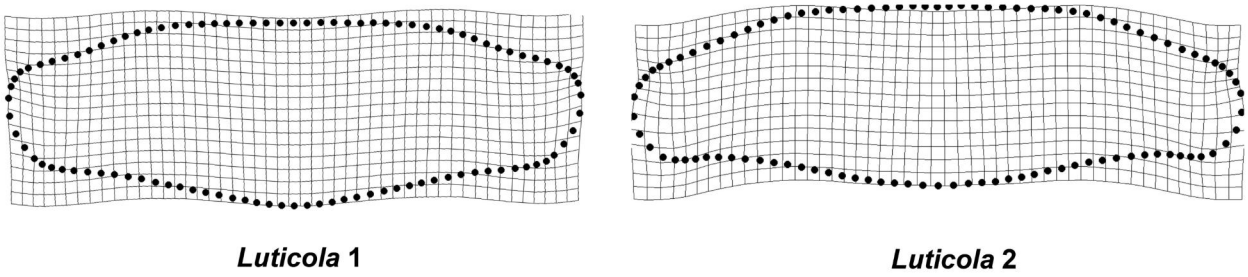

Figure 8. DA shape trends in the strains *Luticola* 1 and *Luticola* 2 represented by 10-times magnified thin-plate splines.

Discussion

Cell size declined markedly during the vegetative phase of the life cycle, and strong allometric effect caused profound shape differences between big and small cells [23]. This pattern was reflected in our Procrustes ANOVA models by components of symmetric variation among the cells (factor “individual”) that revealed highly significant variability in both populations. DA was strongly significant in both populations. Although this asymmetry is slight and cannot be unambiguously discerned via direct microscopic observation, it implies that valve outlines of *L. poulickovae* are systematically asymmetric with respect to the position of their stigma. Slight DA of *L. poulickovae* valve outlines may be related to the general pattern of diatom frustule morphogenesis; in raphid diatoms, the raphe system is deposited first on one side of the valve (the

primary side) and then on the other (the secondary side) [38], an irregularity that may affect the outline and result in DA of valves. Alternatively, it is possible that the observed DA of *Luticola* outline shape is related to the asymmetric central area, and thus genera in which such structures are absent should approximate "ideally" symmetric outline shapes with much more precision than *Luticola* species. As such, it would also be informative to examine whether systematic asymmetry between the left and right sides of the valve occurs in other raphid diatom species and genera, including those lacking any asymmetric structures in the raphe or central area but possessing distinct Voigt discontinuities (such as the genus *Neidium*), which could also be used for recognition of left and right sides of the valves. Conversely, although it is not possible to separate DA and FA in genera that lack distinctly asymmetric valve features, levels of total asymmetry can still be compared. Considering the predominance of DA in *L. poulickovae*, it is plausible to test whether species and genera with asymmetric central areas have consistently higher levels of total asymmetry than do species with symmetrical central areas. These analyses of total asymmetry could be based on PCA of the Procrustes-aligned configurations that form the symmetry group of the biradial object under study [6,12,39]. Specifically, a variant of this method that includes separate PCAs of the symmetry group for each cell would allow straightforward comparison of the datasets with different numbers of cells [23], an analysis closely related to the continuous symmetry measure introduced by Zabrodsky et al. [11,40,41].

Small but detectable levels of FA, indicative of developmental instability during the morphogenetic process, did not change with cell size. Relatively small sample sizes in analyses decomposing DA, FA, and ME in geometric morphometric studies typically lead to low FA estimates with respect to ME [9]. In addition, relatively low F-ratios for FA could have been produced by high ME, which has been affected by the quality of microphotographs and semilandmark placement along the outlines. Higher ME levels may be expected in geometric morphometric studies involving multiple semilandmarks [42] and this may worsen the FA estimates in datasets such as those used in the present study. In addition, FA estimates in analyses based on the mixed-model two-way Procrustes ANOVA may be confounded with antisymmetry [9,43], which cannot be considered as developmental instability. Therefore, application of the Procrustes methods based on registration of curves by semilandmarks for FA quantification may be fundamentally complicated by these issues. However, it should be mentioned that ME levels could possibly be significantly limited by using high-precision microphotographs; and F-ratios for FA could also be higher in analyses based on extensive datasets with high numbers of specimens [9].

Our study showed that total asymmetry was unchanged during the size-diminution period of the life cycle [23]. On the other hand, some studies suggest a possible increase of asymmetric valve

shape and ornamentation deviations with decreasing size [13–15,24]. Our previous study also showed a significant increase of shape variability in clonal populations with decreasing size which is supported by Schmid's [13] hypothesis that morphological inaccuracies during diatom morphogenesis are passed on to next generations, and that their number and magnitude increases during the vegetative phase of the life cycle. However, this above-mentioned increase in variance apparently remained within the symmetric component of the shape variability and therefore the levels of FA and DA were uncorrelated with cell size. On the other hand, independence of FA levels on the life cycle stage of cells highlights its potential for use in environmental assessments based on the morphology of diatom populations. It has previously been shown that FA in aquatic organisms correlates with environmental pollutants that influence the developmental processes [39,44,45]. Falasco et al. [24] also showed that increased occurrence of teratological forms in natural populations of diatoms could be linked to a variety of anthropogenic pollutants. Therefore, provided that reliable estimates of FA in shapes of diatom valves could be obtained by geometric morphometrics or related methods, such as elliptical Fourier analysis (EFA) [46], they might then be used as model systems in biomonitoring of freshwater and marine ecosystems.

Possible drawbacks of the applied methodology, illustrated by relatively high ME estimates in Procrustes ANOVA models, could be overcome by using some of the alternative methods of outline analysis in morphometrics, such as EFA [46]. In that context, decomposition of symmetric variation and individual components of asymmetry (DA, FA) could be based on parallel extraction of coefficients of the harmonic functions characterizing the valve outlines before and after their reflection across the axis of symmetry. Resulting coefficients could then be analyzed in ANOVA models similar to those used in the landmark-based studies. Comparison of such parallel analyses in objects, such as diatom valves, and their ME levels in comparison to detected values of FA could provide a valuable guideline for future research in this field.

With regard to diatom morphological evolution, studies based on cladistic analysis of morphological characters [47], or studies based on analyses of theoretical morphospace [48,49] suggest that strongly asymmetric forms may have evolved from symmetric ancestors. Interestingly, genera with cymbelloid (apical) or gomphonemoid (transapical) types of asymmetry typically have symmetric initial cells (the first cell in the beginning of the life cycle), with apical or transapical asymmetry developing during the vegetative multiplication phase [48,50]. However, molecular phylogenetic research has failed to conclusively support the above-mentioned hypotheses [21]. Nevertheless, if it is taken into account that diatoms with asymmetric central areas may have slightly asymmetric outlines, it is then possible to consider them as theoretical intermediate stages in the evolution of cymbelloid forms with apical asymmetry.

Acknowledgments: The authors express their gratitude to Charles University in Prague for the financial support of this work. The English language and style corrections were made by Editage. We also thank the anonymous reviewers for their critique and recommendations that improved the manuscript.

Author Contributions: Jiří Neustupa conceived and designed the research; Kateřina Woodard performed the experiments; both Jiří Neustupa and Kateřina Woodard analyzed the data and wrote the paper.

Conflicts of Interest: The authors declare no conflicts of interest.

References

1. Neustupa, J.; Hodac, L. Changes in shape of the coenobial cells of an experimental strain of *Pediastrum duplex* var. *duplex* (Chlorophyta) reared at different pHs. Preslia 2005, 77, 439–452.
2. Lenarczyk, J. Morphological plasticity of the microscopic green alga *Pseudopediastrum boryanum* (Chlorophyceae) under varying nutrient concentrations. Nova Hedwig. 2016, 102, 373–390.
3. Verbruggen, H.; Clerck, O.D.; Coppejans, E. Deviant segments hamper a morphometric approach towards *Halimeda* taxonomy. Cryptogam. Algol. 2005, 26, 259–274.
4. Brook, A.J. The Biology of Desmids, 16th ed.; University of California Press: Berkeley, CA, USA, 1981; p. 276.
5. Savriama, Y.; Neustupa, J.; Klingenberg, C.P. Geometric morphometrics of symmetry and allometry in *Micrasterias rotata* (Zygnemophyceae, Viridiplantae). Nova Hedwig. Beih. 2010, 136, 43–54.
6. Neustupa, J. Patterns of symmetric and asymmetric morphological variation in unicellular green microalgae of the genus *Micrasterias* (Desmidiales, Viridiplantae). Fottea 2013, 13, 53–63.
7. Afanasieva, M.S. Radiolarian skeleton: Morphology of spines, internal framework, and primary sphere. Paleontol. J. 2007, 41, 1–14.
8. Potapova, M.; Hamilton, P.B. Morphological and ecological variation within the *Achnanthidium minutissimum* (Bacillariophyceae) species complex. J. Phycol. 2007, 43, 561–575.
9. Klingenberg, C.P. Analyzing fluctuating asymmetry with geometric morphometrics: Concepts, methods, and applications. Symmetry 2015, 7, 843–934.
10. Klingenberg, C.P.; Barluenga, M.; Meyer, A. Shape analysis of symmetric structures: Quantifying variation among individuals and asymmetry. Evolution 2002, 56, 1909–1920.

11. Graham, J.H.; Raz, S.; Hel-Or, H.; Nevo, E. Fluctuating asymmetry: Methods, theory and applications. Symmetry 2010, 2, 466–540.
12. Savriama, Y.; Klingenberg, C.P. Beyond bilateral symmetry: Geometric morphometric methods for any type of symmetry. BMC Evol. Biol. 2011, 11, 280.
13. Schmid, A.M. Aspects of morphogenesis and function of diatom cell walls with implications for taxonomy. Protoplasma 1994, 181, 43–60.
14. Hostetter, H.P.; Hoshaw, R.W. Asexual developmental patterns of the diatom *Stauroneis anceps* in culture. J. Phycol. 1972, 8, 289–296.
15. Hostetter, H.P.; Rutherford, K.D. Polymorphism of the diatom *Pinnularia brebissonii* in culture and a field collection. J. Phycol. 1976, 12, 140–146.
16. Round, F.E.; Crawford, R.M.; Mann, D.G. The Diatoms: Biology and Morphology of the Genera; Cambridge University Press: Cambridge, UK, 1990; p. 131.
17. Edgar, S.M.; Theriot, E.C. Phylogeny of *Aulacoseira* (Bacillariophyta) based on molecules and morphology. J. Phycol. 2004, 40, 772–788.
18. Veselá, J.; Neustupa, J.; Pichrtová, M.; Poulíčková, A. Morphometric study of *Navicula* morphospecies (Bacillariophyta) with respect to diatom life cycle. Fottea 2009, 9, 307–316.
19. Pappas, J.L.; Kociolek, J.P.; Stoermer, E.F. Quantitative morphometric methods in diatom research. Nova Hedwig. Beih. 2014, 143, 281–306.
20. Edgar, R.K.; Saleh, A.I.; Edgar, S.M. A morphometric diagnosis using continuous characters of *Pinnunavis edkuensis*, sp. nov. (Bacillariophyta: Bacillariophyceae), a brackish-marine species from Egypt. Phytotaxa 2015, 212, 1–56.
21. Theriot, E.C.; Ashworth, M.; Ruck, E.; Nakov, T.; Jansen, R.K. A preliminary multigene phylogeny of the diatoms (Bacillariophyta): Challenges for future research. Plant Ecol. Evol. 2010, 143, 278–296.
22. Spaulding, S.A.; Lubinski, D.J.; Potapova, M. Diatoms of the United States. Available online: http://westerndiatoms.colorado.edu (accessed on 5 December 2016).
23. Woodard, K.; Kulichová, J.; Poláčková, T.; Neustupa, J. Morphometric allometry of representatives of three naviculoid genera throughout their life cycle. Diatom Res. 2016, 31, 231–242.
24. Falasco, E.; Bona, F.; Badino, G.; Hoffmann, L.; Ector, L. Diatom teratological forms and environmental alterations: A review. Hydrobiologia 2009, 623, 1–35.
25. Yang, J.R.; Duthie, H.C. Morphology and ultrastructure of teratological forms of the diatoms Stephanodiscus niagarae and *S. parvus* (Bacillariophyceae) from Hamilton Harbour (Lake Ontario, Canada). Hydrobiologia 1993, 269, 57–66.

26. Peres-Weerts, F. Mise en Evidence des Effets Toxiques des Metaux Lourds sur les Diatomees par L'etude des Formes Teratogenes; Agence de l'Eau Artois Picardie: Douai, France, 2000; p. 24. (In French)
27. Poulíčková, A. Morphology, cytology and sexual reproduction in the aerophytic cave diatom *Luticola dismutica* (Bacillariophyceae). Preslia 2008, 80, 87–99.
28. Andersen, R.A. Algal Culturing Techniques; Elsevier Academic Press: London, UK, 2005; p. 578.
29. Poulíčková, A.; Mann, D.G. Sexual reproduction in *Navicula cryptocephala* (Bacillariophyceae). J. Phycol. 2006, 42, 872–886.
30. Rohlf, F.J. The TPS series of software. Hystrix Ital. J. Mammal. 2015, 26, 9–12.
31. Bookstein, F.L. Morphometric Tools for Landmark Data: Geometry and Biology; Cambridge University Press: Cambridge, UK, 1997; p. 436.
32. Adams, D.C.; Otárola-Castillo, E. Geomorph: An R package for the collection and analysis of geometric morphometric shape data. Methods Ecol. Evol. 2013, 4, 393–399.
33. R Development Core Team. R: A Language and Environment for Statistical Computing; R Foundation for Statistical Computing: Vienna, Austria, 2013; Available online: https://www.r-project.org/ (accessed on 9 July 2016).
34. Klingenberg, C.P.; McIntyre, G.S. Geometric morphometrics of developmental instability: Analyzing patterns of fluctuating asymmetry with Procrustes methods. Evolution 1998, 52, 1363–1375.
35. Collyer, M.L.; Sekora, D.J.; Adams, D.C. A method for analysis of phenotypic change for phenotypes described by high-dimensional data. Heredity 2014, 115, 357–365.
36. Slice, D.E. Modern morphometrics. In Modern Morphometrics in Physical Anthropology; Slice, D.E., Ed.; Klewer Press: New York, NY, USA, 2005; pp. 1–45.
37. Hammer, Ø.; Harper, D.A.T.; Ryan, P.D. PAST: Paleontological statistics software package for education and data analysis. Palaeontol. Electron. 2001, 4, 1–9.
38. Mann, D.G. A note on valve formation and homology in the Diatom Genus *Cymbella*. Ann. Bot. 1981, 47, 267–269.
39. Savriama, Y.; Stige, L.C.; Gerber, S.; Pérez, T.; Alibert, P.; David, B. Impact of sewage pollution on two species of sea urchins in the Mediterranean Sea (Cortiou, France): Radial asymmetry as a bioindicator of stress. Ecol. Indic. 2015, 54, 39–47.
40. Zabrodsky, H.; Peleg, S.; Avnir, D. Continuous symmetry measures. J. Am. Chem. Soc. 1992, 114, 7843–7851.

41. Graham, J.H.; Whitesell, M.J.; Flemming, M.; Hel-Or, H.; Nevo, E.; Raz, S. Fluctuating asymmetry of plant leaves: Batch processing with LAMINA and continuous symmetry measures. Symmetry 2015, 7, 255–268.
42. De Groote, I.; Lockwood, C.A.; Aiello, L.C. Technical note: A new method for measuring long bone curvature using 3D landmarks and semi-landmarks. Am. J. Phys. Anthropol. 2010, 141, 658–664.
43. Graham, J.H.; Emlen, J.M.; Freeman, D.C.; Leamy, L.J.; Kieser, J.A. Directional asymmetry and the measurement of developmental instability. Biol. J. Linn. Soc. 1998, 64, 1–16.
44. Lezcano, A.H.; Quiroga, M.L.R.; Liberoff, A.L.; van der Molen, S. Marine pollution effects on the southern surf crab *Ovalipes trimaculatus* (Crustacea: Brachyura: Polybiidae) in Patagonia Argentina. Mar. Pollut. Bull. 2015, 91, 524–529.
45. Trono, D.J.V. Fluctuating asymmetry and developmental instability in *Protoreaster nodosus* (Chocolate Chip Sea Star) as a biomarker for environmental stress. Comput. Ecol. Softw. 2015, 5, 119–129.
46. Lestrel, P.E. Morphometrics for the Life Sciences; World Scientific: Singapore, 2000; p. 261.
47. Kociolek, J.P.; Stoermer, E.F. A preliminary investigation of the phylogenetic relationships among the freshwater, apical pore field-bearing cymbelloid and gomphonemoid diatoms (Bacillariophyceae). J. Phycol. 1988, 24, 377–385.
48. Pappas, J.L. Theoretical morphospace and its relation to freshwater Gomphonemoid–Cymbelloid diatom (Bacillariophyta) lineages. J. Biol. Syst. 2005, 13, 385–398.
49. Pappas, J.L. More on theoretical morphospace and its relation to freshwater gomphonemoid-cymbelloid diatom (Bacillariophyta) lineages. J. Biol. Syst. 2008, 16, 119–137.
50. Cox, E.J.; Willis, L.; Bentley, K. Integrated simulation with experimentation is a powerful tool for understanding diatom valve morphogenesis. Biosystems 2012, 109, 450–459.

4. Geometric Morphometrics of Bilateral Asymmetry in *Eunotia bilunaris* (Eunotiales, Bacillariophyceae) as a Tool for the Quantitative Assessment of Teratogenic Deviations in Frustule Shapes

[published as Woodard, K. & Neustupa, J. (2022). Geometric morphometrics of bilateral asymmetry in *Eunotia bilunaris* (Eunotiales, Bacillariophyceae) as a tool for the quantitative assessment of teratogenic deviations in frustule shapes. Symmetry, 14: 42.]

Abstract

A number of pennate diatom genera typically have teratogenic deformations of their siliceous frustules due to the effects of environmental stress, such as high concentrations of heavy metals and low pH. However, the quantitative assessment of these deformations has rarely been applied. One species in which aberrations have frequently been reported is *Eunotia bilunaris*, which typically has bilaterally symmetric frustules with dorso-ventral differentiation. In this study, we aimed to illustrate the geometric morphometric analysis of symmetry as a tool for assessing the severity of teratogenic deformations. These were quantified by Procrustes superimposition of equidistant points placed along the valvar outlines in pairs of configurations based on their bilateral reflection symmetry. The shape deformations were mostly confined to central parts of the ventral outlines and were captured both by the symmetric and asymmetric subspaces of the variation. The amount of bilateral asymmetry in individual cells was negatively related to frustule size via the allometric power law relationship, illustrating that asymmetry increased in the asexual diminution series. The presented analysis provides a framework for the quantitative assessment of frustule deformations in eunotioid diatoms that can be used for the comparative scoring of teratogenic deviations among cells, populations, or species.

Keywords: *Eunotia; geometric morphometrics; pennate diatoms; phenotypic plasticity; shape asymmetry*

Introduction

Diatoms are one of the most significant groups of protist organisms. They abound in phytoplankton and phytobenthos of aquatic habitats worldwide. It is estimated that they account for as much as 20% of primary production on Earth [1]. Their most important phenotypic synapomorphy is the rigid silica cell wall (frustule), which is composed of two complementary parts (thecae). The upper part of frustules, called the valve, is characterised by various types of symmetric patterns, such as the radial symmetry of the centric diatoms or the biradial and bilateral symmetry of the pennate diatoms [2]. Empty diatom frustules are well preserved in sediments. Therefore, they are a key model group in paleoecological research of aquatic ecosystems [3].

Diatoms are generally sensitive to the environmental conditions of their habitats, which is reflected in the changes of their species composition in natural communities and in the patterns of morphological variation of frustules [4,5]. Teratogenic changes in frustule morphology have been well documented in scientific literature, especially in relation to various stress factors, such as increased sublethal concentrations of heavy metals [6–8], acidification [9,10], increased radiocativity [11], and organic pollution [12]. These teratogenic changes affect different parts of frustules, but the most common are deformities of the frustule outlines compared to their species-specific symmetric shapes.

The incidence of such morphological deformations in the sedimentary record has frequently been used as proxy data for the identification of historical changes in the anthropogenic loading of various aquatic ecosystems [3,5,6,13]. In these studies, the stress rate is usually quantified as the proportion of deformed frustules relative to the “standard” shapes. Thus, the severity of deformation of individual frustules is usually not explicitly quantified in any way. However, in recent years, several studies have been published that have sought to quantify the outline deformations of diatom frustules using the techniques of geometric morphometrics [14–16]. In general, these studies have shown that the degree of teratogenic deviations can be sensitively reflected in the patterns of shape changes of the studied populations. However, they did not separate symmetric and asymmetric variation, but rather focused on the principal components of the overall shape dynamics within the studied datasets that typically correlate with the degree of teratogenic shape deviations. Thus, to the best of our knowledge, no study has yet explicitly quantified shape asymmetries between the corresponding parts of the configurations representing the frustule shapes with teratogenic morphology.

There is, however, a well-founded analytical apparatus based on the geometric morphometric analysis of the configurations, representing a finite symmetry group of the studied

system [17,18]. Principal component analysis (PCA) of such Procrustes-aligned configurations separates symmetric variation among objects from morphometric asymmetry between individual symmetric parts of the studied system. In addition, the Procrustes-aligned coordinates of the configurations, representing the symmetry group of a single object, can be used to quantify the shape asymmetry of that particular specimen [18,19]. Thus, an obvious advantage of such an analysis is the ability to quantify the deformation of each object separately, i.e., without considering the variation of other individuals. With this analytical algorithm, it might be possible to compare the severity of teratogenic deformation of individual frustules without having to re-analyse entire large datasets each time.

From an analytical point of view, however, it is necessary to apply a proper symmetry group corresponding to the geometric arrangement of analysed frustules for the morphometric analysis of symmetry and asymmetry in different diatom lineages. The pennate diatoms, which usually dominate the freshwater phytobenthos, are usually characterised by different types of two-dimensional biradial and bilateral symmetry in the valvar view of their frustules. For example, biradial symmetry, characterised by two perpendicular axes of symmetry dividing the valve into four ideally identical segments, is typical for the genera *Frustulia, Navicula, Luticola*, and *Achnanthidium* [20–23]. However, even in these biradial genera, their ideally symmetric arrangement is usually broken by slight systematic asymmetries of valve morphology, such as the structure of the raphe system or Voigt discontinuities [24–26]. In addition, the bilaterally symmetric valve patterns repeatedly evolved in several pennate diatom lineages [27]. One such evolutionarily significant example of bilaterally symmetric morphology is the eunotioid diatoms (Eunotiales), which are characterised by valves with a distinct asymmetric curvature across the apical axis. Thus, in the valvar view, their cells are distinctly dorsiventral [2]. In contrast, the symmetry across the transapical axis of eunotioid valves is typically preserved, and two cellular halves cannot be distinguished from each other among different individuals. Members of the genus *Eunotia* Ehrenberg, the most frequently distributed genus of this lineage, occur in a wide variety of habitats, including the freshwater phytobenthos and subaerial biofilms and soils [2,9–11,28]. In this study, the eunotioid diatom morphotype was selected to explore the potential of geometric morphometric analysis of asymmetry in assessing the severity of teratogenic deformities. We aimed to identify an analysis that could easily be replicated with different datasets for the comparative analysis of asymmetry in the shapes of eunotioid diatom frustules.

The model system of our study was *Eunotia bilunaris* (Ehrenberg) Schaarschmidt, a diatom species complex occurring mostly in oligotrophic waters with a low pH, such as peatland aquatic habitats in boreal ecosystems. It is composed of several closely related and morphologically very

similar lineages. The valves of *E. bilunaris* are typical for arcuate isopolar outlines with rounded polar ends that are slightly tapered (Figure 1). Interestingly, in the specimens of this species, teratogenic deformations of valvar outlines have been repeatedly reported [3,6,7,9,10,13]. These deformities were largely linked to adverse environmental conditions, such as heavy metal pollution [6,7] or low pH [9,10]. Our study was based on the analysis of cells from a natural population of *E. bilunaris* with a relatively high proportion of visibly deformed cells.

Decomposition of the symmetric and asymmetric components was performed to illustrate the main patterns of shape variation in both these subspaces. Our main goal was to determine whether the different levels of frustule shape deformations could be detected and quantified by geometric morphometric analysis of their bilateral asymmetry. We also determined whether the shape asymmetry of frustules was related to their size, i.e., if the population was constrained by an allometric relationship that could be linked to the changes in cell size during a series of asexual cell divisions.

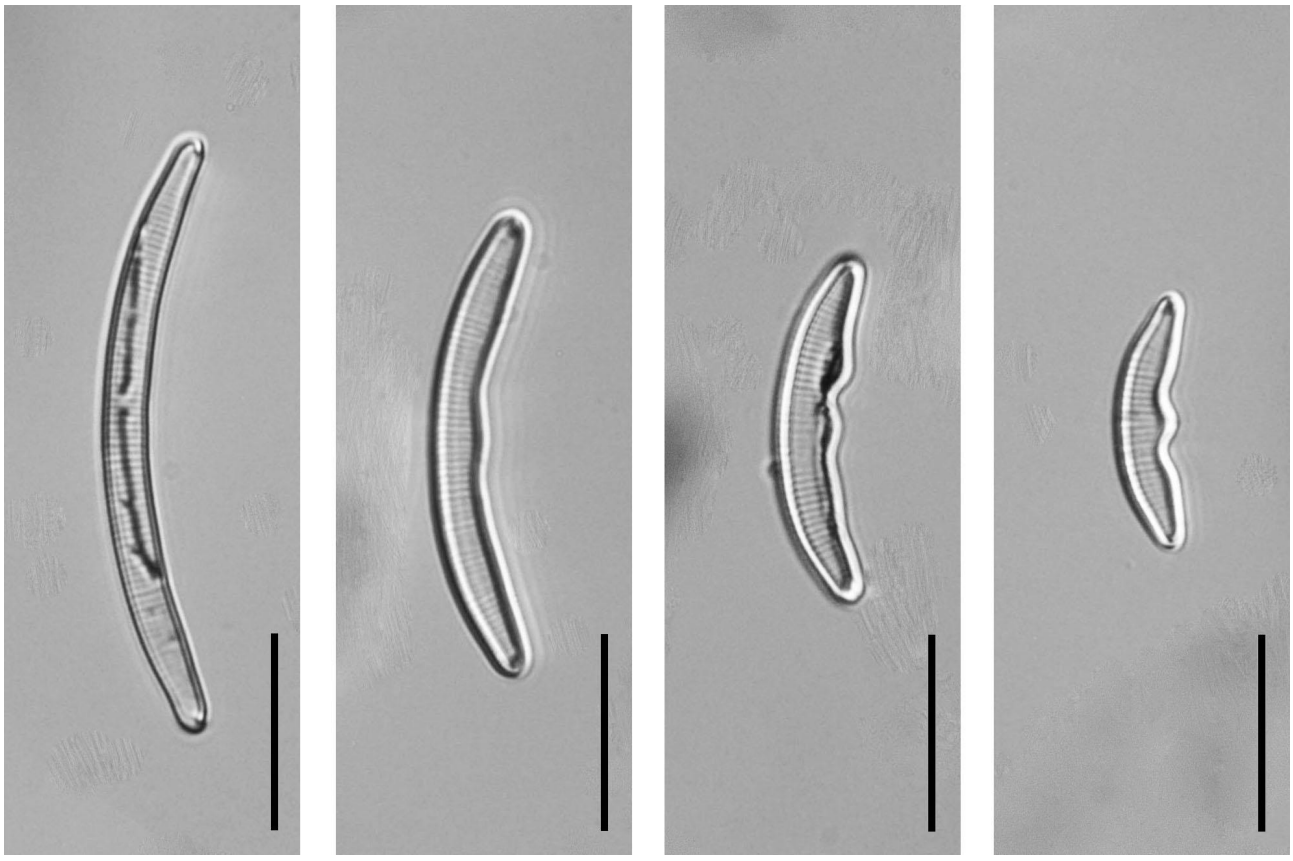

Figure 1. Size diminution series of Eunotia bilunaris cells taken from the studied population. Scale bar = 10 μm.

Materials and Methods

Sampling and Data Acquisition

Algae were sampled on 21 January 2021, in a *Sphagnum*-dominated peat bog ditch located in the mountainous plateau of Krušné hory/Erzgebirge Mts. in Northwest Bohemia, Czech Republic (GPS: 50.536616N, 13.251838E) at an altitude of 827 m above sea level. The pH level of the sampling locality was 4.1, and the conductivity of the water was 112 $S.cm^{-1}$. Immediately after sampling, the diatoms were fixed with ethanol so that the final solution had a 10% concentration of fixative. The valves were cleaned by oxidation with 35% hydrogen peroxide and potassium dichromate for 15 min. Then, they were washed with distilled water and mounted onto permanent slides using Naphrax (Brunel Microscopes Ltd., Wiltshire, UK).

Two-dimensional images of valves were taken on a Leica DM2500 light microscope (Leica Microsystems, Wetzlar, Germany) at 1000 magnification using Bresser Mikro-Cam 5.0 MP (Bresser, Rhede, Germany) digital photographic equipment. Micrographs representing a total of 64 valves were randomly selected, cropped, and rotated in GIMP ver. 2.8.14 [29], with their apical axis horizontal and the dorsal edge of the valves pointing downwards. The outline forms were digitised in TpsUtil, ver. 2.22 [30]. Two fixed landmarks were placed at the apices of each valve. The ventral and dorsal outlines were registered by 61 semi-landmarks placed along each valve side using the semi-automated background_curves tool of TpsDig, ver. 2.22. The equidistant position of these points along the ventral and dorsal valve outlines was achieved using the function digit.curves of the geomorph package, ver. 4.0.0, in R, ver. 4.0.5 [31]. This procedure decreased the number of points in each outline curve by one [32]. Thus, in the final dataset, each valve was registered by 122 two-dimensional outline points. These primary data are available online at https://doi.org/10.5281/zenodo.5732459 (accessed on 16 December 2021).

Geometric Morphometrics

The valvar outline of an eunotioid diatom, registered by a series of two-dimensional points, represents a configuration with bilateral object symmetry [33]. Such a configuration consists of two halves that can be reflected across the axis of symmetry, ideally producing two identical configurations. Any difference between the original and the reflected configuration is due to the presence of asymmetry in the position of the individual points. However, this asymmetry cannot be decomposed into directional and fluctuating components, as in the standard procedure of a two-factor, mixed-effect analysis of variance (ANOVA) model that is frequently used in geometric morphometric studies of bilateral symmetry in multicellular organisms [18]. Consequently,

fluctuating asymmetry could not be used in these diatoms as an explicit measure of individual stress or developmental instability among specimens [34] because frustules of eunotioid diatoms typically lack any unambiguous directional orientation of their two symmetrical halves delimited by the transapical axis. In a set of such objects, the individual halves cannot be unambiguously designated as “right” or “left.” This situation is not at all exceptional and is even typical of most unicellular protist organisms [35–40]. The analysis of a dataset must then be limited to the decomposition of the overall asymmetry and symmetric differences among superimposed objects [17].

In geometric morphometrics, the optimal superimposition of individual configurations is typically achieved using generalised Procrustes analysis (GPA), which optimises the relative position of corresponding points by removing any differences caused by their different position, rotation, and size from the set of configurations [41]. This is accomplished by rotating each configuration to minimise the summed squared distances of landmarks from an iterated estimate of the mean shape. Principal component analysis (PCA) of such Procrustes-aligned coordinates obtained by the GPA of the original and reflected configurations of all objects in the studied dataset yields a set of principal components (PCs) that each describe either purely symmetric shape variation among objects or patterns of bilateral shape asymmetry between their two corresponding halves [17,18]. The ratio of shape variation spanned by the asymmetric and purely symmetric PCs indicates the overall shape asymmetry of the analysed dataset.

Alternatively, pairs of configurations representing a symmetry group of a single eunotioid object, i.e., the original and reflected configurations of a single frustule, can be superimposed separately [18,19]. The residual distances between corresponding landmarks then represent the overall shape asymmetry between the two halves of one object (frustule). An important feature of such a procedure is that it is independent of the other analysed objects, and each individual frustule can be characterised by its own indicator of shape asymmetry [19]. However, it is not possible to visualise the patterns of symmetric and asymmetric variation within the explored morphospace, which is an inherent property of PCA based on the Procrustes aligned coordinates representing the complete symmetry group of the entire dataset.

In this study, we first performed a joint GPA of the entire dataset of original and mirrored configurations. Semi-landmarks were kept in their equidistant positions along the outlines [42]. Although differences between the GPA based on fixed equidistant positions of semi-landmarks and their sliding along the tangents to the outline curve usually only marginally influence the actual shape representation of the objects, introducing an additional step of semi-landmark sliding still slightly alters the actual morphology of the analysed shapes, which may introduce an artificial signal into the data [43]. This is because semi-landmark sliding along the tangents to the outline

curve typically leads to different densities of the aligned semi-landmarks in different parts of the outline [44]. This then leads to increased shape differences between its original and mirrored configurations, thereby increasing the shape asymmetry of individual objects and the entire dataset. The Procrustes aligned configurations were subjected to PCA, and the marginal occupied position on PCs that illustrated the largest proportion of symmetric and asymmetric shape variation in frustules were plotted using the deformation grids of individual configurations from the mean shape of the entire dataset.

To obtain explicit values of the bilateral shape asymmetry of individual frustules, the original and mirrored configurations of each object were separately aligned by GPA (Figure 2). The average Euclidean distances between corresponding landmarks from the original and mirrored configurations of each object were used to illustrate the relative differences in the shape asymmetry of different parts of the analysed frustules. The Procrustes distance (i.e., the square root of the sum of squared differences in the landmark positions of two shapes) between the original and reflected configurations was used to describe the shape asymmetry of individual objects. The same procedure involving a series of GPAs based on the original and mirrored configurations was also performed with the configurations solely spanning the dorsal and ventral valve sides. These analyses were used to identify different levels of asymmetry between these parts of the frustules.

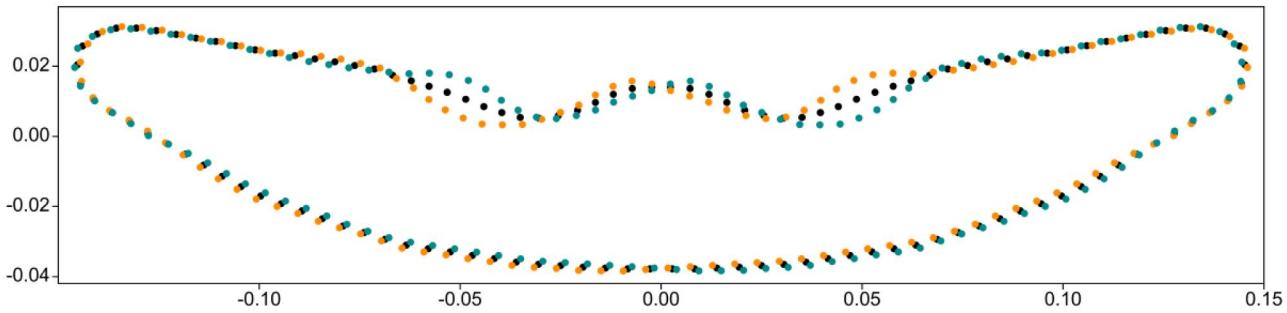

Figure 2. Two Procrustes-aligned configurations of 122 equidistant points representing the bilateral asymmetry of a single Eunotia bilunaris cell (orange and turquoise points). The ideally symmetric mean configuration is depicted by black points.

The frustule size was evaluated by the centroid size of the original landmark configurations. Centroid size, defined as the square root of the sum of squared distances of each landmark from the centroid of each configuration, provides an unbiased morphometric size measure of analysed objects that can be used for subsequent comparison with their shape characteristics [45]. In this study, the centroid size of each frustule was compared with their shape asymmetry evaluated by the

Procrustes distance between the original and mirrored configurations. To investigate the relationship between asymmetry and frustule size, four alternative functions were compared. The linear function was based on the ordinary least squares regression. Then, the quadratic, exponential, and power law functions were also used to evaluate the relationship between the size and asymmetry measures of individual frustules. The Akaike information criterion (AIC) was used to compare these four models and determine which one might be the best fit for the observed data [46].

GPA was implemented using the function *procGPA* in the *shapes* package, ver. 1.2.6 [47], in R, ver. 4.0.5 [48]. PCA of the dataset consisting of the Procrustes aligned original and mirrored configurations was conducted in TpsRelw, ver. 1.65 [29]. The deformation grids illustrating shapes typical for individual PCs were also obtained using this software. Analyses examining the relationship between size and shape asymmetry of frustules were performed in PAST, ver. 4.04 [49]. The R scripts used for the analyses are available online at https://doi.org/10.5281/zenodo.5732459 (accessed on 16 December 2021).

Results

Variation among individual frustules of *E. bilunaris* accounted for 92.3% of the total shape variability that was described by symmetric PCs yielded by PCA of the original and mirrored configurations of frustules. The remaining 7.7% of the variation was accounted for by asymmetric axes that described the bilateral asymmetry of configurations.

The single dominant feature of shape variation was a bilaterally symmetric pattern distinguishing cells with narrowly elongated shapes from those that were typically relatively shorter and wider with a central projection on the ventral side (Figure 3). This trend accounted for 80.5% of the total variation, as illustrated by PCA of the Procrustes aligned data of the original and mirrored configurations. Changes in the shape of the central part of the ventral outlines were also a prominent feature of the symmetric variation patterns described by PC2 and PC4, which accounted for 5.8% and 2.1% of the total shape variability, respectively. In these cases, however, the changes in the shape of this central part of the ventral outline were not associated with any notable morphological changes in other parts of the valves (Figure 3). Two main patterns of bilateral shape asymmetry were illustrated by PC3 and PC5, accounting for 2.9% and 1.5% of the variation, respectively. Interestingly, both patterns largely involved asymmetric deviations of the ventral sides (Figure 3).

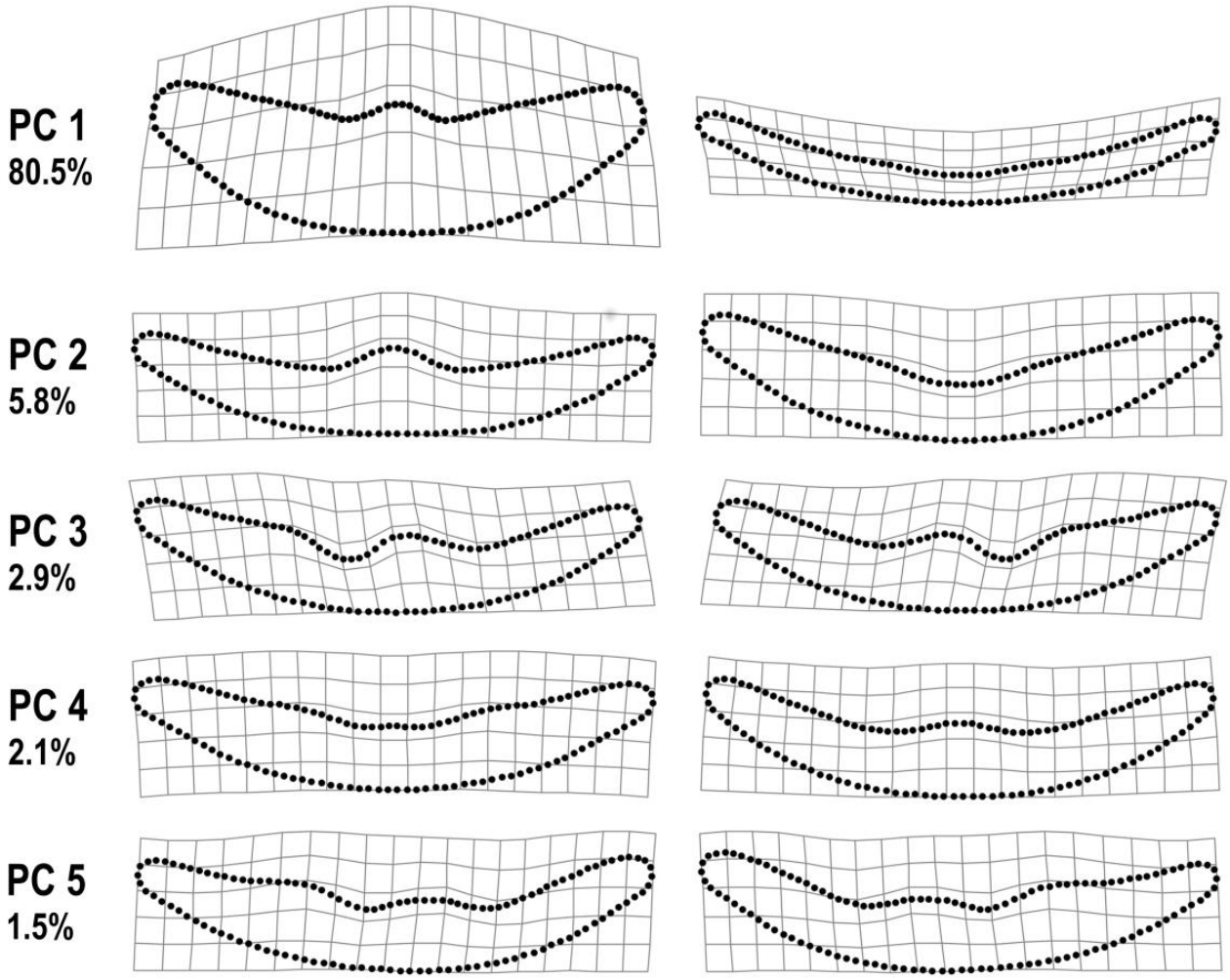

Figure 3. Deformation grids showing the configurations typical for the most marginal occupied positions on the five principal components (PC) that described most variation in the shape space of the original and mirrored configurations of 64 analysed valves. The shape dynamics associated with PC1, PC2, and PC4 involved both symmetric halves of the frustules equally. In contrast, PC3 and PC5 described the bilaterally asymmetric shape changes within the dataset.

When looking at the average asymmetric variability of the individual frustules, the ventral side of the valve outlines was clearly more asymmetric than the dorsal side (Figures 4 and 5). Moreover, most of the asymmetry of the frustules was due to shape deviations on their ventral sides. The highest levels of asymmetry were concentrated in the central parts of the ventral curve (Figure 5), except for the central portion itself, where the shape variability was primarily manifested in the symmetric components.

Comparison of the different models for the analysis of the relationship between frustule size and asymmetry (Table S1) favoured the power law relationship with a negative scaling coefficient of -0.38 (95% C.I. (-0.32, -0.43)). This was corroborated by a strongly significant linear log-log relationship between these variables ($r = -0.80$, $R^2 = 0.64$, $p = 0.0001$), indicating that the relatively large frustules within the dataset were usually considerably less asymmetric than the smaller cells

Additionally, 20% of the smallest frustules in the sample accounted for approximately half the range of the observed bilateral asymmetry (Figure 6).

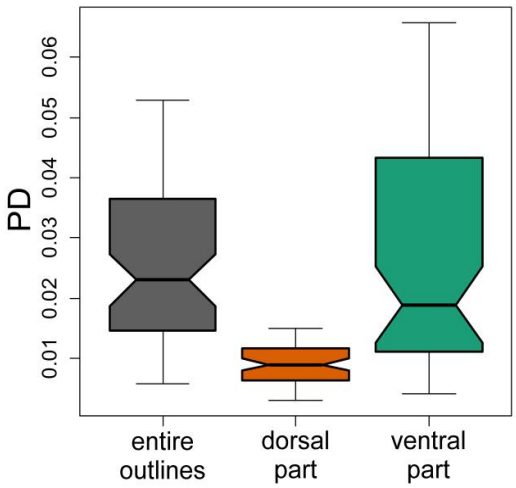

Figure 4. Boxplots showing bilateral asymmetry of frustules evaluated by the Procrustes distances (PD) between their original and mirrored configurations. The entire outlines (grey) and their dorsal (orange) and ventral (green) parts were analysed separately.

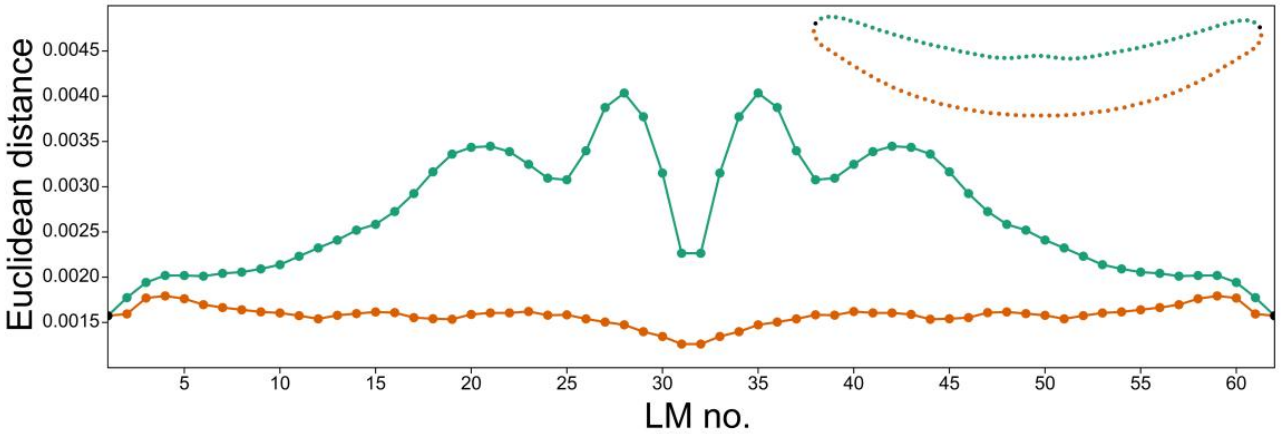

Figure 5. Average Euclidean distances between corresponding points (LM) of the Procrustes aligned original and mirrored configurations of each frustule. The ventral outline values are depicted in green, and the dorsal outline values are shown as orange points and lines.

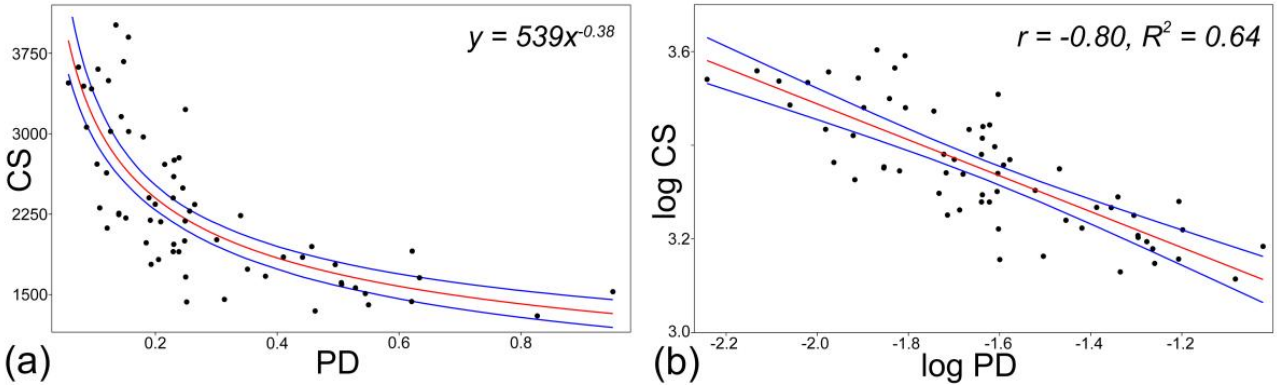

Figure 6. Graphs showing (**a**) the allometric power law relationship between centroid sizes of individual frustules (CS) and their bilateral asymmetry evaluated by the Procrustes distance (PD) between the original and mirrored configurations and (**b**) their log-log linear relationship.

Discussion

The analysed deformations in the shape of the valves of *E. bilunaris* were visually similar to those illustrated in the genus *Eunotia* in several previous studies [3,7,9,10,50,51]. These deformations primarily affected the ventral part of the frustules. In addition, our morphometric analysis also showed that the overall rate of these deformations increased significantly with decreasing cell size. In diatoms, this basically means that the cell outlines were more distorted as they underwent more vegetative divisions because the cell size decreased with each binary division throughout the asexual vegetative cycle [2,52]. However, not all shape deformations were asymmetric with respect to the bilaterally symmetric *Bauplan* of eunotioid diatoms. The most significant shape trend in our data, which was captured by PC1 as illustrating more than 80% of the total symmetric and asymmetric variation, was clearly related to the allometric shape-to-size relationship in which cells progressively shrink during a series of vegetative divisions while also changing shape symmetrically in both halves of the frustule. This phenomenon of shape allometry associated with a diminution series during the vegetative cycle has been illustrated in pennate diatoms by several examples [19,21,23,53,54]. In *E. bilunaris*, it mainly involves a gradual shortening of the cells, while largely maintaining their relatively stable width [52,55]. In terms of shape variation, this process also included the production of a central bump on the ventral side of the valves, as shown by the shape changes associated with PC1. However, these allometric shape changes were detected in *E. bilunaris* both in natural populations and in clonal cultures under optimal growth conditions and are therefore unlikely to be a manifestation of teratogenic morphogenesis [52,55]. Thus, the formation of a central bump in small cells is probably an intrinsic part of the allometric shape pattern in this species.

The asymmetric deviations from bilaterally symmetric shapes captured by our morphometric analysis also visually resembled those previously recorded in various species of the genus *Eunotia* in recent populations or in fossil material associated with various types of environmental stress, such as acidification or heavy metal contamination [3,7,9,10,13,56]. Our analysis showed that the regions of the ventral outline near the central part of the valves were the most prone to asymmetric deformations, while the average degree of asymmetry decreased significantly towards the apical cell poles. The allometric pattern of markedly increasing frustule asymmetry with decreasing size, observed in *E. bilunaris*, represents a distinctly different phenomenon from the more or less stable rate of subtle asymmetric variation and individual fluctuating asymmetry of frustules during the asexual diminution series that were previously illustrated in various species of the genera *Navicula, Luticola*, and *Sellaphora* [19,22,57]. These results confirm that when a teratogenic deformity arises in a population, it typically persists and becomes increasingly amplified through the asexual reproduction series [9,58]. The strong allometric relationship of the asymmetric deformations in *E. bilunaris*, contrasting with the absence of similar patterns in the subtle shape fluctuation asymmetry in the aforementioned genera grown under optimal conditions, provides indirect evidence that the observed variation represented a teratogenic response at the population level that was accentuated in the course of the vegetation cycle.

Several previous studies and reviews have stressed that assessing the severity of frustule teratology is an important step for further advancing research on the relationship between these morphogenetic deformities and their causative environmental factors [4,5,58,59]. We suggest that the presented geometric morphometric framework for the analysis of bilateral asymmetry across the transapical axis of eunotioid diatoms represents one such approach for quantifying shape teratogeny in this diatom group. Previous geometric morphometric studies that addressed teratogenic deformations of diatom frustules were mostly based on the analysis of overall shape variability in the valves, i.e., without explicitly distinguishing symmetric and asymmetric subspaces of the variation [11,14–16]. This obviously resulted in a situation when most of the detected patterns (described by the first few PCs) highlighted symmetric differences among individual frustules. Importantly, the specific position of frustules in relation to the average shape also necessarily depended on the structure of the particular dataset under study [60].

In contrast, the geometric morphometric analysis of the asymmetry of individual frustules allowed us to quantify their individual degree of deviation from the ideal bilaterally symmetric pattern regardless of other analysed cells. With the same number of equidistant points registering the valve outlines, the results could be compared among populations, studies, or even different taxa with eunotioid frustule outlines. When investigating diatoms with different types of valvar

symmetry, the design of the asymmetry analysis would have to be adjusted to their respective symmetry groups. For example, three perpendicular geometric components of shape asymmetry can be decomposed in configurations with biradial symmetry that are typical for most araphid diatoms and several raphid genera, such as *Frustulia, Luticola, Navicula*, and *Achnanthidium* [19,20,23,57]. In addition, teratogenic shape asymmetry in genera with heteropolar valves, such as *Gomphonema, Licmophora,* and *Didymosphenia* [61], needs to be quantified based on the reflection of configurations across the apical axis. However, in all cases, the Procrustes-based decomposition of the shape asymmetry could represent a well-applicable framework for scoring the severity of diatom frustule teratology in relation to different types of environmental stress, such as the metal contamination, acidification, eutrophication, or increased radioactivity [5].

Supplementary Materials: The following are available online at https://www.mdpi.com/article/10.3390/sym14010042/s1, Table S1: Comparison of the different models for the analysis of the relationships between frustule size and shape asymmetry of *E. bilunaris*.

Funding: This research was funded by Charles University Prague; project number "Progres no. 43".

Data Availability Statement: The primary data and the R scripts used for the analyses are available online at https://doi.org/10.5281/zenodo.5732459 (accessed on 16 December 2021).

Acknowledgments: The algae were sampled based on the field research permit awarded to the authors by the Department of Environment and Agriculture of the Regional Authority of Northern Bohemia (no. KUUK/073894/2021).

Conflicts of Interest: The authors declare no conflict of interest. The funders had no role in the design of the study; in the collection, analyses, or interpretation of data; in the writing of the manuscript, or in the decision to publish the results.

References

1. Malviya, S.; Scalco, E.; Audic, S.; Vincent, F.; Veluchamy, A.; Poulain, J.;Wincker, P.; Iudicone, D.; de Vargas, C.; Bittner, L.; et al. Insights into Global Diatom Distribution and Diversity in the World's Ocean. Proc. Nat. Acad. Sci. USA 2016, 113, 1516–1525.

2. Round, F.E.; Crawford, R.M.; Mann, D.G. The Diatoms. Biology and Morphology of the Genera; Cambridge University Press: Cambridge, UK, 1990; p. 747.

3. Sienkiewicz, S.; Gasiorowski, M. The Evolution of a Mining Lake—From Acidity to Natural Neutralization. Sci. Total Environ. 2016, 557, 343–354.

4. Falasco, E.; Bona, F.; Badino, G.; Hoffmann, L.; Ector, L. Diatom Teratological Forms and Environmental Alterations: A Review. Hydrobiologia 2009, 623, 1–35.

5. Falasco, E.; Ector, L.; Wetzel, C.E.; Badino, G.; Bona, F. Looking Back, Looking Forward: A Review of the New Literature on Diatom Teratological Forms (2010–2020). Hydrobiologia 2021, 848, 1675–1753.

6. Cattaneo, A.; Couillard, Y.;Wunsam, S.; Courcelles, M. Diatom Taxonomic and Morphological Changes as Indicators of Metal Pollution and Recovery in Lac Dufault (Quebec, Canada). J. Paleolimnol. 2004, 32, 163–175.

7. Furey, P.C.; Lowe, R.L.; Johansen, J.R. Teratology in *Eunotia* Taxa in the Great Smoky Mountains National Park and Description of *Eunotia macroglossa* sp. nov. Diat. Res. 2009, 24, 273–290.

8. Morin, S.; Cordonier, A.; Lavoie, I.; Arini, A.; Blanco, S.; Duong, T.T.; Tornés, E.; Bonet, B.; Corcoll, N.; Faggiano, L.; et al. Consistency in Diatom Response to Metal-contaminated Environments. In Emerging and Priority Pollutants in Rivers; Guasch, H., Ginebreda, A., Geiszinger, A., Eds.; Springer: Berlin/Heidelberg, Germany, 2012; pp. 117–146.

9. Smith, T.; Manoylov, K. Diatom Deformities from an Acid Mine Drainage Site at Friendship Hills National Historical Site, Pennsylvania. J. Fresh. Ecol. 2007, 22, 521–527.

10. Grabowska, M.; Hindák, F.; Hindáková, A. Phototrophic Microflora of Dystrophic Lake Seczek, Masuria, Poland. Oceanol. Hydrobiol. Stud. 2014, 43, 337–345.

11. Millan, F.; Izere, C.; Breton, V.; Voldoire, O.; Biron, D.G.;Wetzel, C.E.; Miallier, D.; Allain, E.; Ector, L.; Beauger, A. The Effect of Natural Radioactivity on Diatom Communities in Mineral Springs. Bot. Lett. 2020, 167, 95–113.

12. Dziengo-Czaja, M.; Matuszak, J.A. Teratological Forms of Diatoms (Bacillariophyceae) as Indicators of Water Pollution in the Western Part of Puck Bay (Southern Baltic Sea). Oceanol. Hydrobiol. Stud. 2008, 37, 119–132.

13. Sienkiewicz, E.; Ga˛siorowski, M. Natural Evolution of Artificial Lakes Formed in Lignite Excavations based on Diatom, Geochemical and Isotopic Data. J. Paleolimnol. 2019, 62, 1–13.

14. Olenici, A.; Blanco, S.; Borrego-Ramos, M.; Momeu, L.; Baciu, C. Exploring the Effects of Acid Mine Drainage on Diatom Teratology using Geometric Morphometry. Ecotoxicology 2017, 26, 1018–1030.

15. Olenici, A.; Baciu, C.; Blanco, S.; Morin, S. Naturally and Environmentally Driven Variations in Diatom Morphology: Implications for Diatom-based Assessment of Water Quality. In Modern Trends in Diatom Identification. Fundamentals and Applications; Cristóbal, G., Blanco, S., Bueno, G., Eds.; Springer: Cham, Switzerland, 2020; pp. 39–52.

16. Cerisier, A.; Vedrenne, J.; Lavoie, I.; Morin, S. Assessing the Severity of Diatom Deformities using Geometric Morphometry. Bot. Lett. 2019, 166, 32–40.

17. Savriama, Y.; Klingenberg, C.P. Beyond Bilateral Symmetry: Geometric Morphometric Methods for any Type of Symmetry. BMC Evol. Biol. 2011, 11, 280.

18. Klingenberg, C.P. Analyzing Fluctuating Asymmetry with Geometric Morphometrics: Concepts, Methods, and Applications. Symmetry 2015, 7, 843–934.

19. Woodard, K.; Kulichová, J.; Poláčková, T.; Neustupa, J. Morphometric Allometry of Representatives of Three Naviculoid Genera throughout their Life Cycle. Diat. Res. 2016, 31, 231–242.

20. Potapova, M.; Hamilton, P.B. Morphological and Ecological Variation within the *Achnanthidium minutissimum* (Bacillariophyceae) Species Complex. J. Phycol. 2007, 43, 561–575.

21. Veselá, J.; Neustupa, J.; Pichrtová, M.; Poulíčková, A. Morphometric Study of *Navicula* Morphospecies (Bacillariophyta) with Respect to Diatom Life Cycle. Fottea 2009, 9, 307–316.

22. Woodard, K.; Neustupa, J. Morphometric Asymmetry of Frustule Outlines in the Pennate Diatom *Luticola poulickovae* (Bacillariophyceae). Symmetry 2016, 8, 150.

23. Kulichová, J.; Urbánková, P. Symmetric and Asymmetric Components of Shape Variation in the Diatom Genus *Frustulia* (Bacillariophyta). Symmetry 2020, 12, 1626.

24. Mann, D.G. Symmetry and Cell Division in Raphid Diatoms. Ann. Bot. 1983, 52, 573–581.

25. Mann, D.G. Protoplast Rotation, Cell Division and Frustule Symmetry in the Diatom *Navicula bacillum*. Ann. Bot. 1984, 53, 295–302.

26. Cox, E.J. Ontogeny, Homology, and Terminology - Wall Morphogenesis as an Aid to Character Recognition and Character State Definition for Pennate Diatom Systematics. J. Phycol. 2012, 48, 1–31.

27. Kociolek, J.P.; Williams, D.M.; Stepanek, J.; Liu, Q.; Liu, Y.; You, Q.; Karthick, B.; Kulikovskiy, M. Rampant Homoplasy and Adaptive Radiation in Pennate Diatoms. Plant Ecol. Evol. 2019, 152, 131–141.

28. Fazlutdinova, A.; Gabidullin, Y.; Allaguvatova, R.; Gaysina, L. Diatoms in Volcanic Soils of Mutnovsky and Gorely Volcanoes (Kamchatka Peninsula, Russia). Microorganisms 2021, 9, 1851.

29. The GIMP Development Team. 2014. Available online: https://www.gimp.org (accessed on 31 October 2021).

30. Rohlf, F.J. The tps Series of Software. Hystrix Ital. J. Mammal. 2015, 26, 9–12.

31. Adams, D.C.; Otárola-Castillo, E. Geomorph: An R Package for the Collection and Analysis of Geometric Morphometric ShapeData. Meth. Ecol. Evol. 2013, 4, 393–399.

32. Adams, D.C.; Collyer, M.; Kaliontzopoulou, A. Package “Geomorph”. 2020. Available online: https://cran.r-project.org/web/packages/geomorph/geomorph.pdf (accessed on 31 October 2021).

33. Klingenberg, C.P.; Barluenga, M.; Meyer, A. Shape Analysis of Symmetric Structures: Quantifying Variation among Individuals and Asymmetry. Evolution 2002, 56, 1909–1920.

34. Zakharov, V.M.; Shadrina, E.G.; Trofimov, I.E. Fluctuating Asymmetry, Developmental Noise and Developmental Stability: Future Prospects for the Population Developmental Biology Approach. Symmetry 2020, 12, 1376.

35. McManus, H.A.; Lewis, L.A.; Schultz, E.T. Distinguishing Multiple Lineages of *Pediastrum duplex* with Morphometrics and a Proposal for Lacunastrum gen. nov. J. Phycol. 2011, 47, 123–130.

36. Neustupa, J. Patterns of Symmetric and Asymmetric Morphological Variation in Unicellular Green Microalgae of the Genus *Micrasterias* (Desmidiales, Viridiplantae). Fottea 2013, 13, 53–63.

37. Lenarczyk, J.; McManus, H.A. Testing the Boundaries of the Green Algal Species *Pediastrum alternans* (Chlorophyceae) Using Conventional, Geometric Morphometric and Phylogenetic Methods. Phycologia 2016, 55, 515–530.

38. Neustupa, J. Asymmetry and Integration of Cellular Morphology in *Micrasterias compereana*. BMC Evol. Biol. 2017, 17, 1.

39. Lenarczyk, J. Evolution of Morphological Variability and Modularity in Single Cells of Algal Colonies: A Case Study *Pseudopediastrum* (Hydrodictyaceae, Sphaeropleales, Chlorophyceae). Phycologia 2019, 58, 180–191.

40. Neustupa, J.; Woodard, K. Geometric Morphometrics Reveals Increased Symmetric Shape Variation and Asymmetry Related to Lead Exposure in the Freshwater Green Alga *Micrasterias compereana*. Ecol. Indic. 2020, 111, 106054.

41. Rohlf, F.J.; Slice, D. Extensions of the Procrustes Method for the Optimal Superimposition of Landmarks. Syst. Zool. 1990, 39, 40–59.

42. MacLeod, N. Morphometrics: History, Development Methods and Prospects. Zool. Syst. 2017, 42, 4–33.

43. MacLeod, N. Use of Landmark and Outline Morphometrics to Investigate Thecal Form Variation in Crushed Gogiid Echinoderms. Palaeoworld 2015, 24, 408–429.

44. Neustupa, J.; Nemcova, Y. Morphological Allometry Constrains Symmetric Shape Variation, but not Asymmetry, of *Halimeda tuna* (Bryopsidales, Ulvophyceae) Segments. PLoS ONE 2018, 13, e0206492.

45. Zelditch, M.L.; Swiderski, D.L.; Sheets, D.H. Geometric Morphometrics for Biologists: A Primer, 2nd ed.; Elsevier Academic Press: London, UK, 2012; p. 478.

46. Burnham, K.P.; Anderson, D.R. Multimodel Inference: Understanding AIC and BIC in Model Selection. Sociol. Meth. Res. 2004, 33, 261–304.

47. Dryden, I.L. Shapes: Statistical Shape Analysis. R Package Version 1.2.6. 2021. Available online: https://CRAN.R-project.org/package=shapes (accessed on 2 November 2021).

48. R Core Team. R: A Language and Environment for Statistical Computing. 2021. Available online: https://www.r-project.org/ (accessed on 2 November 2021).

49. Hammer, Ø.; Harper, D.A.T.; Ryan, P.D. PAST: Paleontological Statistics Software Package for Education and Data Analysis. Palaeont. Electron. 2001, 4, 1–9.

50. Cox, J.D. Deformed Diatoms. Proc. Am. Soc. Micr. 1890, 12, 178–183.

51. Jahn, R.; Kusber, W.H. Algae of the Ehrenberg Collection: 1. Typification of 32 Names of Diatom Taxa Described by C. G. Ehrenberg. Willdenowia 2004, 34, 577–595.

52. Mann, D.G.; Chepurnov, V.A.; Idei, M. Mating System, Sexual Reproduction, and Auxosporulation in the Anomalous Raphid Diatom *Eunotia* (Bacillariophyta). J. Phycol. 2003, 39, 1067–1084.

53. Geitler, L. Der Formwechsel der Pennaten Diatomeen (Kieselalgen). Arch. Protistenkd. 1932, 78, 1–226.

54. English, J.D.; Potapova, M.G. Ontogenetic and Interspecific Valve Shape Variation in the Pinnatae Group of the Genus *Surirella* and the Description of *S. lacrimula* sp. nov. Diat. Res. 2012, 27, 9–27.

55. Vanormelingen, P.; Chepurnov, V.A.; Mann, D.G.; Sabbe, K.; Vyverman, W. Genetic Divergence and Reproductive Barriers among Morphologically Heterogeneous Sympatric Clones of *Eunotia bilunaris* sensu lato (Bacillariophyta). Protist 2008, 159, 73–90.

56. Falasco, E.; Bona, F.; Ginepro, M.; Hlúbiková, D.; Hoffmann, L.; Ector, L. Morphological Abnormalities of Diatom Silica Walls in Relation to Heavy Metal Contamination and Artificial Growth Conditions. Water SA 2009, 35, 595–606.

57. Kulichová, J.; Neustupa, J.; Vrbová, K.; Levkov, Z.; Kopalová, K. Asymmetry in *Luticola* species. Diatom Res. 2019, 34, 67–74.

58. Lavoie, I.; Hamilton, P.B.; Morin, S.; Tiam, S.K.; Kahlert, M.; Gonçalves, S.; Falasco, E.; Fortin, C.; Gontero, B.; Heudre, D.; et al. Diatom Teratologies as Biomarkers of Contamination: Are all Deformities Ecologically Meaningful? Ecol. Indic. 2017, 82, 539–550.

59. Fernández, M.R.; Martín, G.; Corzo, J.; De La Linde, A.; García, E.; López, M.; Sousa, M. Design and Testing of a New Diatom-based Index for Heavy Metal Pollution. Arch. Environ. Contam. Toxicol. 2018, 74, 170–192.

60. Wishkerman, A.; Hamilton, P.B. Shape outline extraction software (DiaOutline) for elliptic Fourier analysis application in morphometric studies. Appl. Plant Sci. 2018, 6, e1204.

61. Coquillé, N.; Morin, S. Fitness of Teratological Morphotypes and Heritability of Deformities in the Diatom *Gomphonema gracile*. Ecol. Indic. 2019, 106, 105442.

5. Morphometric variation and allometric trajectories in the genus *Eunotia* (Bacillariophyceae, Eunotiophycideae)

[submitted as Woodard, K. & Neustupa, J. Morphometric variation and allometric trajectories in the genus *Eunotia* (Bacillariophyceae, Eunotiophycideae). "Biological Shape Analysis - Proceedings of the International Symposium".]

Abstract

We explored diversity of ontogenetic allometric trajectories in the diatom genus *Eunotia* (Bacillariophyceae, Eunotiophycideae). The frustules of diatoms decrease in size over the vegetative part of their life cycle and this size diminution is related to a shape change of their silica frustules. We explored whether the allometric trajectories of morphologically close species tend to be similar. This would mean that the shape changes throughout the vegetative part of the life cycle are constrained by the initial morphology of the largest cells at the beginning of the vegetative life cycle. On the other hand, if the trajectories are divergent, they may be driven by different factors. We obtained the diminution series of 70 *Eunotia* species and captured outline morphology of frustules via 40 equidistant landmarks and semilandmarks. Morphospaces of the largest and smallest cells of individual diminution series were constructed via principal component analysis of Procrustes aligned landmarks with semilandmarks slid according to the minimum bending energy criterion. The allometric space of investigated species was based on slope values yielded by shape-to-size linear regression analyses. The results showed that shape changes throughout the life cycle are relatively conservative across the genus-level diversity except of a few species whose allometric trajectories were profoundly divergent, which may indicate their potential for morphological and subsequent evolutionary diversification.

Key words: *allometric trajectories, ontogeny, geometric morphometrics, diatoms*

Introduction

Diatoms are ubiquitous single celled algae with peculiar morphology. Their rigid cell walls, frustules, consist of polymeric silicon dioxide. Diatom frustule is composed of two parts, an epivalve and a hypovalve. In most cases, both valves have the same morphology and ornamentation, only epivalve is slightly larger and it fits over the hypovalve in similar way as a lid of a box (1). Diatoms abound in number of various shapes and ornamentations that are traditionally used for taxonomic determination. The morphology of the diatom frustule is closely related to the life cycle of these algae. During the life cycle, long lasting (several months up to several years) vegetative division phases are alternated by short periods of sexual reproduction (2). During the long periods of vegetative division, the cell size decreases in populations (1;3). This is due to the fact that during the vegetative division, new valves are synthesized inside the original frustule. Therefore, cells of every new generation are slightly smaller. When the population reaches a certain minimum cell size, it triggers sexual reproduction and the maximum cell size is restored. The size reduction was considered as an inevitable consequence of the way of vegetative division (4;5), however, it has been proved that this process can be overcome (6) and now most researchers are inclined to the theory that the size diminution is a way of timing the sexual reproduction (7;8;9).

Shape changes of the frustules that take place during the long phase of vegetative reproduction and size reduction have been documented in numerous studies (3;10;11;12;13). These shape changes are highly correlated with size change of the frustules (14;15). In this case, it is size diminution, which is a difference from most other organisms, where allometric shape change is related to their growth. The shape changes throughout the diatom life cycle can be caused by the changes of the inner cell environment connected to size reduction and change of the cellular S/V ratio (3;12). It has been proposed that during vegetative division, mother valves serve as molds for synthesis of the new valves (12). Consequently, some inaccuracies can be passed on to the next generations (12). Finally, frustule shape can be affected by the environmental conditions (16;17). Several studies of ontogenetic allometric trends in diatoms have been carried out for the purpose of taxonomic investigation (14;18;19). The authors aimed to distinguish between closely related species based not only on morphological characteristics of the frustules but also on possible differences in the trajectories of the shape changes throughout the vegetative phase of the life cycle.

In this study, we examined whether the allometric trajectories of diatom species are constrained by the morphology of the largest initial cells that occur in the beginning of the vegetative phase, or whether the allometric trajectories are rather flexible and may be driven by other factors. We hypothesized that if the allometric trajectories of morphologically similar species

are relatively divergent, such allometric diversity may be a substrate for subsequent morphological and evolutionary diversification of the genus. On the contrary, high correlation of the among-species morphospace and their allometric trajectories would indicate that the shape changes throughout the vegetative phase are strongly constrained by the frustule morphology and therefore they are evolutionarily conserved.

To depict the pattern of allometric diversity of the diatom species, we used the concept of allometric space which is a multivariate space where each allometric trajectory is represented by a unique point. This concept was first introduced by Gerber et al. (20) in a study exploring the role of development in the evolution of morphological disparity and since then, it was used in several studies (21;22;23). In these studies, the allometric space was carried out as an ordination analysis of first principal component from PCA of morphological data. This approach is based on the Huxley-Jolicoeur school which defines allometry as the covariation among morphological features (linear measurements) that all contain size information (24;25). In the diatomology, this approach was applied in the classic work of Geitler (3) where the author studied covariation of different measurements of the diatom frustule (typically cell length and width) during the size reduction period of life cycle. In contrast, the Gould-Moismann school defines allometry as a correlation between size and shape, while the size is a scalar property that can be quantified by a single number, and shape is defined geometrically and it is size free (25). This concept lies in the basics of the geometric morphometrics where allometry is carried out as a shape-to-size regression. Within the framework of geometric morphometrics, the concept of allometric spaces was used in a study where the allometric patterns of individual populations of *Micrasterias* were compared to the degrees of allometric scalling of S:V ratio (26). For construction of allometric spaces in this study, the slope values from linear shape-to-size regressions of individual populations were used.
The present study follows the geometric morphometrics approach. For analysis of the allometric trajectories of diatoms throughout the vegetative phase of the life cycle, we chose a model genus *Eunotia* Ehrenberg that is characterized by bilateral symmetry and semilunar frustule outline. We analyzed the data for 70 species based on the microphotographs representing their size diminution series illustrated in a monograph of Lange-Bertalot et al. (27). The frustule outlines were registered by 2 landmarks and 38 semilandmarks and they were analyzed by methods of geometric morphometrics (28). Finally, in order to study allometric trajectories and their relation to frustule morphology we compared the morphospaces of the largest and smallest cells of each species with the allometric space of all the species.

Material and Methods

Data acquisition

In order to obtain cell outline data, we used the microphotographs of the characteristic diminution series of *Eunotia* species from the authoritative taxonomic monograph Diatoms of Europe, Vol. 6 (27). The dataset consisted of 70 *Eunotia* species and each species was represented by a size diminution series of 6 to 20 cells (Tab. 1). The entire dataset consisted of 804 cells. The cell outlines were registered via equidistant landmarks captured in the program TpsDig ver. 2.17 (29). Overall 40 landmarks were positioned along the cell outline, out of which 2 landmarks were placed in a fixed position (nos 1; 20) and 38 equidistant landmarks were treated as semilandmarks (nos 2 – 19; 20 – 40), (Fig. 1). This means that they were allowed to slide iteratively along tangents to the respective curve and their final position was determined by the smallest possible bending energy between each configuration and the mean shape of the dataset (30;31). The two fixed landmarks were placed on the intersections of the apical axis of the cells. The cell outlines represented by the landmark configurations were symmetrized along the transapical axis (32). The subsequent analyses were conducted on the symmetrized data.

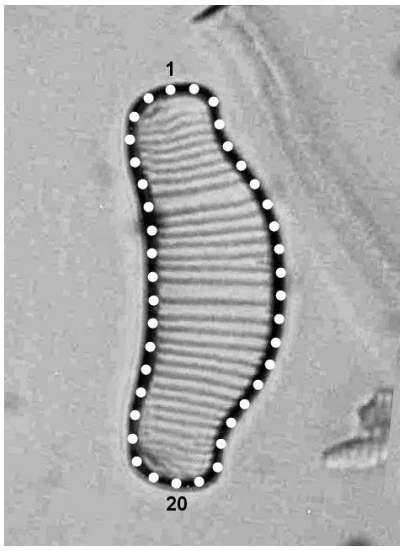

Fig. 1. 40 landmarks along the cell outline. 2 fixed landmarks (nos 1; 20) and 38 equidistant landmarks treated as semilandmarks.

Morphospace construction

The landmark configurations of the largest cells from each series corresponding to each species were superimposed by the generalized Procrustes analysis (GPA) in TpsRelw ver. 1.46 (29).

Principal component analysis (equivalent to the relative warps analysis, RWA, with $\alpha = 0$) of the aligned coordinates was performed in order to construct the morphospace of the largest cells. For illustration of the morphospace, the first two relative warps were plotted against each other and the margins of the realized morphospace were visualized via deformation grids based on the thin-plate spline interpolation (28). The morphospace of the smallest cells of each species was constructed in similar way using the configurations of the smallest cells from each series.

Allometric space construction

For the construction of the allometric space, the landmark configurations of the cells from each size diminution series (i. e. each species) were subjected to a generalized Procrustes superimposition. Subsequently, a series of linear shape-to-size regression analyses was conducted for each species separately in PAST, ver. 2.17 (33). In these regression analyses, the shape was represented by all *x* and *y* coordinates of every landmark in each configuration and the size was represented by the centroid size (CS) values of the landmark configurations. The slope values from the shape-to-size regressions of each species were subjected to a PCA analysis (26). As a result, each allometric trajectory of each species was represented by a unique point in the ordination space of the principal components. A point representing a hypothetical species with no allometric shape change was included in the dataset with values of the slopes $a = 0$ (26). The visualizations of the shape differences between the biggest and the smallest cells of selected species were conducted in TpsRegr 1.41 (29).

Procrustean tests

The correspondence of two morphospaces and the allometric space was tested using the Procrustean tests (34;35) in R, ver. 2.15.3, package *vegan*, function *protest* (36).

First, the principal components of the morphospace of the largest and smallest cells and the allometric space data were subjected to a three-dimensional non-metric multidimensional scaling (NMDS) procedure (33). The result of the NMDS for each dataset (both morphospaces and the allometric space) was three axes that represented variation between species. Then, pairs of these configurations were rotated in order to maximize their fit using Procrustes superimposition. The significance of the Procrustes fit was tested via permutation procedure *protest* with 9999 repetitions. Using this method we compared and tested the allometric space vs. morphospace of the largest

cells, allometric space vs. morphospace of the smallest cells, and morphospace of the largest cells vs. morphospace of the smallest cells.

Table 1. List of species including the plate numbers in the original publication and sizes of the largest and smallest cells of the diminution series expressed via centroid size of landmark configurations.

Species	**Plate**	**Centroid size max.**	**Centroid size min.**
E. ambivalens	13	4612.87	2020.29
E. genuflexa	16	4921.23	3948.26
E. mucophila	23	1981.18	690.75
E. jettnerae	26	3786.00	1599.57
E. cantonatii	28	3834.25	1433.28
E. bilunaris b	30	1506.75	566.47
E. bilunaris c	31	3686.38	1577.19
E. bilunaris d	32	3169.40	1761.38
E. mertensiae	34	1600.45	1045.08
E. incisa	38	1360.49	522.31
E. boreoalpina	39	1735.81	741.52
E. rhomboidea	41	1167.20	668.34
E. exsecta	46	2127.23	1072.21
E. sedina	47	2684.12	1152.70
E. julii	51	2503.63	1398.96
E. novaisiae	52	1369.70	876.11
E. hexaglyphis	57	1482.50	1091.10
E. obtusinasuta	58	2327.33	746.00
E. dorofeyukae	60	2350.13	956.50
E. circumborealis	61	1211.82	549.26
E. islandica	63	1761.90	559.05
E. cisalpina	67	1641.48	535.34
E. meridionalis	69	829.16	625.44
E. macaronesica	71	1145.90	948.24
E. neoscandinavica	75	4274.20	1923.17
E. diodon	77	2337.44	1643.81

E. suecica	88	2188.65	1405.97
E. papiliofalsa	91	1077.23	795.61
E. herkiniensis	94	982.90	907.44
E. implicata	97	1154.48	551.05
E. varioundulata	101	765.44	637.72
E. paratridentula	110	705.86	281.06
E. trinacria	112	520.17	325.63
E. muscicola	113	895.59	511.23
E. perminuta	114	868.17	568.25
E. exigua	115	820.14	277.05
E. meisteri	118	543.64	395.84
E. nymanniana	120	1625.33	550.22
E. elegans	124	1087.81	718.98
E. arculus	125	1797.02	504.54
E. boreotenuis	126	1448.51	358.62
E. botuliformis	128	1459.66	489.49
E. tenella	129	766.94	336.52
E. pseudogroenlandica	132	1458.20	520.36
E. falacoides	135	856.52	916.32
E. neofallax	136	1079.21	679.68
E. groenlandica	137	1424.68	912.95
E. silesioscandica	139	1111.35	638.88
E. nanolusitanica	139	1484.42	542.70
E. pexii	139	1054.39	618.37
E. ferefalcata	139	1530.92	682.84
E. wiltschkorum	141	910.24	582.50
E. seminulum	144	724.77	407.41
E. chelonia	145	719.55	470.72
E. paludosa	146	1628.79	536.80
E. superpaludosa	148	2041.34	1454.60
E. ursamaioris	152	1373.60	469.43
E. scandiorussica	154	2254.58	685.85
E. intermedia	156	1713.03	636.92

E. minor	162	1483.22	651.39
E. michaelis	165	1222.24	776.70
E. pectinalis	166	4736.65	914.61
E. soleirolii	168	1765.62	577.53
E. fennica	175	1362.63	773.28
E. arcus	183	2299.19	790.46
E. insubrica	194	1258.03	825.28
E. compactarcus	194	1561.27	880.21
E. curtagunrowii	195	1021.59	594.31
E. excelsa	200	2369.15	741.15
E. valida	213	2593.45	891.29

Results

Morphospace of the largest and smallest cells

The morphospace of the largest cells (i.e. those occurring at the beginning of the vegetative phase of the life cycle) mainly differentiated between robust rounded cells with capitate apices and elongated narrow cells (Fig. 2). This morphological trend was captured by PC1 and it accounted for 70.5% of total morphospace variability. At one margin of the morphospace along this axis, there were extremely elongated, thin cells with no undulations similar to *E. ambivalens, E. genuflexa* and *E. cantonatii*, and at the other margin, the cells were robust and they had distinct capitate apices similar to *E. insubrica, E. michaelis* and *E. curtagunrowii*. PC2 accounted for 18.5% of variability and it corresponded to curvature of the cells. At the negative margin of this axis, there were almost straight cells similar to *E. boreoalpina, E. rhomboidea* and *E. neoscandinavica* with no curvature, while on the other margin, the cells were markedly curved as *E. elegans, E. pexii* and *E. scandiorussica*.

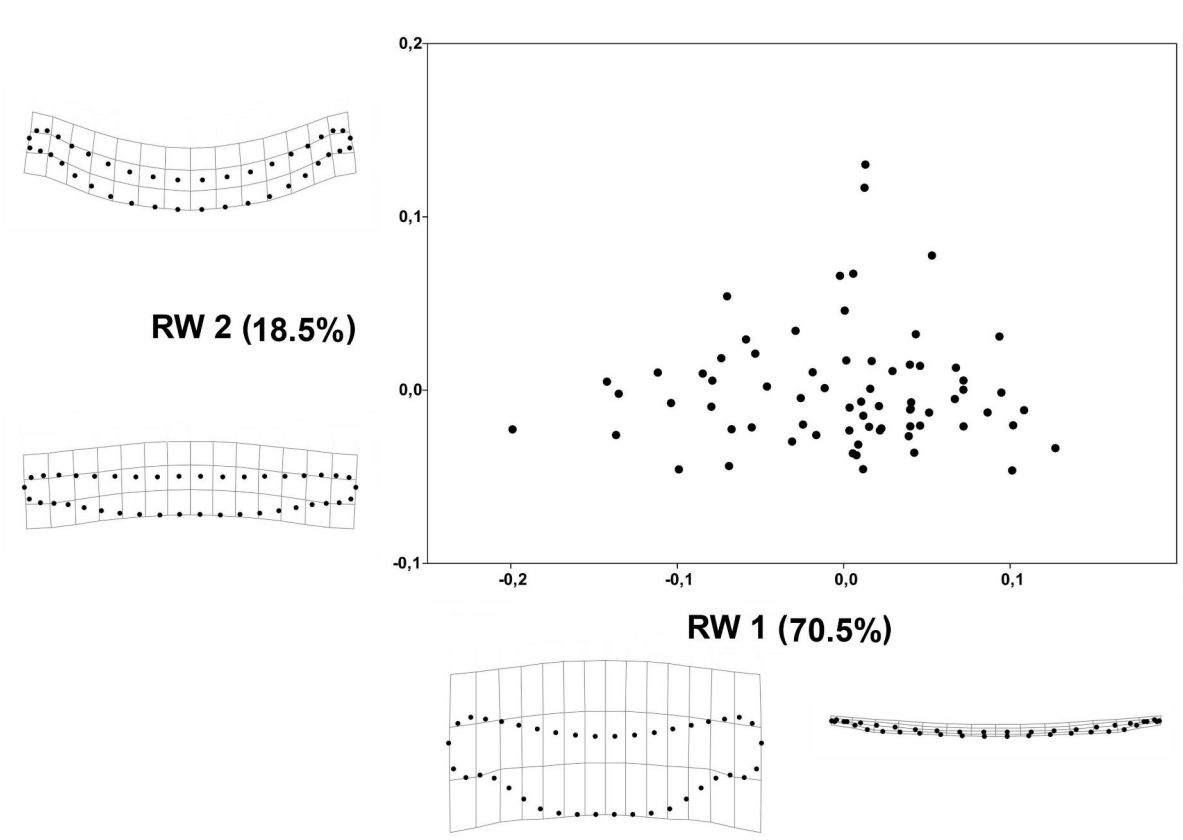

Fig. 2. Ordination plot of the second (RW2) vs. first (RW1) relative warps representing the shape differences in the largest cells of the diminution series of each species. Thin-plate splines represent the margins of the realized morphospace on a particular warp.

The first principal component (PC1) of the morphospace of the smallest cells (i.e. those occurring at the end of the vegetative diminution phase) accounted for 80% of the variability (Fig. 3) and it corresponded to the cell robustness in a way quite similar to the PC1 of the morphospace of the large cells. PC2 accounted for 6.4% of the variability and it corresponded to the curvature of the cells and, at the same time, undulation of the dorsal margins of the cells. On one margin of the PC2, there were almost straight cells with slight curvature on the dorsal margins and with no undulations similar to *E. paludosa*, *E. intermedia* and *E. soleirolii*. On the opposite margin of the PC2, there were cells with strong curvature on both margins and undulated dorsal margins similar to *E. elegans, E. suecica* and *E. pexii*. Comparing the overall outline of the two morphospaces, the outlines of the smallest cells were generally more robust and rounded than the outlines of the large cells. Also the curvature and the capitate shape of the apical parts were less pronounced in the smallest cells. However, overall trends in both morphospaces were relatively similar and in both cases, the morphospace was evenly occupied by the species.

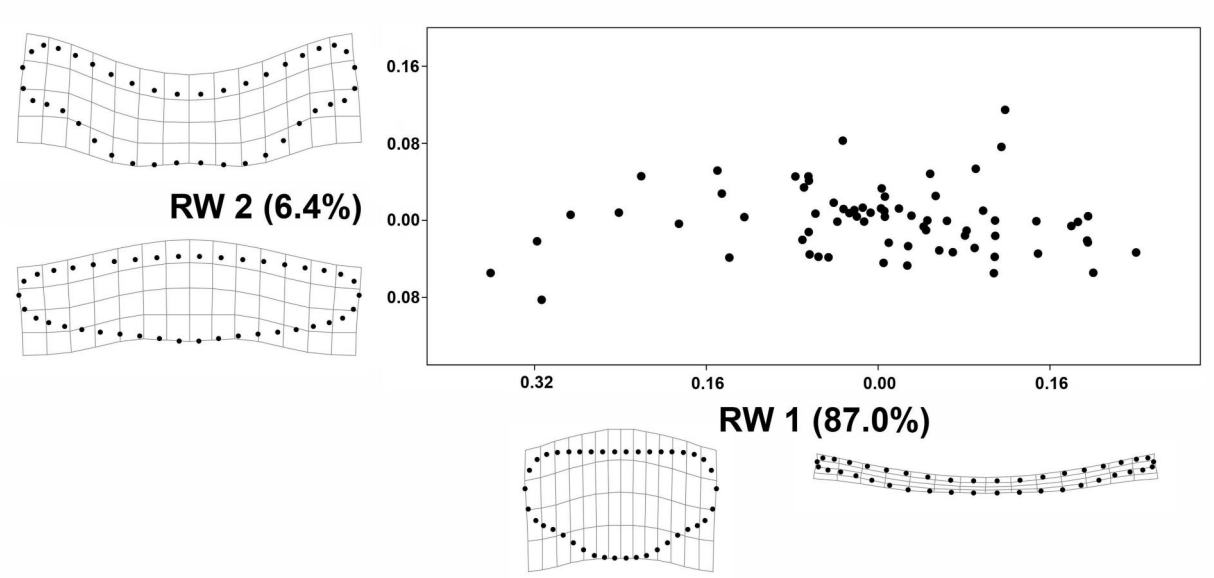

Fig. 3. Ordination plot of the second (RW2) vs. first (RW1) relative warps representing the shape differences in the smallest cells of the diminution series of each species. Thin-plate splines represent the margins of the realized morphospace on a particular warp.

Allometric space

Allometric space was based on PCA of slope values from individual shape-to size linear regression analyses of individual species. PC1 accounted for 82.8% of variability and PC2 accounted for 6.5% of variability. In contrast to both morphospaces, allometric space was occupied strongly unevenly. The species typical by narrow, elongated, straight or slightly curved cells with no undulations clustered tightly together (Fig. 4). Thus, the allometric trajectories of the species with this rather simple, semilunar outline were remarkably similar. By visual inspection the cell shape of these species changed only modestly during the vegetative part of the life cycle. Typical representative of this group is *E. genuflexa* with very narrow, elongated, slightly curved cells that stayed almost unchanged during the size diminution phase; or *E. groenlandica* with semilunar cells with slight curvature of the dorsal margins.

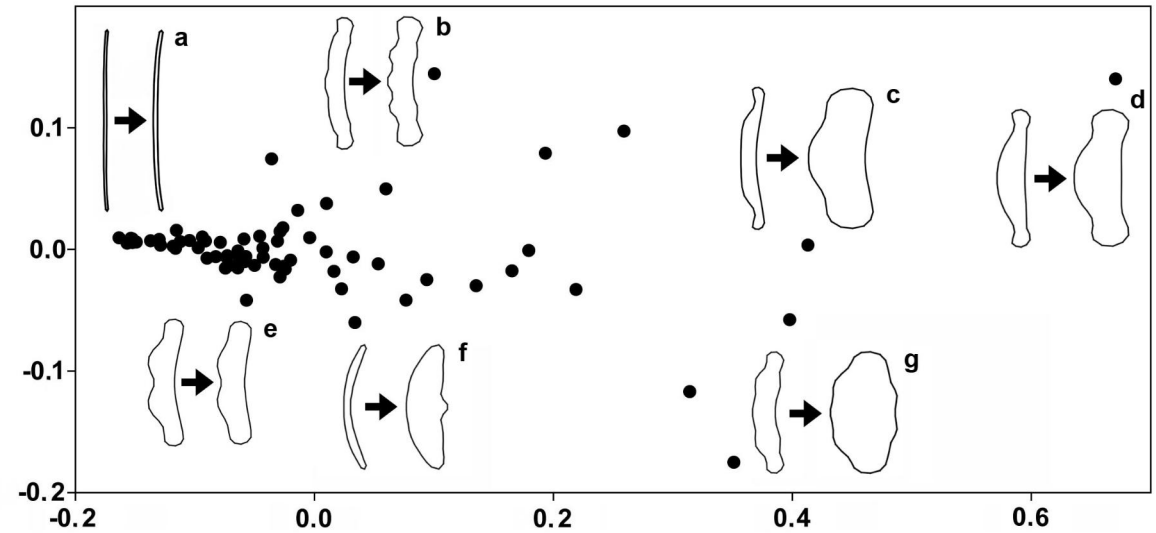

Fig. 4. Allometric space representing diversity of ontogenetic allometric trajectories of individual species. Visualizations of cell outlines represent shape differences between the largest and smallest cells. Arrows represent direction of the ontogenetic change. (a) *E. genuflexa*; (b) *E. perminuta*; (c) *E. tenella*; (d) *E. meisteri*; (e) *E. macaronesica*; (f) *E. bilunaris b*; (g) *E. paratridentula*.

Besides these species with simple elongated shapes and homogeneous allometric trajectories, there were species whose allometric trajectories were quite divergent and, thus, they occupied marginal positions of the allometric space. In these taxa, the final shape at the end of the vegetative phase often differed markedly from the initial shape at the beginning of the life cycle. During the size diminution of these species, different shape patterns and structures on the cell outline arose or disappeared. Specifically, the large cells of one morphotype of *E. bilunaris* had elongated semilunar shape with smooth frustule outline and similar curvature of both dorsal and ventral margins. During the size diminution phase, a central inflation appeared on the ventral margin of the frustules. In several species, the capitate apices become less pronounced or they disappeared completely as in *E. tenella* of *E. trinacria*. The large cells of *E. exigua* had strong curvature on both dorsal and ventral margins and pronounced capitate apices. Compared to that, the smallest cells were almost round with no curvature on the ventral margin and with less pronounced capitate apices. In the *E. paratridentula,* the large cells were slightly curved and they had undulations on both dorsal and ventral margins. In contrast, the ventral margin of the small cells was curved outwards. The large cells of *E. perminuta, E. paratridentula* and *E. muscicola*, the number of the dorsal undulations decreased.

Correlation of the allometric space and the morphospaces

Three Procrustean tests were conducted to detect possible correlations between three ordination spaces: the allometric space and two morphospaces based on the largest and the smallest cells of individual diminution series. The tests revealed a consistent significant relationship between the three ordination spaces (Tab. 2). However, the tests also showed a considerable residual variability that could not be removed by the superimposition of the ordination spaces. This residual variability was the highest in the comparison of the allometric space and the morphospace of the largest cells. Nevertheless, even in this case, the result of the permutation test showed strongly significant relationship between the structure of the allometric space and the morphospace of the largest cells.

Table 2. Correlation of the allometric space and the morphospaces – results of the Procrustean tests.

Matrices compared	Procrustes Sum of Squares (m12 squared)	Correlation in a symmetric Procrustes rotation	p-value
Allometric space VS **morphospace** of the largest cells	0.78	0.47	0.0001
Allometric space VS **morphospace** of the smallest cells	0.65	0.60	0.0001
Morphospace of the largest cells VS **morphospace** of the smallest cells	0.63	0.61	0.0001

The comparison of two morphospaces based on the largest and smallest cells of each species revealed the highest correlation from all three Procrustean tests. This result reflected a fact that in many of the tested species the specific morphological characters were relatively stable throughout the entire size diminution phase. In addition, higher Procrustes sums of squares in the tests evaluating relation of both morphospaces and the allometric space reflected the conservative pattern of allometric trajectories in a number of morphologically diverse species whose shape did not change profoundly during the vegetative part of the life cycle.

Discussion

The frustule outlines of *Eunotia* species included in this study fell into three major shape types – *E. bilunaris*-like species characterized by elongated semilunar smooth cell outlines with no undulations and slight to strong curvature of both dorsal and ventral parts; robust species characterized by pronounced capitate apices and slight to strong curvature; and finally species characterized by undulations typically occurring on the dorsal margins of the cells. This trend was reflected in the morphospace based on PCA of the superimposed coordinates of the largest cells of each species. In this morphospace, robustness or narrowness of the cell outlines accounted for the most of the morphological variation in the studied set and constituted its most distinctive morphological feature. Other significant features that dominated this morphospace were the extent of the cell curvature and presence or absence of the capitate apices.

The morphospace based on the smallest cells was quite similar to the morphospace of the large cells. The robustness or the narrowness accounted for the most of the variability followed by the cell curvature. Even though the two morphospaces were quite similar, there are several differences. The ventral margins of the small cells are more often bulged outwards, and, in addition, the undulations on the dorsal margins of the cells are slightly more pronounced in the morphospace of the small cells.

In overall comparison, the outline of the small cells was more robust and, by visual inspection, their length-to-width ratio was smaller than in the large cells. In other words, during the vegetative phase of the life cycle the cell outline became more rounded. This trend of shape change that was detected in the genus *Eunotia* is typical for most of the bilateral diatom genera (1;2;37;38;39;40;41;42) and it is strongly allometric, i.e. related to size change. In the classic Geitler's monograph (3), the author describes that during the size reduction phase of the life cycle, the apical axis of the cells tends to shorten more rapidly than the transapical axis. It can also be described as increase in circularity of the cell outlines that is expressed by isoperimetric quotient (15;43). Increasing circularity of the cell outlines is related to several phenomena. In isometrically scaled objects, volume decreases faster than surface and therefore, the S-to-V ratio increases with decreasing size (44). For single celled organisms, the change of the S-to-V ratio directly affects metabolism and physiology since the cell walls are the areas of the contact with environment and substance exchange. However, in diatoms, the increasing circularity during the size diminution phase may decelerate the increase of the S-to-V ratio during the size reduction phase. Therefore, the impact of the cell size diminution might be mitigated by the gradual shape change of the cells.

In total, about 70% of the analyzed species formed a tight cluster in the allometric space, which indicated that their allometric trajectories were very close. The species that were represented by these trajectories often had similar shapes as well. They were mostly characterized by the *E. bilunaris*-like morphology, i.e. they had narrow, elongated, slightly curved outlines with no undulations. Throughout the size reduction phase, the shape changes of the cell outlines of these species were not excessive. Their shape changed mostly via shortening of the apical length, and if the capitate apices were present, they became less pronounced. At the same time, width of the frustules decreased much slower than the apical length. Similar allometric trends were observed in different taxons such as in *Stauroneis, Surirella* or *Luticola* (14;15;37). On the other hand, there was a number of species, whose positions in the allometric space were more distant from the aforementioned cluster. Interestingly, these species typical by divergent allometric trajectories often had more complex/elaborate shapes (i.e. capitate apices, undulations along the cellular margins) than those with *E. bilunaris*–like morphology. Shape changes associated with the allometric dynamics in some of these species (*E. paratridentula, E. muscicola, E. perminuta*) involved decrease in number of undulations on the dorsal margins of frustules. It should be noted that the number of the undulations on the dorsal margin of some species, such as *E. zygodon*, was considered stable and it was used as a taxonomic character. However, it was found that it can change during the size reduction phase of the life cycle (45). In general, the species with divergent trajectories distant from the center of the allometric space were characterized by more heterogeneous shape changes during the size reduction phase. However, the complexity of the outlines and the heterogeneity are not necessarily related and testing this hypothesis may be a future area of research.

When comparing the relationship of the allometric space and the morphospaces of the largest and smallest cells, the three ordination spaces were generally strongly correlated. This result implicates that the allometric trajectories were relatively conservative and the differences in morphological characteristics of individual taxa were relatively stable throughout the size reduction phase. However, there was a notable residual variability that was based on relatively few species. These species with divergent and heterogeneous allometric trajectories require closer examination. It has been hypothesized that new morphological variants may arise via extension or early interruption of developmental pathways (46). The species with heterogeneous, complex and divergent trajectories therefore provide a substrate for a different type of morphological diversification, which may then lead to occupation of new parts of the morphospace (20;25;47;48). Subsequently, such morphological heterogeneity may lead to additional evolutionary

diversification. Thus, the species with divergent allometric trajectories might play an important role in the morphological evolution of the genus *Eunotia*.

The most characteristic feature of diatom phenotype is their bipartite silica frustule and their life cycle that is directly linked to frustule's topology and structure. Unlike most organisms that grow during their ontogeny, diatom cell size decreases in the time of their life cycle. This size diminution is accompanied by a shape change of repeated phenotypic expressions of a single clonal genotype and, therefore, it has been considered as ontogenetic allometry (14). These ontogenetic allometric trajectories of diatoms proved to be a useful taxonomic character. Even if the species specific morphology in one stage of life cycle is identical in multiple taxa, their trajectories may be different (14;19;49;50;51;52). Allometric trajectories may also be a substantive feature that affects ecology of diatoms. Large cell size range of diatoms throughout the vegetative life cycle of every clonal population causes variability in the S:V ratios. Therefore, it significantly expands their niche breadth in relation to some of the key environmental factors such as temperature, nutrients or pH (53). This phenomenon has been considered one of the reasons of widespread and ecological dominance of diatoms in microphytobentos (54). It has also been suggested that different size classes in the life cycle of a single diatom species may be selected by varying environmental conditions among the habitats (55).

Finally, based on the outcomes of the present study, exploration of allometric spaces of diatoms may bring new insights into morphological diversification of diatom lineages. In this context, correlation of allometric diversity of diatom lineages with their phylogenetic history will be especially interesting. However, current lack of molecular data for most of the diatom species hinders research in this field. Advances in this research area will enable formal testing of real significance of the allometric diversification for evolutionary radiation of this extremely important group of eukaryotic microorganisms.

References

1. Round FE, Crawford RM, Mann DG. (1990) The Diatoms: Biology and Morphology of the Genera. Cambridge University Press, Cambridge.

2. Edlund MB, Stoermer EF. (1997) Ecological, evolutionary, and systematic significance of diatom life history. J Phycol 33: 897–918.

3. Geitler L. (1932) Der Formwechsel der pennaten Diatomeen (Kieselalgen). Arch Protistenkunde 78: 1–226.

4. MacDonald JD. (1869) On the structure of diatomaceous frustule, and its genetic cycle. Ann Mag Nat Hist 3: 1–8.

5. Pfitzer E. (1869) Über den Bau und die Zellteilung der Diatomeen. Bot Ztg 27: 774–776.

6. Chepurnov VA, Chaerle P, Roef L, Van Meirhaeghe A, Vanhoutte K. (2011) Classical breeding in diatoms: scientific background and practical perspectives. In: J Secbach & JP Kociolek (eds), The diatom world, pp. 167–194. Springer, Dordrecht.

7. Lewis WM Jr. (1984) The diatom sex clock and its evolutionary significance. Am Nat 123: 73–80.

8. Jewson DH. (1992) Size reduction, reproductive strategy and the life cycle of a centric diatom. Philos Trans R Soc B 336: 191–213.

9. Mann DG. (2011) Size and sex. In: J Secbach & JP Kociolek (eds), The diatom world, pp. 145–166. Springer Dordrecht.

10. Theriot E, Ladewski TB. (1986) Morphometric analysis of shape of specimens from the neotype of *Tabellaria flocculosa* (Bacillariophyceae). Am J Bot 73: 224–229.

11. Cox EJ. (1993) Diatom systematics – a review of past and present practice and a personal vision for future development. Beih Nova Hedwigia 106: 1–20.

12. Schmid AM. (1994) Aspects of morphogenesis and function of diatom cell walls with implications for taxonomy. Protoplasma 181: 43–60.

13. Mann DG, Chepurnov VA. (2005) Auxosporulation, mating system, and reproductive system in *Neidium* (Bacillaiophyceae). Phycologia 44: 335–350.

14. English JD, Potapova MG. (2012) Ontogenetic and interspecific valve shape variation in the Pinnatae group of the genus *Surirella* and the description of *S. lacrimula* sp. nov. Diat Res 27: 9–27.

15. Woodard K, Kulichová J, Poláčková T, Neustupa J. (2016) Morphometric allometry of representatives of three naviculoid genera throughout their life cycle. Diat Res, 31: 231–242.

16. Falasco E, Bona F, Badino G, Hoffmann L, Ector L. (2009) Diatom teratological forms and environmental alterations: a review. Hydrobiologia 623: 1–35.

17. Kociolek JP, Stoermer EF. (2010) Variation and polymorphism in diatoms: the triple helix of development, genetics and environment. A review of the literature. Vie et Milieu 60: 75–87.

18. Cox E J. (2005) Defining morphological characters in diatoms: ontogeny as an aid to inferring homology. Phycologia 44: 24–24.

19. Edgar RK, Saleh AI, Edgar SM. (2015) A morphometric diagnosis using continuous characters of *Pinnunavis edkuensis*, sp. nov. (Bacillariophyta: Bacillariophyceae), a brackish–marine species from Egypt. Phytotaxa 212: 1–56.

20. Gerber S, Eble GJ, Neige P. (2008) Allometric space and allometric disparity: a developmental perspective in the macroevolutionary analysis of morphological disparity. Evolution 62: 1450–1457.

21. Wilson LAB, Sánchez–Villagra MR. (2010) Diversity trends and their ontogenetic basis: an exploration of allometric disparity in rodents. Philos Trans R Soc B 277: 1227–1234.

22. Watanabe A, Slice DE. (2014) The utility of cranial ontogeny for phylogenetic inference: a case study in crocodylians using geometric morphometrics. J Evol Biol 27: 1078–1092.

23. Tavares WC, Pessôa LM, Seuánez HN. (2016) Phylogenetic and size constrains on cranial ontogenetic allometry of spiny rats (Echimyidae, Rodentia). J Evol Biol 29: 1752–1765.

24. Huxley J. (1993) Problems of relative growth. The Johns Hopkins University Press. Baltimore, Md.

25. Klingenberg, CP. (2016) Size, shape, and form: concepts of allometry in geometric morphometrics. Dev Genes Evol 226: 113–137.

26. Neustupa, J. (2016) Static allometry of unicellular green algae: scaling of cellular surface area and volume in the genus *Micrasterias* (Desmidiales). J Evol Biol 29: 292–305.

27. Lange–Bertalot H (Ed.), Bak M, Witkowski A, Tagliaventi N. (2011) Diatoms of Europe: Diatoms of the European Inland Waters and Comparable Habitats. Volume 6: Eunotia and some related genera. Gantner Verlag, Ruggell.

28. Zelditch ML, Swiderski DL, Sheets HD. (2012) Geometric morphometrics for biologists: a primer. Elsevier, London.

29. Rholf FJ. (2013) TPS software series. Department of Ecology and Evolution, State University of New York, Stony Brook.

30. Perez SI, Bernal V, Gonzalez PN. (2006) Differences between sliding semi-landmark methods in geometric morphometrics, with an application to human craniofacial and dental variation. J Anat 208.6: 769–784.

31. MacLeod N. (2015) Use of landmark and outline morphometrics to investigate thecal form variation in crushed gogiid echinoderms. Palaeoworld 24: 408–429.

32. Klingenberg CP, Barluenga M, Meyer A. (2002) Shape analysis of symmetric structures: quantifying variation among individuals and asymmetry. Evolution 56: 1909–1920.

33. Hammer O, Harper DAT, Ryan PD. (2001) PAST: paleontological statistics software package for education and data analysis. Palaeont Electr 4: 1–9.

34. Jackson DA. (1995) PROTEST: a Procrustean randomization test of community environment concordance. Écoscience 2: 297–303.

35. Peres–Neto PR, Jackson DA. (2001) How well do multivariate data sets match? The advantages of a Procrustean superimposition approach over the Mantel test. Oecologia 129: 169–178.

36. Oksanen J, Blanchet FG, Kindt R, Legendre P, Minchin PR, O'Hara RB et al. (2013) *vegan*: Community Ecology Package. R package version 2.0–10. See http://CRAN.Rproject.org/package=vegan

37. Hostetter HP, Hoshaw RW. (1972) Asexual developmental patterns of the diatom *Stauroneis anceps* in culture. J Phycol 8: 289–296.

38. Tropper CB. (1975) Morphological variation of *Achnanthes hauckiana* (Bacillariophyceae) in the field. J Phycol 11: 297–302.

39. Stoermer EF, Ladewski TB. (1982) Quantitative analysis of shape variation in type and modern populations of *Gomphoneis herculeana*. Beih Nova Hedwigia.

40. Amato A, Orsini L, D'Alelio D, Montresor M. (2005) Life cycle, size reduction patterns, and ultrastructure of the pennate planktonic diatom *Pseudo-nitzschia delicatissima* (Bacillariophyceae). J Phycol 41: 542–556.

41. Cox E J. (2014) Diatom identification in the face of changing species concepts and evidence of phenotypic plasticity. Micropalaeontology 33: 111–120.

42. Rovira L, Trobajo R, Sato S, Ibáñez C, Mann DG. (2015) Genetic and physiological diversity in the diatom *Nitzschia inconspicua*. J Eukaryot Microbiol 62: 815–832.

43. Osserman R. 1978. The isoperimetric inequality. Bull Amer Math Soc 84: 1182–1238.

44. Okie JG. (2013) General models for the spectra of surface area scaling strategies of cells and organisms: fractality, geometric dissimilitude, and internalization. Amer Nat 181: 421-439.

45. Taylor JC, Cocquyt C, Mayama S. (2016) New and interesting *Eunotia* (Bacillariophya) taxa from the Democratic Republic of the Congo, tropical central Africa. Plant Ecol Evol 149: 291–307.

46. Strelin MM, Benitez–Vieyra S, Fornoni J, Klingenberg CP, Cocucci AA. (2016) Exploring the ontogenetic scaling hypothesis during the diversification of pollination syndromes in *Caiophora* (Loasaceae, subfam. Loasoideae). Ann Botany 117: 937–947.

47. Klingenberg CP, McIntyre GS. (1998). Geometric morphometrics of developmental instability: analyzing patterns of fluctuating asymmetry with Procrustes methods. Evolution, 52: 1363–1375.

48. Wilson LAB. (2013) Allometric disparity in rodent evolution. Ecol Evol 3: 971–984.

49. Potapova MG, Ponader KC. (2004) Two common North American diatoms, *Achnanthidium rivulare* sp. nov. and *A. deflexum* (Reimer) Kingston: morphology, ecology and comparison with related species. Diat Res 19: 33–57.

50. Edgar SM, Theriot EC. (2004) Phylogeny of *Aulacoseira* (Bacillariophyta) based on molecules and morphology. J Phycol 40: 772–788.

51. Edgar RK, Kociolek JP, Edgar SM. (2004) Life cycle–associated character variation in *Aulacoseira krammeri* sp. nov., a new Miocene species from Oregon, USA. Diat Res 19: 7–32.

52. Veselá J, Neustupa J, Pichrtová M, Poulíčková A. (2009) Morphometric study of *Navicula* morphospecies (Bacillariophyta) with respect to diatom life cycle. Fottea 9: 307–316.

53. Neustupa J, Veselá J, Šťastný J. (2013) Differential cell size structure of desmids and diatoms in the phytobenthos of peatlands. Hydrobiologia 709: 159–171.

54. Snoeijs P, Busse S, Potapova M. (2002). The importance of diatom cell size in community analysis. J Phycol 38: 265–281.

55. Kulichová J, Fialová M. (2016). Correspondence between morphology and ecology: morphological variation of the *Frustulia crassinervia–saxonica* species complex (Bacillariophyta) reflects the ombro–minerotrophic gradient. Cryptogam Algol 37: 15–28.

6. Key results and Conclusions

A study of three naviculoid genera revealed substantial amounts of ontogenetic allometry. These patterns indicated that size reduction is associated with the vast majority of shape variation of frustules in populations. Thus, it can be stated that in pennate diatoms, morphological allometry is the dominant element of their phenotypic variability. This variability is primarily manifested by increasing circularity of valve outlines and, on the other hand, by a gradual increase in shape variability among cells during the size reduction series. Slight shape differences among cells accumulate throughout the vegetative cycle, which may indicate a real physical inheritance of shape in the sense of David Mann's (1994) treatise on shape and form of diatom frustules. Interestingly, asymmetry within cells does not increase in clonal cultures during size reduction. This means that the symmetry of frustules is robust against developmental noise and it also means that developmental stability of small individuals may not be reduced even after many cycles of mitotic division compared to large cells at the beginning of the cycle. Raphid pennate diatoms, however, also have an inherent cryptic asymmetry that originates in the morphogenesis of individual frustules. In this context, my research showed that valve outlines of clonal strains of *Luticola poulickovae* exhibited a side-oriented shape asymmetry that was apparently related to the position of the primary and secondary valve sides.

In addition to side-oriented asymmetry, which typically reflects genus-level evolutionary processes, individual asymmetric deviations of diatoms are manifested at the level of individuals or populations. In many cases, they can be considered to be the result of environmental stress. Since these deviations are often slight and irregular, their description and quantification is not trivial. Therefore, the analyses in this thesis focused on the construction of a morphometric framework for the evaluation of individual asymmetry using the model system *Eunotia bilunaris*. The applied methodology based on the geometric morphometric analysis of symmetry showed that teratogenic shape deformations do not actually affect all parts of the valve outlines with the same frequency. Thus, it was possible to identify specific regions of the frustule that may be particularly sensitive to stress.

While ontogenetic allometric trends involve considerable variation among cells within a size reduction series, they also involve a substantial amount of stability at the species level. This intriguing phenomenon has traditionally been the basis for the morphological characterization of individual species. Analysis of these typical size reduction series in the raphid pennate genus *Eunotia* showed that most species have relatively closely similar allometric trajectories. On the other hand, a few species with more complex morphologies were typical for more divergent

ontogenetic allometric patterns. This might indicate their increased potential for morphological evolutionary diversification.

The general objective of this thesis was to show that biological shape analysis can provide a meaningful way of asking questions and exploratory research of shape variation in pennate diatoms. However, geometric morphometrics is still a relatively dynamic research field with a variety of recently introduced analytical tools. It is therefore obvious that future morphometric analyses of diatoms should take these advances into account. For example, future studies of their ontogenetic and evolutionary allometric trajectories might benefit from a newly developed method of centric allometry, that is based on Procrustes form space or Boas coordinates. In this analysis, the quantitative morphometric description includes both size and shape together. Bookstein (2019) suggested that this analysis may be useful especially in systems with significant allometric effects. Thus, the diatom frustules represent a prime example of a system suitable for the analysis of centric allometry. In this respect, application of the Boas coordinates or Procrustes form space in diatom analyses could result in a more holistic description of their natural variability and it could also be more relatable with traditional diatomological studies.

List of references

Bookstein, F. L. (2019). Reflections on a Biometrics of Organismal Form. Biological Theory, 14:177-211.

Mann, D. G. (1994). The origins of shape and form in diatoms: the interplay between morphometric studies and systematics. In: Ingram, D. & Hudson, A. (eds.). Shape and Form in Plants and Fungi, pp. 17-38. Academic Press, New York.